Copy 8
Contains 117 Pages

GER 10882 Rev. A
30 November 1962

CODE 25500

GOODYEAR

GOODYEAR AIRCRAFT CORPORATION

AKRON, OHIO

QUARTERLY PROGRESS REPORT NUMBER ONE
STUDY ON METHODS OF STRUCTURALLY EVALUATING EXPANDABLE STRUCTURES HAVING POTENTIAL SPACE APPLICATIONS

N. L. Jeppesen

B. W. Reynolds

N. C. Costakos

N. E. Houtz

E. Rottmayer

Contract No. NAS w-471

Reporting Period 1 August 1962 to 1 November 1962

(Supersedes and Cancels GER 10882 dated 10 November 1962)

218-52 (1-60)M

THIS DOCUMENT CONTAINS GOODYEAR AIRCRAFT CORPORATION PROPRIETARY INFORMATION AND IS SUBJECT TO RETURN UPON REQUEST.
IT IS TRANSMITTED FOR THE SOLE PURPOSE OF AIDING THE TRANSACTION OF BUSINESS BETWEEN GOODYEAR AIRCRAFT CORPORATION AND THE RECIPIENT. ALL INFORMATION, DATA, DESIGNS, AND DRAWINGS CONTAINED HEREIN ARE PROPRIETARY TO AND THE PROPERTY OF GOODYEAR AIRCRAFT CORPORATION, AND MAY NOT BE REPRODUCED OR COPIED, NOR APPROPRIATED TO USES IN ANY WAY DETRIMENTAL TO THE INTERESTS OF GOODYEAR AIRCRAFT CORPORATION INCLUDING DISCLOSURE TO OUTSIDE PARTIES, DIRECTLY OR INDIRECTLY, WITHOUT SPECIFIC WRITTEN CONSENT OF GOODYEAR AIRCRAFT CORPORATION.

ABSTRACT

This report summarizes the progress made during the first quarter of a one-year contract (NASw-471) for a "Study on Methods of Structurally Evaluating Expandable Structures Having Potential Space Applications."

The objective of the study is to determine the relative importance of each of the parameters that influence the structural weight of pliable, expandable, orbital space structures.

Major areas in which studies were initiated during this period were:

1. Determination of the important parameters that affect the weight of expandable structures.
2. The relationship of these parameters to the total structural weight.
3. The effect of shape and method of construction on structural weight.
4. The possibility of using the cumulative damage theory to determine safety factors.
5. Significance of long-time loading (creep) on design of expandable structures.

TABLE OF CONTENTS

Section		Page
	ABSTRACT	iii
I	INTRODUCTION	1
	A. General	1
	B. Approach	1
II	DETAILS OF APPROACH	4
	A. Philosophy	4
	B. Basic Assumptions	8
	C. Classification of Structures	14
	D. Outline of Method for Structural Evaluation	16
	E. Summary Curves	16
III	WORK ACCOMPLISHED TO DATE	23
	A. Basic Structural Weight	23
	1. General	23
	2. Values of C_1 for Various Shapes and Methods of Construction	24
	3. Creep-Rupture at Room Temperature	25
	4. Environmental Effects on Creep-Rupture, k_1	29
	5. Cumulative Damage and Safety Factors	34
	6. Pressure Ranges	38
	7. Volumes for Various Shapes	38
	B. Secondary Structural Weight	43
	C. Supporting Studies	43
IV	ANALYSIS OF RESULTS TO DATE	44
	A. Interpretation of Results	44
	B. Recommended Action	45
	C. Success in Meeting Objectives	45
V	WORK TO BE ACCOMPLISHED NEXT QUARTER	46
VI	REFERENCES	47

TABLE OF CONTENTS (Continued)

Appendix		Page
A	BASIC STRUCTURAL WEIGHT OF PRESSURE VESSELS IN THE FORM OF SURFACES OF REVOLUTION	A-1
	A. General Analysis	A-1
	B. Ellipsoids of Revolution	A-3
	C. Paraboloid and Spherical Segment	A-8
	D. Circular Torus	A-12
	E. Cone and Spherical Segment	A-15
	F. Cylinder with Hemispherical Ends	A-19
	G. Sphere	A-20
	H. Summary of Basic Structural Weight Analysis	A-20
B	ULTIMATE TENSILE STRENGTH-TO-WEIGHT RATIO AT STANDARD ATMOSPHERE AND ROOM TEMPERATURE	B-1
	A. General	B-1
	B. References	B-1
C	CREEP-RUPTURE DATA	C-1
	A. General	C-1
	B. References	C-1
D	CUMULATIVE DAMAGE AND FACTOR OF SAFETY	D-1
	A. Creep-Rupture	D-1
	B. Operating Margin and Factor of Safety	D-8
	C. Comparison of Safety Factors of Polymeric Fabrics and Metals	D-15
	D. References	D-18

LIST OF ILLUSTRATIONS

Figure		Page
1	Outline of Method for Structurally Evaluating Expandable Structures Having Potential Space Applications	17
2	Optimum Design Curve for Spherical, Wire-Film, Passive Communication Satellite	19
3	Optimum Wire Weight for Aluminum	20
4	Volume Requirements for Manned Space Station	21
5	Creep-Rupture Loading Experiment Schematic	28
6	Typical Material Creep-Rupture Data at Room Temperature	30
7	Type 51 Dacron Creep-Rupture Data at Various Temperatures	31
8	Maximum and Minimum Surface Temperatures as a Function of the Orbital Angle	35
9	Extreme Maximum Temperatures as a Function of α/ϵ and ϵ	36
10	Creep-Rupture and Operating Margin	37
11	Volume and Surface Area of a Sphere	40
12	Volume of a Torus (8-Foot Diameter Cross-Section)	41
13	Volume of Cylinders of Various Lengths and Diameters	42
A-1	Surface of Revolution	A-1
A-2	Geometry of the Ellipse	A-3
A-3	Plot of Coefficient, C, for Ellipsoids of Revolution	A-7
A-4	Paraboloid and Spherical Segment Geometry	A-8
A-5	Plot of Coefficient, C, for Paraboloid and Spherical Segment	A-11
A-6	Circular Torus Geometry	A-12
A-7	Plot of Coefficient, C, for Toroidal Pressure Vessel	A-14
A-8	Cone and Spherical Segment Geometry	A-15
A-9	Plot of Coefficient, C, for Cone and Spherical Segment Pressure Vessel	A-18
A-10	Cylinder	A-19
D-1	Plot of Creep-Rupture Curve Representing Original Data	D-5
D-2	Plots of Equations 1b and 1f	D-6
D-3	Plots of Equations 1a through 1f	D-7

LIST OF ILLUSTRATIONS (Continued)

Figure		Page
D-4	Operating Margin	D-9
D-5	Confidence Limit and Safety Factor Curves	D-11
D-6	Relation Between Operating Margin and Factor of Safety, $n = \overline{Q}_E/Q_E$	D-13
D-7	Comparison of Two Safety Factor Concepts and Related Operating Margins	D-16

LIST OF TABLES

Table		Page
1	Structural Classification of Expandable Space Vehicles	15
2	Variation of C_1 with Shape and Construction	26
3	Range of Pressures for Various Types of Vehicles	39
A-1	Coefficient, C, in the Basic Weight Equation, $W = \frac{CnpV}{k_1}$	A-21
B-1	Ultimate Tensile Strength-to-Weight Ratio at Standard Atmosphere and Room Temperature	B-2
C-1	Fabric Construction	C-2
C-2	Creep-Rupture Data	C-4
D-1	Survival Times, Reliability, and Factor of Safety	D-12
D-2	Ratio of Moduli of Elasticity to Ultimate Strengths for Polymers and Metals	D-17
D-3	Factor of Safety and Percent Elongation	D-17

SECTION I - INTRODUCTION

A. GENERAL

Goodyear Aircraft Corporation (GAC) under Contract NAS w-471 is conducting a study to determine the relative importance of each of the parameters that influence the weight of pliable expandable structures having space potential. This study is limited to vehicles operating below an altitude of 500 nautical miles, but does not include re-entry vehicles. In addition, areas in which research is required to provide significant improvements in structural efficiency will be indicated. The program is under the direction of Office of Advanced Research and Technology, NASA Headquarters, Washington, D. C.

This report summarizes the progress made during the first quarter of the one year study. The major effort during the first quarter was spent in determining the parameters that affect the weight of expandable space structures and their basic relationship to the total weight of the structure. Other major areas that were studied during this period were:

a. The effect of shape and method of construction on structural weight.
b. Cumulative damage and safety factors for expandable space structures.
c. Significance of long-time loading (creep) on design of expandable space structures.

No supporting studies are included in this report, but they will appear in subsequent reports as they are completed. The progress report concludes with an analysis of results to date The analysis includes an interpretation of the results, recommended future action, and success in meeting objectives.

B. APPROACH

A preliminary analysis was made to determine the significant parameters influencing the weight of expandable structures. It was found that the weight

determining parameters that are significant for Echo type vehicles at one end of the spectrum are not necessarily equally significant for the manned space stations at the other end of the spectrum. It was decided, therefore, to individually determine the relative importance of the weight parameters for each type of vehicle. Accordingly, the vehicles were categorized into types and classified according to structure. The structural classifications and vehicle types being considered in this study are shown in Table 1 with a preliminary listing of the important parameters for each vehicle.

A first attempt to indicate the basic relationships of each parameter to the total structural weight resulted in the preparation of Figure 1 as a schematic representation of a method for structurally evaluating expandable structures having potential space applications. This figure shows the fundamental equation for total structural weight and denotes the relationship of each factor to the total weight.

In general these factors have no simple mathematical relationship with one another or with the total weight, except that they might be some function of the volume or surface area of the vehicle. It is necessary therefore to determine most of these relationships empirically from test data gathered from industry and various government agencies. Figure 1 shows the type of parametric curves that will have to be generated for each weight factor. This is only a first attempt to indicate what information is needed and how it should be presented, and it is expected that a closer look at each factor may bring about some changes.

Using Table 1 as a guide and using the Figure 1 data gathered, it will be possible to determine the relative importance of each of the parameters that influence the weight of each type of vehicle. It will then be possible to plot summary curves similar to those shown in Figures 2, 3, and 4 that will more graphically display the influence of some of the important parameters on the design of each type of vehicle or on the utility of various designs.

In developing the empirical relationships and in determining the relative

importance of each parameter it will be readily apparent where information is completely lacking or inadequate. These areas will be noted, and a suggested program to obtain the information required will be prepared along with a listing of the relative importance of each parameter.

SECTION II - DETAILS OF APPROACH

A. PHILOSOPHY

Generally speaking, true parametric studies or optimization studies are confined out of necessity to a rather narrow scope in order to reduce the tremendous number of combinations of parameters that must be considered. A parametric study such as this one, that encompasses all orbiting vehicles, from Echo-type satellites to manned space stations, made from any type of expandable material and made by any method of construction, is much too broad to be accomplished in a reasonable length of time unless the study is divided into smaller, more manageable sections.

This division can best be accomplished by segmenting the study according to the type of vehicle being considered. A first attempt to categorize the study is shown in Table 1 which shows the structural classification, the types of vehicles to be considered, the parameters to be considered for each type of vehicle, and in some cases the range through which some of the parameters must be considered.

Breaking down the study by types of vehicles has many distinct advantages:

(1) Only those parameters applicable to a particular vehicle will have to be considered for that vehicle.

(2) In many instances the range of values of each parameter to be considered can be narrowed to fit the particular vehicle being considered.

(3) The important parameters for each type of vehicle will be clearly spelled out; therefore, those associated with a particular type of vehicle will not have to search out this information for themselves.

(4) With the important parameters established for each type of vehicle, the proper perspective will be provided for planning research and development programs by vehicles rather than for orbital space vehicles in general.

The prime consideration when evaluating an orbiting structure is its weight. Although cost should not be overlooked, the structure usually represents a small part of the total cost when the launch vehicle and the launching complex are considered. Therefore, for this study the weight of the structure will serve as the basis for evaluation.

The types of structures to be considered for this study will be confined to pliable, expandable structures for low, earth-orbit applications. In general, the structures will be pressure vessels in the form of surfaces of revolution.

In order to determine the effect of the many parameters on the weight of the structure, an initial weight shall be established that represents the weight of the structure as it is prior to considering all the external effects, such as environment, seams, shape, method of construction, etc. For comparison, then, a final weight is determined, taking into account the effect of all the parameters. In addition, the degree to which each parameter affects the weight can also be established.

This initial weight is herein defined as the total weight of the filamentous material required to resist the internal pressure of an inflated structure made up entirely of filaments that are loaded to identical stress levels. Structures such as these have recently come to be known as "isotensoid" structures. This initial weight shall herafter be designated as the Isotensoid Weight (W_I). The Isotensoid Weight can be determined (References 1 and 2) from the following equation:

$$W_I = \frac{C_o V p n}{k_o}$$

where:

C_o = Coefficient for isotensoid structures = 3.0

V = Volume of structure

p = Internal pressure

n = Safety factor

k_o = Strength-weight ratio of material filament under creep load at room temperatures

It should be pointed out that the Isotensoid Weight does not include the weight of the binder usually associated with this type of construction but is just the weight of the structural material alone. Another interesting feature of this equation is the fact that for all isotensoid structures, regardless of shape, the coefficient (C_o) is equal to 3.0. As a result it can be seen that the structural weight is proportional to the volume of the structure irrespective of the shape. In determining W_I the strength-weight ratio of the material (k_o) will be based on room temperature creep strength. The final weight or Total Weight (W_{TOT}) as it shall hereafter be known will be broken down into two categories:

(1) Basic Structural Weight (W_B)

(2) Secondary Structural Weight (W_S), or:

$$W_{TOT} = W_B + W_S$$

The Basic Structural Weight is nothing more than the Isotensoid Weight modified to reflect the effect of methods of construction, other than filament winding, on the structural weight, as well as the effect of environment and fabrication process on the material, which in turn affects the structural weight. This relationship can be written:

$$W_B = W_I \left(\frac{k_o}{k_1}\right)\left(\frac{C_1}{C_o}\right)$$

or

$$W_B = \left(\frac{C_o\, V\, p\, n}{k_o}\right)\left(\frac{k_o}{k_1}\right)\left(\frac{C_1}{C_o}\right)$$

where:

k_1 = Strength-weight ratio of material based on effects on fabrication processes and environment.

C_1 = Coefficient based on shape and method of construction.

It should be noted that the factor $\left(\frac{k_o}{k_1}\right)$ actually is a non-dimensional number which reflects the importance of material strength as affected by environment and fabrication processes, in determining structural weight. Likewise $\left(\frac{C_1}{C_o}\right)$

is a measure of the importance of shape and method of construction on the weight. W_B, like W_I, defines only the weight of the structural material required to resist the internal pressure and does not include such things as the binder, seams, etc included in the Secondary Structural Weight.

The Secondary Structural Weight is herein defined as the sum of the weights of those items, exclusive of the Basic Structural Weight, that make up the structural wall of the space vehicle or that are necessary to insure the structural integrity of the wall. The items considered here as making up the Secondary Structural Weight are as follows:

W_E = Weight of the elastomer or binder

W_D = Weight of material added to resist dynamic loads.

W_{SM} = Weight of material and cement added for seams.

W_C = Weight of reinforcing material around cutouts.

W_J = Weight of material added for reinforcement of joint at intersection of two structures.

W_P = Weight of partitions required for reasons of safety.

W_{SL} = Weight of sealant required to seal seams, joints, or walls.

W_{PS} = Weight of pressurization system, if pressure must be maintained for structural integrity.

The equation defining the Secondary Structural Weight can be written as follows:

$$W_S = W_E + W_D + W_{SM} + W_C + W_J + W_P + W_{SL} + W_{PS}$$

These factors, in general, have no simple mathematical relationship to the total weight or to one another, except that they might be some function of the vehicle volume or area. It is intended that these relationships be established empirically from test data presently available or where possible by calculation (see Figure 1). The equation for the total weight can then be written:

$$W_{TOT} = \frac{C_o V p n}{k_o}\left(\frac{k_o}{k_1}\right)\left(\frac{C_1}{C_o}\right) + W_E + W_D + W_{SM} + W_C + W_J + W_P + W_{SL} + W_{PS}$$

As the study progresses and more information is compiled this equation may be modified as more definite relationships are established.

The next step will be to determine the relative importance of each parameter in the above equation for each type of vehicle listed in Table 1. From these data summary curves can be prepared, as well as suggested research and development programs.

B. BASIC ASSUMPTIONS

This study is being conducted on the basis of the following limits and assumptions:

1. Structural Materials

All structural materials considered for this study are to be pliable, and will depend upon internal pressure for structural integrity, or at least for initial deployment. Comparisons will be made using other methods of deployment.

2. Structural Weight

The structural weight is defined as the sum of the weights of the following items:

a. The primary structural material (including seams and reinforcements).
b. The sealant or elastomer
c. The pressurizing gas (when retained)
d. The pressurization system
e. Any partitions required for reasons of safety

3. Meteoroid Protection

Many vehicles require meteoroid protection in the form of a "Whipple bumper" or mechanical atmosphere. Such protection can reduce the severity of the environmental conditions experienced by the inner or structural wall. Where applicable, this reduction is to be taken into account in this study.

4. Vehicles Considered

Only vehicles in earth orbit up to 500 nautical miles and that do not re-enter the earth's atmosphere are being considered in this study.

5. Shapes to be Considered

The shapes to be considered may be surfaces of revolution, or the structure may consist of several combinations of surfaces of revolution. Since the primary inflation stresses are always tensile, some oblate spheroids are eliminated because they are subjected to hoop compression when inflated. The shapes to be considered are:

a. Sphere
b. Circular Cylinders
c. Circular Torus
d. Isotensoid Torus
e. Cone
f. Paraboloid
g. Prolate Spheroid
h. Oblate Spheroid
i. Combinations

6. Range of Pressures to Be Considered

Inflation pressures range from practically zero as in the case of "Echo" type spheres to a pressure not exceeding one atmosphere for manned structures. It is possible that pressures higher than one atmosphere will be used for special storage containers; these, however, wouldprobably be small diameter containers.

7. Parameters of Construction to Be Considered

a. Types of Construction

(1) One or more plies of woven or braided cloth
(2) Cord type cloth
(3) Filament wound
(4) Sheet material - structure formed with or without gores.
(5) Combinations of sheet and (1), (2), or (3)
(6) Gas retention accomplished by an elastomer impregnating the cloth, by a separate bladder, or by combination of an elastomer and bladder; or added material. May not be necessary as could be the case in (4).

b. Effect of Seams

(1) Lap seams that are cemented, sewn and cemented, heat sealed, or welded insofar as they affect the strength

(2) Seaming techniques that can be used under controlled manufacturing conditions and those that can be used under severe environmental conditions for repair

c. Effects of Cutouts

For simplicity only cutouts that are essentially circular are being studied to determine the effect of their size and purpose on the structural weight. The kind of structure as well as the structural shape into which the cutout is made will probably be significant.

d. Effect of Intersections

When one surface of revolution intersects another, the resulting curve is a plane curve in particular cases only; usually it is a skew curve. In either case a bulkhead or ring capable of supporting thrusts, shears, and moments in any direction may be necessary. Certain cases can be handled with membranes of the right shape; however, undesirable partitions may be required. Because of the complexity of the curves of intersection, the study is being limited to cylinder-sphere, cylinder-cylinder, sphere-sphere, sphere-torus, and cylinder-torus curves of intersection.

8. Dynamic Loads

a. Deployment

As the structure is being inflated or expanded by pressurization, entrapped air, or mechanical means and as it attempts to reach its stable shape, the structure and its contents are subjected to dynamic forces. The magnitude of these forces and their effect upon the weight will be estimated.

b. Attitude Stabilization and Simulated Gravity

The attitude stabilization and simulated gravity forces will be determined for a 400-ft diameter space station as an upper limit.

c. Docking Loads

Since supplies may be taken aboard or personnel returned or exchanged, some structure must be added to support the loads expected during the docking operation. These loads will be determined for the docking of an Apollo capsule, as an upper limit. The inherent capability of various shapes to resist docking loads will also be considered.

9. Structural Instability

The weight (W_o) is based on a stable structure; therefore, instability will result in a weight penalty. All the shapes listed in paragraph 5 above can become unstable under certain conditions. Some such conditions that are likely to be met in service will be studied. An example is the instability of a circular torus with a rigid hub.

10. Compartmentation Requirements

Most vehicles will require simple partitions for safety as well as for convenience or privacy. The number of safety partitions will be a function of the requirements to prevent catastrophic failure if the vehicle is punctured by a meteoroid. Only the safety partitions will be considered in the structural weight.

11. Safety Factors

Factors of safety depend upon whether the structure is manned or unmanned, fabric or metal, time under load, fatigue, and environmental conditions. An example of factors of safety (in accordance with Reference 3) used in the Goodyear Aircraft INFLATOPLANE* are:

Metal Structure, Yield	1.15
Metal Structure, Ultimate	1.50
Fabric Structure, Wrinkling	1.00
Fabric Structure, Ultimate	1.75

*TM - Goodyear Aircraft Corporation, Akron, Ohio

In addition to these factors additional material factors of safety for the fabric components (in accordance with Reference 3) are:

Inflation only	4
Limit Load	3
Ultimate Load	1.5

These latter factors take into account time under load, and to some extent, fatigue as well. Similar factors of safety will be established in the study.

12. Environment Ranges

a. Temperature

Limiting outer skin temperature are those obtainable on a black body in space.

b. Vacuum

Pressure should be that associated with operating up to 500 nautical miles altitude.

c. Radiation

Various types of radiation in space are solar infrared, solar ultraviolet, Inner Van Allen Belt, Outer Van Allen Belt, and solar flares. The intensities of these radiations are dependent on the flight parameters of the space vehicle.

Below 500 nautical miles ultraviolet radiation is the only electromagnetic radiation known to greatly affect the strength of unprotected polymeric materials. In this study the effect of radiation on material properties will be primarily that resulting from ultraviolet radiation.

d. Ozone

It is believed that layers of ozone will occur below possible orbit altitudes and will not present a problem. Ozone is known to deteriorate rubber elastomer. The Goodyear Tire and Rubber has been investigating this problem. Once ozone environment has been determined the Goodyear Tire and Rubber data will be investigated.

13. Material Ranges

a. Types of materials to be considered

(1) Woven fabric

(2) AIRMAT* fabric

(3) Cord fabric

(4) Filament wound fabric

(5) Film

(6) Combinations

b. Re-inforcing material to be considered.

(1) Nylon

(2) Dacron

(3) New polymers

(4) Metal (stainless steel wires, etc.)

(5) Aluminum oxide whiskers

c. Elastomers to be considered

(1) Neoprene

(2) Butyl

(3) Hypalon

(4) Polyurethane

(5) Silicone

d. Coatings to be considered

Specific coating materials are not outlined at this time. Basically they can be used as additives to the elastomer in a dispersed form or may be painted to the outside of the elastomer. GAC is presently evaluating the following additives: zinc oxide, zinc sulfate, and carbon black. Inquiries are being made regarding Echo coatings used by NASA. What is required for a coating will be compared with what is available.

e. Films to be considered

Specific film materials are not outlined at this time. On lighter fabrics

*TM - The Goodyear Tire and Rubber Company, Akron, Ohio

films can be used to obtain low permeability. In case of the GAC developed film-cloth laminate, a Mylar film is used to provide shear stiffness to the single-ply cloth.

f. Strength Range

Depending on structural requirements, the strength requirements can vary from close to zero on up to that of aluminum oxide whiskers.

g. Duration of Flight

The duration of flight is considered as ranging from a minimum of one week to a maximum of one year.

C. CLASSIFICATION OF STRUCTURES

In an effort to break down the parametric study into smaller, more manageable pieces it seemed logical to study each type of structure separately. In categorizing the various structures the first logical division is to separate the manned vehicles from the unmanned vehicles (Table 1). In general, unmanned vehicles will operate at a much lower pressure than will a manned vehicle. One exception would be fuel storage tanks which would operate at high pressures, but would be unmanned.

The next logical breakdown would be by the intensity of the loads to which the structure would be subjected. In the case of unmanned structures three sub-divisions seem necessary: (1) extremely lightly loaded, (2) lightly loaded, and (3) highly loaded. In the manned category, however, there are no extremely lightly loaded vehicles, and hence, only two sub-divisions are required: (1) lightly loaded and (2) highly loaded.

Listing the various expandable space vehicles in accordance with the above structural classifications, it becomes apparent that there are only eight types of vehicles listed under five structural classifications. There are not many more vehicle types than structural classifications, and hence, the decision to

Table 1. Structural Classification of Expandable Space Vehicles

Structural Classification		Type of Vehicle	Meteoroid Protection or Insulation Required		Material or Method of Construction									Environment of Structural Material													
														Temperature			Time in Orbit			Time Loaded			Radiation Intensity			Vacuum			
			Yes	No	Film	Film and Foam	Plied Fabric	Film W'N'D	Film Cage	Air-Mat*	Seam Eff'y	Cut-Out Reinf	Joint Eff'y	Low	Mod	High	Short	Med	Long	Short	Med	Long	Low	Mod	High	Low	Mod	High	None
Unmanned	Extremely Lightly Loaded	Passive Comm'n Satellite		▲	▲						▲			▲	▲	▲			▲	▲					▲			▲	
	Lightly Loaded	Solar Concentrator		▲		▲					▲					▲			▲	▲					▲			▲	
		Antenna		▲		▲					▲			▲	▲	▲			▲	▲					▲			▲	
		Expandable Camera	▲				▲	▲		▲	▲				▲				▲	▲			▲					▲	
	Highly Loaded	Fuel Storage Tank	▲				▲	▲			▲	▲		▲					▲			▲	▲					▲	
Manned	Lightly Loaded	Space Hangar		▲			▲	▲		▲	▲	▲		▲	▲	▲		▲			▲			▲				▲	
	Highly Loaded	Space Station	▲				▲	▲	▲		▲	▲	▲		▲				▲			▲	▲					▲	
		Escape Vehicle	▲				▲	▲			▲	▲			▲			▲			▲		▲					▲	

Structural Classification		Type of Vehicle	Pressure Requirements				Method of Deployment				Compartment Required		Shape							Structural Instability		Safety Factor		
			One Shot	Low	Mod	High	Infl	Mech	Rotation	Foaming	Yes	No	Sphere	Torus	Cyl	Cone	Parab-oloid	Prol Sph	Comb.	Yes	No	Low	Mod	High
Unmanned	Extremely Lightly Loaded	Passive Comm'n Satellite	▲	▲			▲		▲			▲	▲				▲	▲			▲	▲		
	Lightly Loaded	Solar Concentrator	▲	▲			▲	▲		▲		▲					▲	▲			▲	▲		
		Antenna	▲	▲			▲	▲		▲		▲					▲	▲			▲	▲		
		Expandable Camera			▲		▲	▲				▲			▲						▲	▲		
	Highly Loaded	Fuel Storage Tank			▲		▲				▲		▲		▲						▲		▲	
Manned	Lightly Loaded	Space Hangar			▲		▲					▲			▲						▲			▲
	Highly Loaded	Space Station				▲	▲				▲		▲	▲	▲	▲	▲	▲	▲	▲				▲
		Escape Vehicle				▲	▲						▲		▲	▲	▲	▲			▲		▲	

* TM - GOODYEAR TIRE & RUBBER COMPANY AKRON, OHIO

make parametric studies by vehicles rather than by structural classifications will result in far less work and much more meaningful results. For example, if the study were to be done by structural classification,every shape listed in the table would have to be considered, as well as each material, and the complete range of each environment etc for each classification. If, however, the study is done by type of vehicle, only those shapes, materials, environments, etc specifically applicable to each vehicle need be considered. The coded blocks in Table 1 represent a "first pass" at tabulating the factors that will have to be considered for each type of vehicle in this study. As the study progresses it is conceivable that some changes will have to be made in the table, but it will be brought up to date from time to time.

D. OUTLINE OF METHOD FOR STRUCTURAL EVALUATION

In an effort to obtain a clear picture of the type of data needed for this study and of the relationships of all the factors involved, Figure 1 was prepared. The illustration breaks down the Total Weight Equation into its various factors, defines each parameter, indicates the factors involved in determining each parameter, and shows schematically how the data might be presented.

E. SUMMARY CURVES

From the many graphs and tables generated according to the plan outlined in Figure 1, other graphs summarizing these results can be prepared. They will be drawn specifically for each type of vehicle and will graphically display the influence of some of the important parameters on the design of each type of vehicle or on the utility of various configurations.

Figure 2 is an example of the type of curve that could be drawn to show the effects of some of the important parameters in the design of spherical, wire-film, passive communication satellites.

It is easily shown that the minimum weight film that is considered practical today is the major portion of the antenna weight until very large diameter spheres are considered. Nevertheless, in anticipation that either large diameters will

$$W_I = \frac{C_o V p n}{k_o} \quad \text{(Isotensoid Weight)}$$

$$W_{TOT} = W_B + W_S$$

$$W_B = W_I \left(\frac{k_o}{k_1}\right)\left(\frac{C_1}{C_o}\right) \quad \text{(Basic Structural Weight)}$$

$$W_S = W_1 + W_2 + W_3 + W_4 + W_5 + \ldots W_n \quad \text{(Secondary Structure Weight)}$$

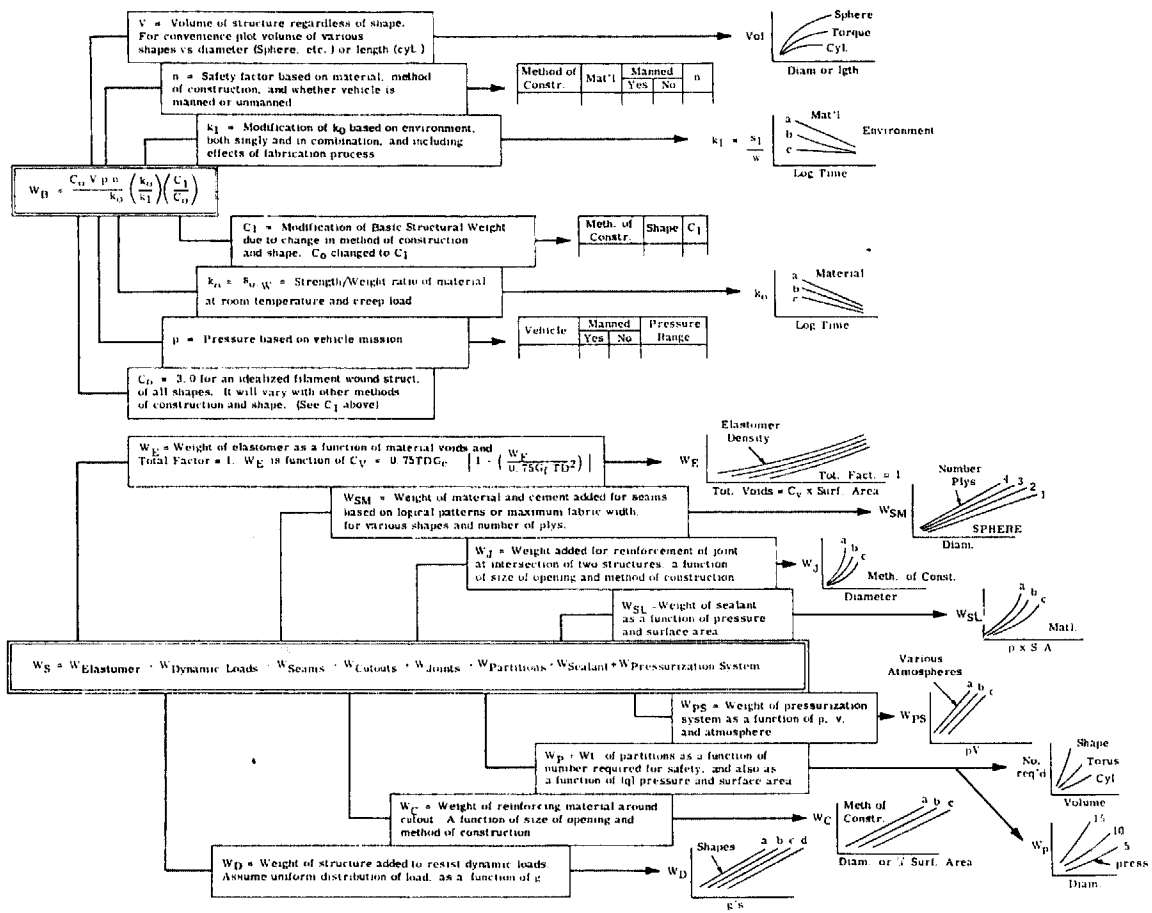

Figure 1. Outline of Method for Structurally Evaluating Expandable Structures Having Potential Space Applications

be of interest or that much lighter film weight becomes practical, it is of interest to optimize the wire weight required, subject to the constraints of buckling due to solar pressure and effective radar cross-section.

The variables to be considered are:

1. Wire material
2. Operating Frequency - f
3. Wire diameter - d
4. Wire spacing - s
5. Radius of sphere - R
6. Reflected power coefficient - r_p

The optimum wire weight to satisfy these two constraints may be found in the following manner for a particular material. The wire weight required to satisfy buckling due to solar pressure can be plotted on log-log scale as a function of wire spacing, s, using wire diameter, d, and sphere radius, R, as parameters as shown in Figure 2. Each point in this figure is a combination of s, d, and R that satisfies the buckling equation.

The reflected power coefficient, r_p, is a function of s, d, and the operating frequency, f. Therefore, if f is assumed, then each combination of s and d corresponds to a particular value of r_p. Curves of constant r_p can be determined and plotted as shown in Figure 2. Once there are available curves of the radius required to give the same radar effectiveness, these radii can be plotted from the relationship:

$$r_p R^2 = \text{constant.}$$

Such a curve is indicated in Figure 2 and shows minimum weight for particular combinations of s and d.

It is planned to determine such curves for various operating frequencies and wire materials. For each material a plot of wire weight versus effective radius with operating frequency as a parameter will be constructed. It is anticipated the curve will appear as shown in Figure 3.

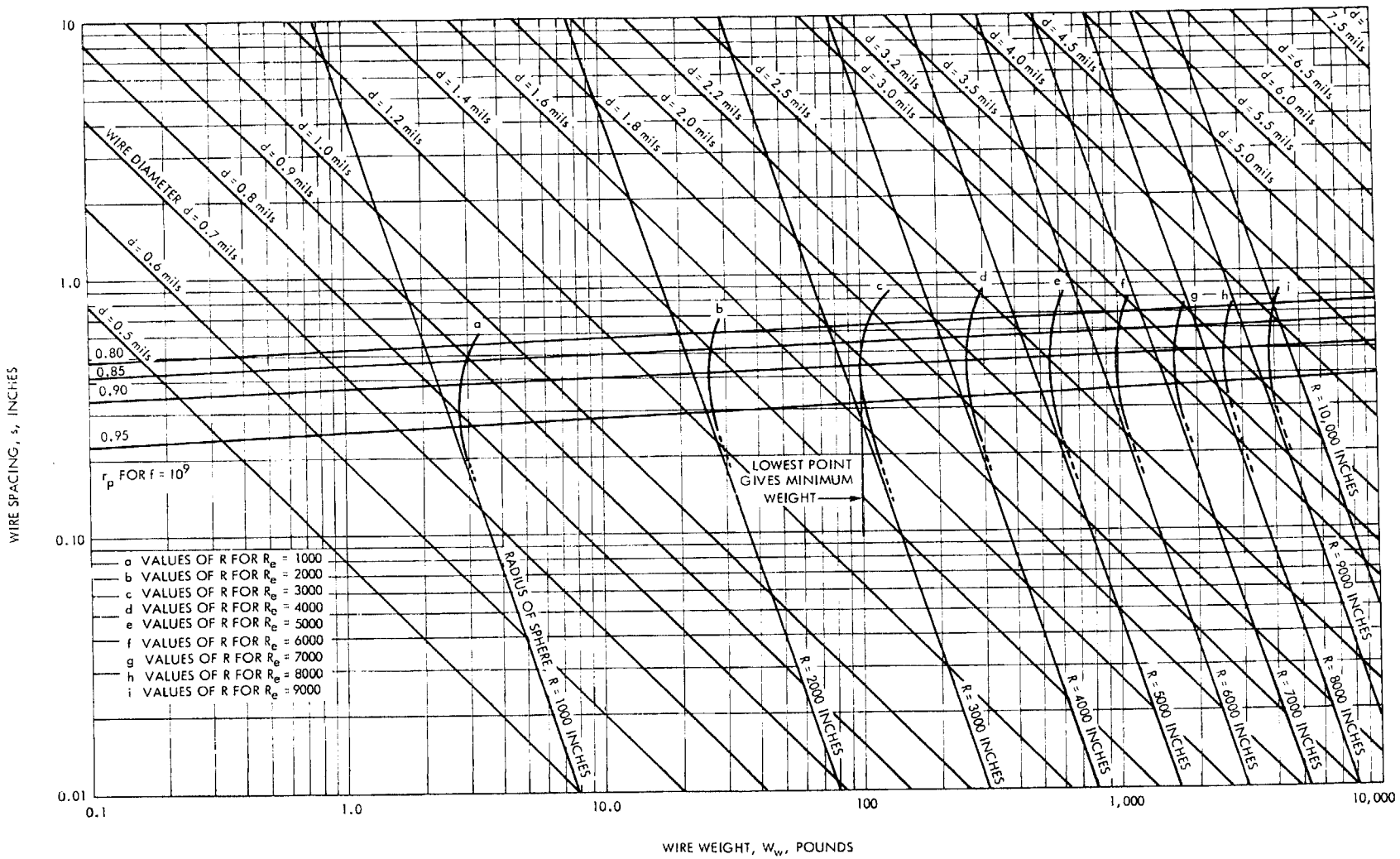

Figure 2. Optimum Design Curve for Spherical, Wire-Film, Passive Communication Satellite

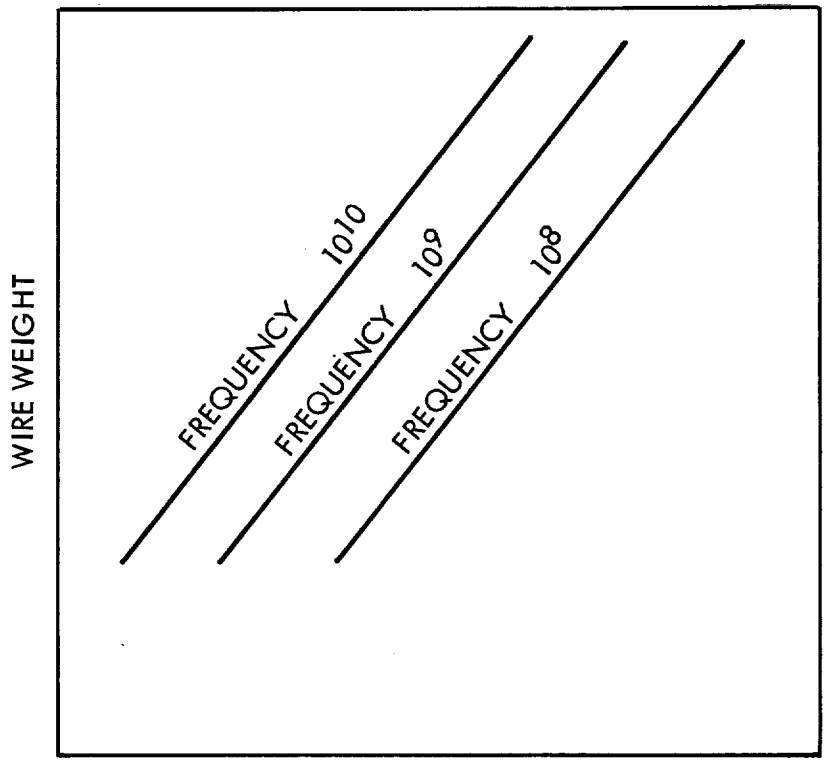

Figure 3. Optimum Wire Weight for Aluminum

Figure 4 is an example of another type of curve that shows the relative utility of some shapes for use as a manned space station. The shapes considered are a sphere, a torus, and a cylinder. Both the torus and the cylinder have an 8-foot diameter cross-section. The plot is that of the volume enclosed by each shape versus its major diameter (sphere and torus) or length (cylinder). Along the upper abscissa is plotted the g's developed at the outer rim for a rotation speed of approximately 4 rpm. Along the right ordinate is plotted the volume required for various crew sizes up to thirty men based on 1000 cubic feet per man.

Let us assume that it is desired to design a 20-man space station that can develop an artificial gravity of 1/2 g at approximately 4 rpm. This can be done with a station having a rotation diameter of 200 feet. At this diameter the volume of the sphere is 4 million cubic feet, the torus volume is 30,000 cubic feet, and the cylinder volume is 4500 cubic feet. The volume required for a

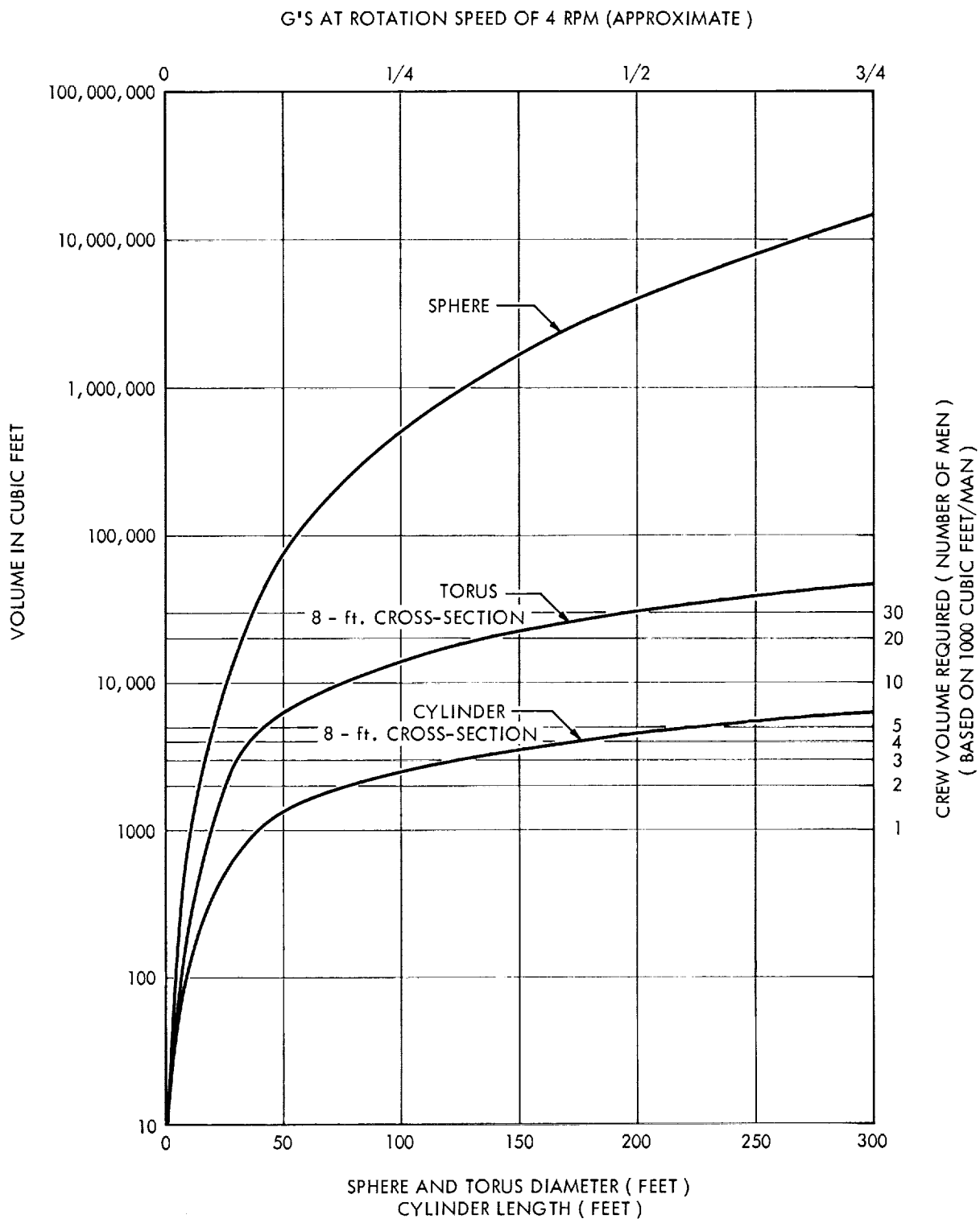

Figure 4. Volume Requirements for Manned Space Station

20-man crew is 20,000 cubic feet. From this it can be concluded that the sphere provides a volume far in excess of that which is required, while the cylinder provides far too little, and the torus comes closest to meeting the requirements.

These are limited samples of the types of curves to be developed as the study progresses. By means of the curves some valid conclusions can be drawn regarding the optimum arrangement of material, configuration, and method of construction for each type of vehicle.

SECTION III - WORK ACCOMPLISHED TO DATE

A. BASIC STRUCTURAL WEIGHT

1. General

The work accomplished to date has been confined entirely to those items associated with the Basic Structural Weight:

$$W_B = \left(\frac{C_o V p n}{k_o}\right)\left(\frac{k_o}{k_1}\right)\left(\frac{C_1}{C_o}\right)$$

The coefficient (C_o) is a constant when the structure is constructed by a continuous filament that is stressed uniformly throughout its entire length. However if the structure is made up of a film of uniform thickness, or of varying thickness such that the stresses are uniform throughout its surface, different coefficients result depending on the shape of the structure. These coefficients, denoted by C_1, are tabulated in Table 2.

Work has been started but not yet completed on the tabulation and assimilation of test data from which values of k_o and k_1 can be established for various materials and environmental conditions.

In the event insufficient test data is available to establish values of k_1 for combined environments, the possibility of establishing combined environment allowables from single environment test data, by use of the cumulative damage theory, is being investigated. This theory is also being considered as a means of determining the safety factor, n, for a structure subjected to a time-dependent load and environment (refer to part 5 of this section). More work must be done in this area.

A brief study of the creep-rupture phenomenon as applied to fabrics has been started. It is important that this phenomenon be thoroughly understood for it is one of the most important factors affecting the allowable stress of a material designed for long-time use. Valid comparisons of the load carrying capability of different materials cannot be made without knowledge of their creep-rupture characteristics (refer to parts 3 and 4 of this section).

The possible range of pressures, p, that can be expected for the vehicles to be studied during this program can be found in Table 3.

A comparison of the relative volumes of spherical, toroidal and cylindrical shapes can be made from Figures 11, 12, and 13.

2. Values of C_1 for Various Shapes and Methods of Construction

The basic structural weight of a pressure vessel in the shape of a surface of revolution is given (Reference 4) as:

$$W_B = \frac{C_1 V p n}{k_1}$$

where:

V = volume

p = pressure

n = safety factor

k_1 = strength-weight ratio

and C_1 is a constant that is dependent upon the shape and construction except when the construction is an isotensoid construction, in which case $C_1 = C_o = 3$.

Besides the isotensoid method of construction, two other methods, both employing sheet material, are considered. The optimum weight is achieved if the vessel is constructed of sheet material whose thickness varies in such a manner that at each point the maximum principal stress is constant. Another

method of construction is one that employs sheet of constant thickness. In this case the sheet thickness is determined by the largest of all the maximum principal stresses.

When constant sheet thickness is used, the structural coefficient, C_1, varies between the optimum value and the isotensoid value of three, or C_1 may equal one or the other of the latter two values except for the torus.

The results are given in the form of Table 2. When the structure consists of two surfaces of revolution, the constant sheet thickness coefficient is given as two numerical values; one in which both surfaces are made with the same uniform thickness, and one in which the thickness is uniform in each surface but not the same in both. (See Appendix A for detailed analysis.)

3. Creep-Rupture at Room Temperature (k_o)

Materials for which we have an interest in developing the strength-weight ratio term, k_o, used in the basic structural weight equation are those which carry the primary structural loads (this excludes binder weight). The pliable materials which will be used as load-carrying members in expandable space structures fall under several material classifications. These classifications are: whiskers, fibers (which includes yarns and cloths), and films.

The strength-weight ratio term, k, is defined as the ultimate tensile strength divided by the unit weight of the load-carrying member. The term k_o represents the value at room temperature and sea level atmospheric conditions under creep load. The effects of the environment, creep-rupture, and fabrication processes will all be considered in establishing the structural material strength-weight ratio term, k_1. The environmental effects on the term, k_1, will be discussed in part 4 of this section.

When conventional engineering materials are used, the term k is equal to the ultimate tensile strength divided by the unit structural weight. For this study, the engineering unit for expressing k will be inches.

Table 2. Variation of C_1 with Shape and Construction

SHAPE	LIMITS OF C_1 WITH STRUCTURAL DIMENSIONS	
	OPTIMUM	UNIFORM
SPHEROIDS PROLATE $b > a$ SPHERICAL $b = a$ OBLATE $b < a$ 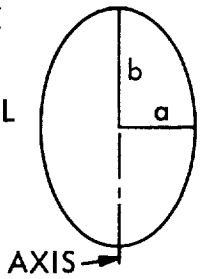 	$2 \geq C_1 \geq 1.5$; $0 \leq \frac{a}{b} \leq 1$ $C_1 = 1.5$ $1.5 \leq C_1 \leq 2$; $1 \leq \frac{a}{b} \leq \sqrt{2}$	$2.36 \geq C_1 \geq 1.5$; $0 \leq \frac{a}{b} \leq 1$ $C_1 = 1.5$ $1.5 \leq C_1 \leq 2.43$; $1 \leq \frac{a}{b} \leq \sqrt{2}$
PARABOLOID WITH SPHERICAL END 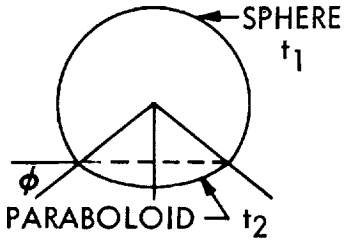 	$1.5 \leq C_1 \leq 2$ $0 \leq \phi \leq 90^\circ$	$t_1 = t_2$ $1.5 \leq C_1 \leq 2.79$; $0 \leq \phi \leq 77^\circ$ $2.79 \geq C_1 \geq 2.66$; $77^\circ \leq \phi \leq 90^\circ$ $t_1 \neq t_2$ $1.5 \leq C_1 \leq 2.66$; $0 \leq \phi \leq 90^\circ$
CONE WITH SPHERICAL END 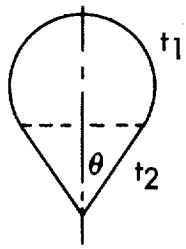 	$2 \geq C_1 \geq 1.5$ $0 \leq \theta \leq 90^\circ$	$t_1 = t_2$ $C_1 = 3$ $0 \leq \theta \leq 90^\circ$ $t_1 \neq t_2$ $3 \geq C_1 \geq 1.5$ $0 \leq \theta \leq 90^\circ$
CYLINDER WITH SPHERICAL ENDS 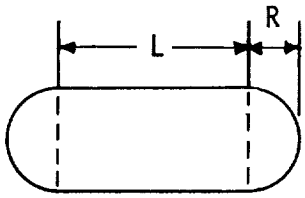 	$1.5 \leq C_1 \leq 2$ $0 \leq \frac{L}{R} \leq \infty$	$t_1 = t_2$ $3 \geq C_1 \geq 2$ $0 \leq \frac{L}{R} \leq \infty$ $t_1 \neq t_2$ SAME AS OPTIMUM
TORUS 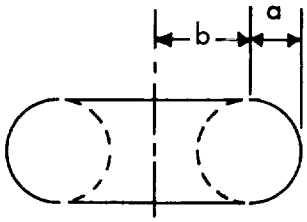 	$C_1 = 2$	$2.0 \leq C_1 \leq \infty$ $0 \leq \frac{a}{b} \leq 1$ FOR $\frac{a}{b} = 0.5$ $C_1 = 3$

A creep-rupture phenomenon is exhibited by nearly all the pliable materials used structurally in expandable vehicles. This characteristic increases the complexity of obtaining the term k, because the strength or strength-weight ratio must be related to the vehicle loading history.

In orbital, expandable, space structures the loading history is simply the tension load induced by a pressure. The other loads are for the most part a small percentage of the pressure load. This then implies that a simple uniaxial tension experiment will provide the needed data.

Goodyear and other investigators have conducted a large number of uniaxial creep-rupture tests over a wide variety of materials under many environmental conditions. This type of experiment is depicted in Figure 5. Specimens are loaded varying amounts, and the time to rupture is measured for each. When the load (or strength-weight ratio) is plotted versus the log of the time to rupture a straight line can be established.

The quick-break tensile strength is another term used to describe the ultimate tensile strength of materials exhibiting room-temperature creep-rupture. Quick-break tensile strength is defined as the load which causes rupture in approximately 20 seconds from the time of application divided by the original cross-sectional area. The equipment used to measure quick-break strength varies (Instron, Scott, and Baldwin-Southwark), resulting in different testing speeds and dissimilar failure times.

The best strength criteria for evaluating manufacturing and environmental parameters would be creep-rupture data. But most investigators invariably use quick-break strengths for evaluating these effects. This then necessitates gathering quick-break strengths for this study.

Ultimate tensile strength-weight ratios, using quick-break strength for polymeric materials, have been compiled for certain materials in various forms such as whiskers, fibers, yarns, woven cloth, coated cloth, and film. This

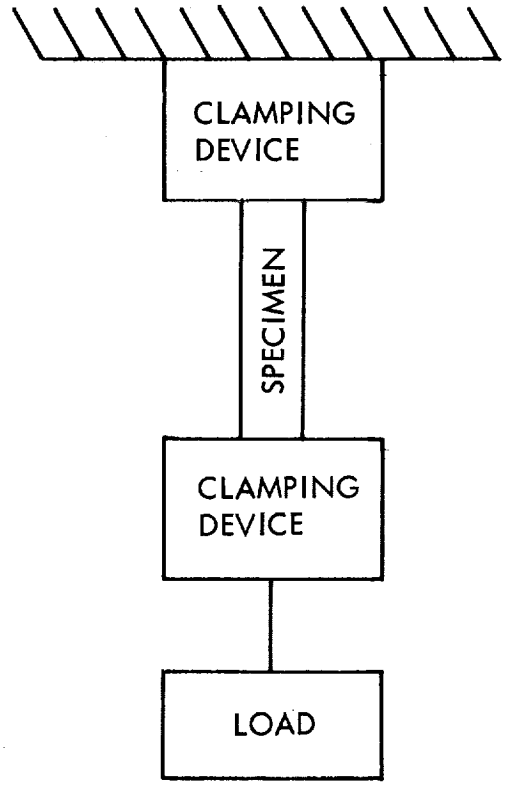

Figure 5. Creep-Rupture Loading Experiment Schematic

information is presented in tabular form in Appendix B. Materials considered to date are: Fortisan, nylon, Dacron, DuPont HT-1, cotton, fiberglass, iron, copper, gold, silicone, sodium chloride, aluminum oxide, graphite, René 41, 304 stainless steel, and Monel. This information will be organized into classes and presented in graphical form to facilitate the structural evaluation of expandable space structures.

Since one of the most important factors in the evaluation of expandable space structures is the creep-rupture strength, a considerable portion of the materials effort will be spent in compiling and organizing such data into the most usable form.

Appendix C presents the creep-rupture strength-weight ratio data prepared in a form currently useful to the program. Figure 6 summarizes typical creep-rupture data at room temperature for the materials Dacron, nylon, Orlon, cotton, and Fortisan.

It must be emphasized that there are many types of materials under the general classes of Dacron, nylon, etc. It must also be emphasized that the form and state of the material prior to testing can greatly affect the strength-weight ratio, k. For example, Dacron can be purchased in several types of yarn or cord, all of which have different strength and ultimate elongation properties. In fact, tenacity, which is a strength-weight ratio term, is one method used to classify these different types. This can be seen from the quick-break strength given in Appendix B, where type 52 Dacron is shown to be the strongest Dacron presently available commercially. Note that the Dacron data presented in Figure 6 is for type 51 Dacron.

4. Environmental Effects on Creep Rupture, k_1

Part 3 of this section has indicated the importance of using creep-rupture data for evaluating the effects of various phenomena on polymeric materials. Unfortunately, such information is extremely limited for the effects of vacuum, radiation, etc. Temperature seems to be the only parameter on which there is considerable information, and even this is for short durations. This lack of data is not deleterious to the evaluation of expandable space structures because in general it can be shown that the structural members loaded for long periods can easily be protected from the harmful aspects of the space environment. This is discussed more fully in the following paragraphs.

The environmental test data presently accumulated for determining k_1 is presented in Appendix C. Figure 7 shows the effect of temperature on a woven,

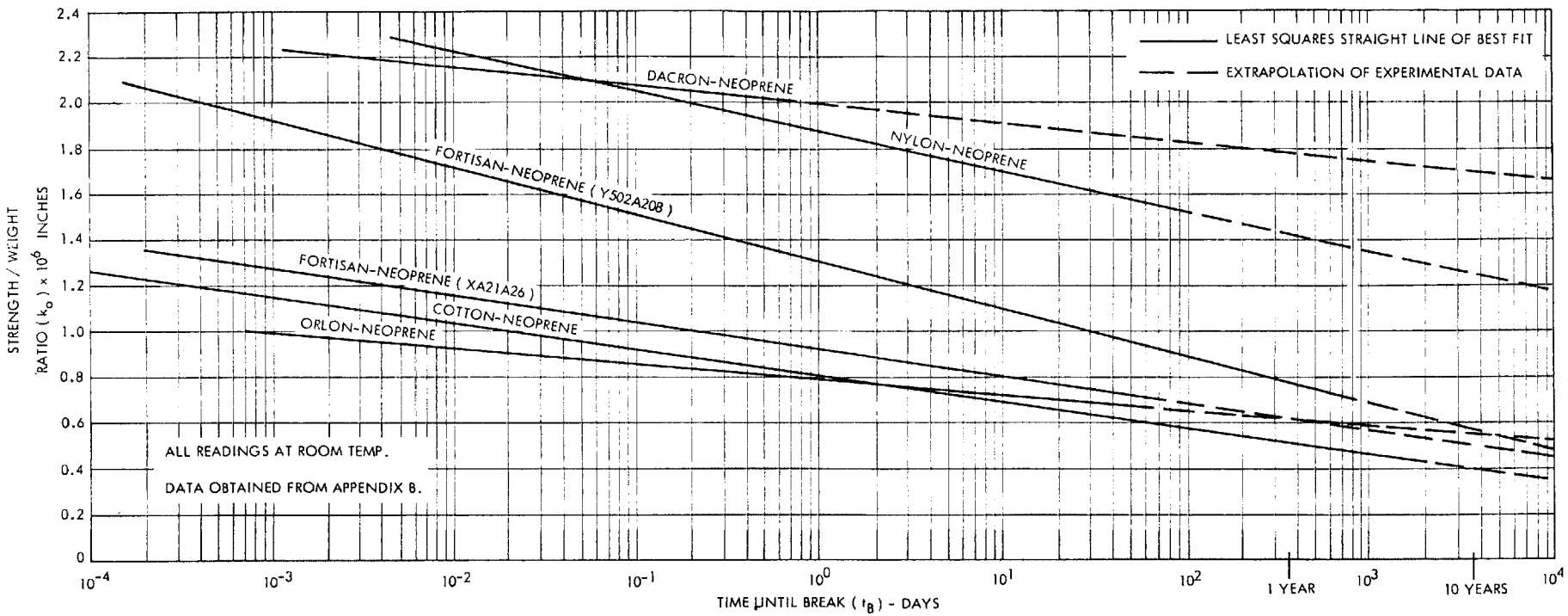

Figure 6. Typical Material Creep-Rupture Data at Room Temperature

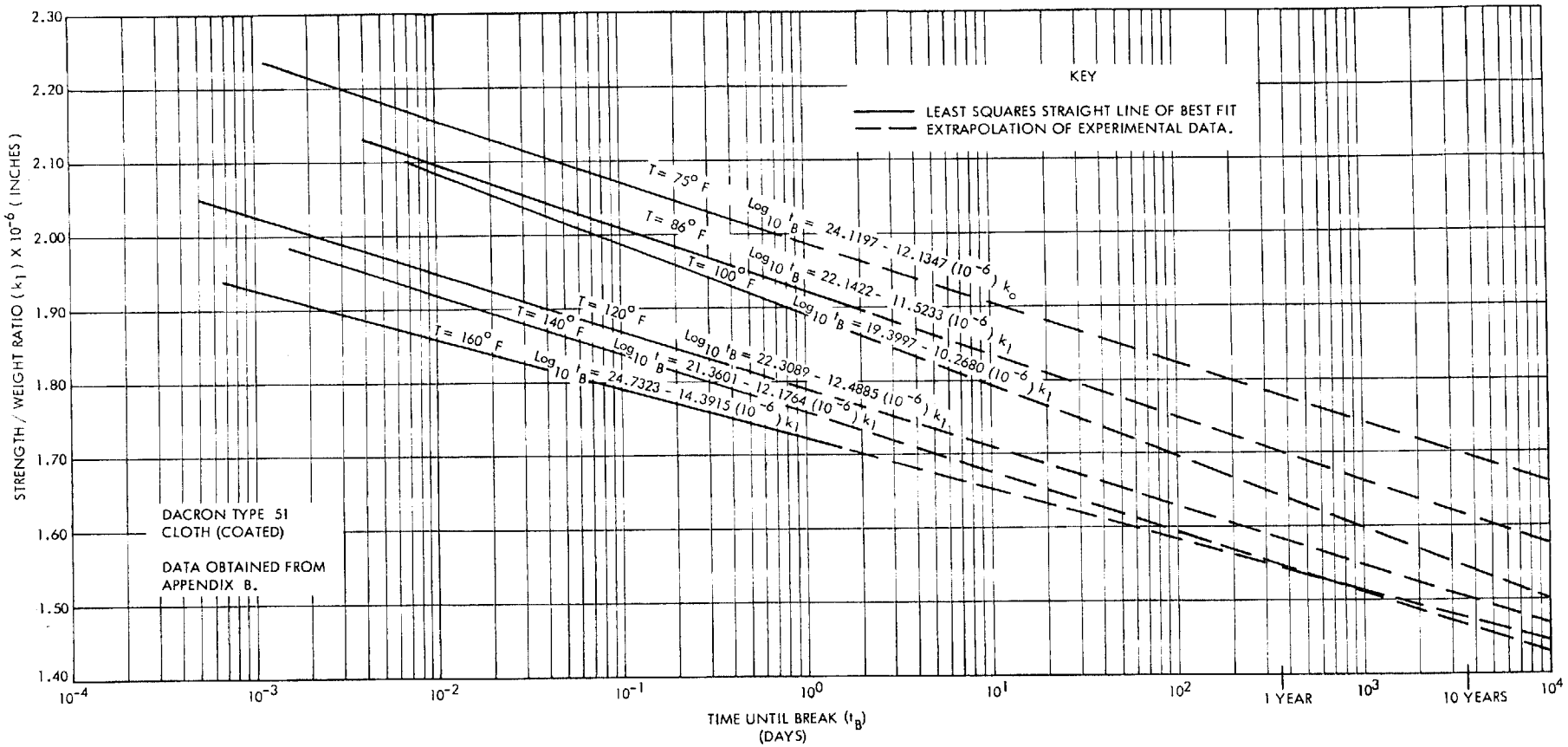

Figure 7. Type 51 Dacron Creep-Rupture Data at Various Temperatures

type 51 Dacron cloth (warp loading direction) that was tested as a neoprene-coated, two-ply, bias-straight fabric.

a. Atmosphere

An atmosphere is defined herein to mean the medium which surrounds the material in space or under test. It can be measured by indicating gas partial pressures.

In space a vacuum of 10^{-8} to 10^{-9} torr will be obtained (in the region of interest), usually on the outer surface of the material. The minimum pressure expected in space is 10^{-11} torr. A gas atmosphere, causing the important creep-rupture loads, is usually maintained on the inside surface.

The internal atmospheric composition depends on the mission of the vehicle. For example, a manned space station will have an atmosphere very similar to that experienced on earth.

Ultra-low pressure (10^{-9} torr) can cause material evaporation or other phenomena that could ultimately affect the creep-rupture strength of a material. The rate of evaporation is a function of the molecular weight and temperature of the material. The materials of interest are of high-molecular weight and are very stable under low pressures as long as the temperature does not become a factor. Any decrease in strength induced by low pressure is believed to be insignificant compared to the structural material creep-rupture life measured in the earth's atmosphere.

The effect of temperature and reduced atmospheric pressure on the creep-rupture characteristics of uncoated and neoprene-coated nylon -6 yarn (Reference 5) has been investigated. Although the results of this experiment are inconclusive, the effect of decreasing the pressure indicated an increase in creep-rupture strength. This work requires a more

thorough investigation over the range of all the polymers of interest, but nevertheless the work gives an indication that earth-atmospheric data are conservative when projected into space applications and, therefore, may be very useful as conservative design criteria in the selection of structural materials.

b. Radiation

Ultraviolet radiation is the only electromagnetic radiation known to greatly affect the strength of unprotected polymeric materials (Gamma radiation is included in the discussion as high-energy particles). The solar energy referred to as ultraviolet acts between 1 to 3800Å which consists of 8 percent of the total solar flux. (Total solar flux is 2 cal/m^2-day.) Little data is available on the strength effects of polymeric materials below 2000Å. This represents only approximately 0.2 percent of the total solar flux.

The effect of high-energy particles on the strength of polymeric materials has been evaluated using cobalt-60 energy sources. It is therefore necessary to extrapolate that data to the spectrum of high-energy particle fluxes encountered in space.

Polymeric materials can be protected from ultraviolet radiation by thin, flexible, opaque coatings. The high-energy particle radiation flux below the Van Allen belts (the region of interest) is sufficiently low that its effects are considered unimportant. For these and other reasons the creep-rupture properties of polymeric materials under either ultraviolet or cobalt-60 radiation have not been measured.

Work on radiation effects on polymeric materials has just been initiated and a more thorough analysis will be given in a later report.

c. Temperature

Many factors influence wall temperatures of an expandable space structure; i.e., earth and solar absorptance; infrared emittance; vehicle orbit,

orientation, and rotational characteristics; and heat transfer coefficient (vacuum), internally generated heat, and skin thickness all affect equilibrium wall temperatures. Both extremely high and extremely low temperatures are possible. Figures 8 and 9 present the maximum and minimum wall temperatures that a space station would experience for the orbit indicated. Figure 8 shows the outer wall temperatures varying from 257°F to -135°F. Figure 9 gives the maximum temperatures which are possible for the given variables, the highest point exhibiting a 770°F outer wall temperature.

The black body solar equilibrium temperature at one astronomical unit is 253°F, assuming a flat plate.

Therefore, the temperature extremes and temperature history of a space vehicle are extremely complex and are defined by the particular application.

High temperatures cause increases in the rate that chemical changes take place in polymeric materials. They cause immediate losses in tensile-strength, modulus, adhesion, and creep-rupture properties. High temperatures also affect the loss of ultimate tensile strength in metal structural materials. If the temperature is high enough, metal structural materials also exhibit creep-rupture characteristics.

Low temperatures cause polymers to become stiffer and sometimes to change state. The creep-rupture strength should increase as the temperature is lowered. Metal structures also experience an embrittlement and an increase in ultimate tensile strength as the temperature is decreased.

5. Cumulative Damage and Safety Factors

The creep-rupture characteristics of many natural and man-made polymeric materials are such that a straight line results when the breaking strength is plotted versus the logarithm of the breaking time. A cumulative damage theory

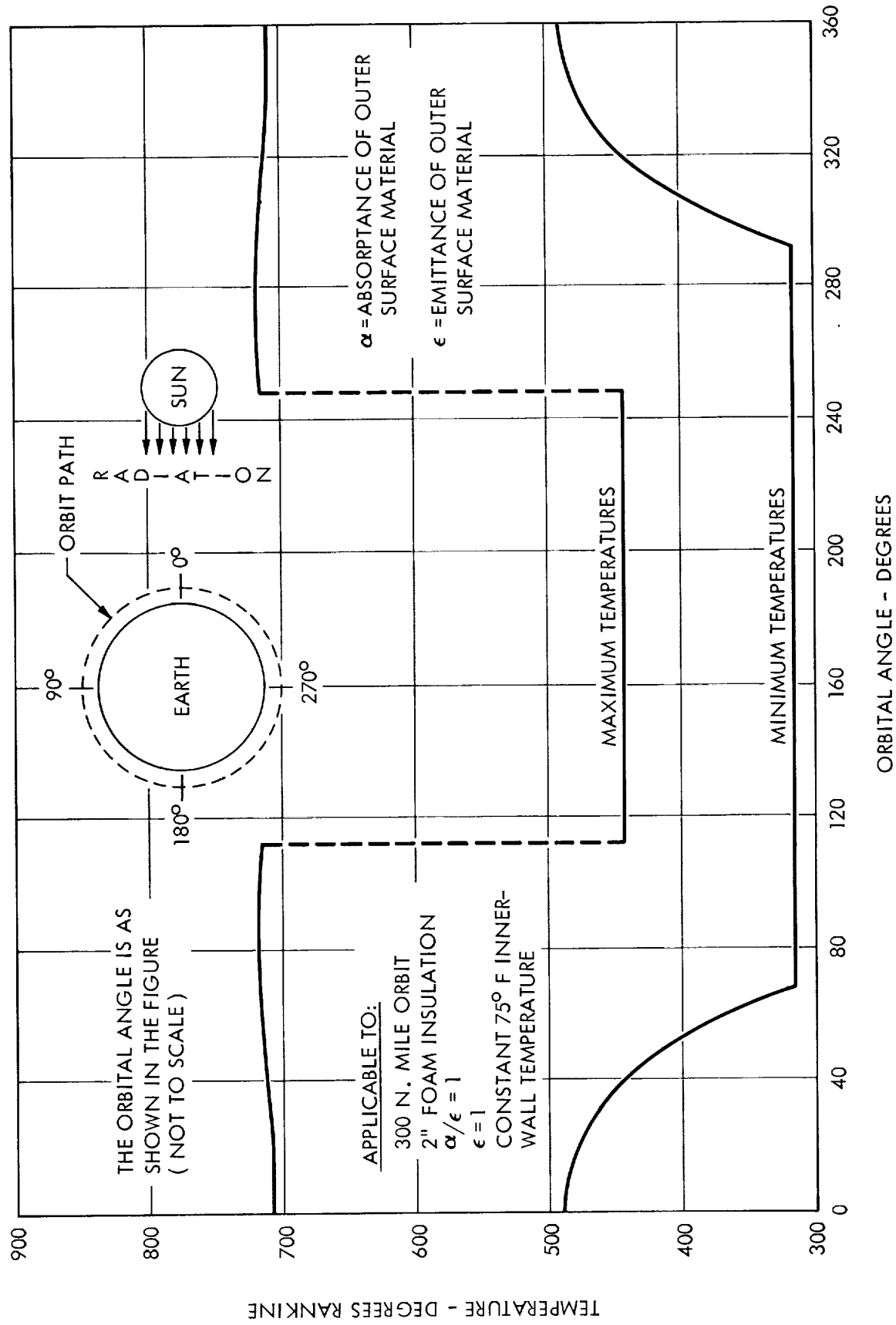

Figure 8. Maximum and Minimum Surface Temperatures as a Function of the Orbital Angle

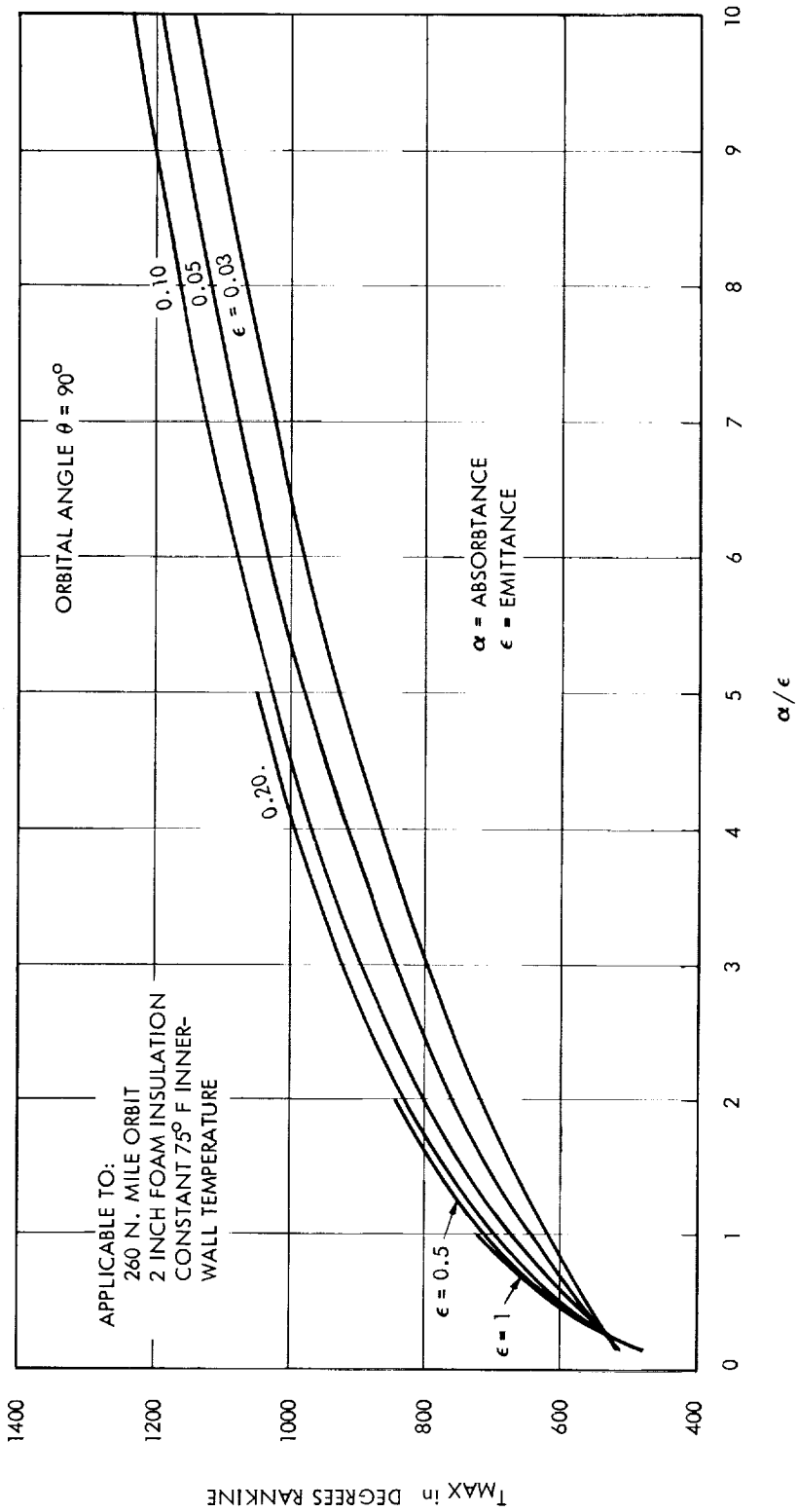

Figure 9. Extreme Maximum Temperatures as a Function of α/ϵ and ϵ

based on this fact is proposed in Reference 6. An explanation of the theory is made with the aid of Figure 10.

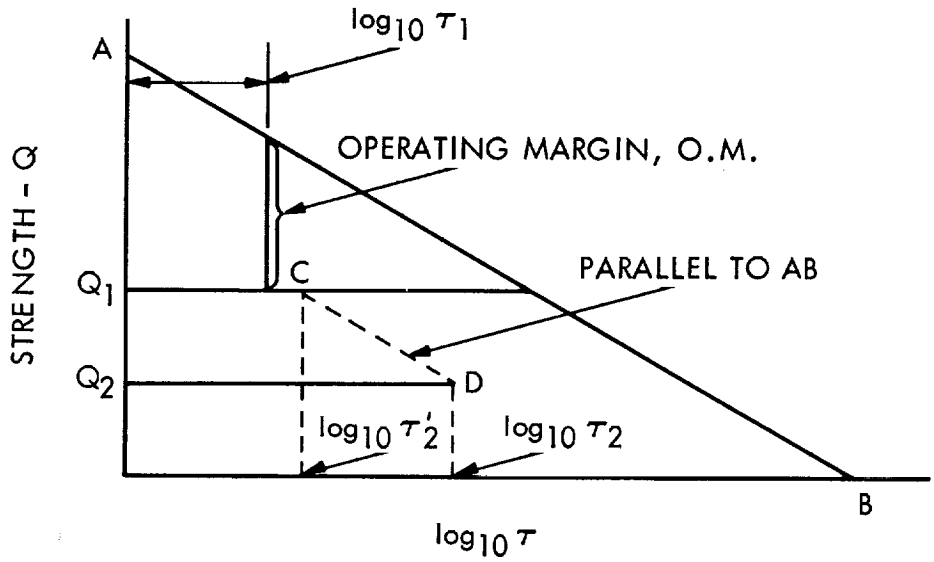

Figure 10. Creep-Rupture and Operating Margin

Let AB be the creep-rupture curve. If a load Q_1 is applied and maintained, failure will result at a time given by the intersection of AB and a horizontal line through Q_1. The operating margin is defined as the vertical distance between AB and a point on the horizontal through Q_1; e.g., OM is the operating margin for the stress Q_1 acting for time τ_1.

The theory of Reference 6 states simply that the damage corresponding to point C is equivalent to that at point D because both points have the same operating margin; i.e., Q_1 for a time τ'_2 is equivalent to Q_2 for a time τ_2. A natural extension of the theory is that any combination of Q_i and τ_i can be converted to a common Q_a and time τ_{ai}. Then if all the times τ_{ai} are added up, the operating margin is given by Q_a acting for a time $\Sigma\tau_{ai}$.

Other environments or loads such as fatigue give similar damage characteristics. For instance fatigue-rupture curves give straight lines when the stress

causing failure is plotted versus the logarithm of the cycles to failure. An operating margin for fatigue can be determined in a manner exactly analogous to that just described for creep-rupture.

Another natural extension of the cumulative damage theory just described is the conversion of a fatigue-rupture operating margin to an equivalent creep stress and creep time in order to combine fatigue damage with creep damage. Other damage such as creep damage at higher temperatures, radiation, vacuum, etc could also be converted to damage at, say, room temperature. See Appendix D for more detailed calculations.

6. Pressure Ranges

In the process of determining the structural classification of each type of vehicle it was necessary to establish the range of pressures under which each vehicle might be expected to operate. These pressures serve to establish whether a vehicle is Extremely Lightly Loaded, Lightly Loaded, or Highly Loaded. Tabulation of the possible range of pressures for each type of vehicle is found in Table 3.

7. Volumes for Various Shapes

Because the volume (V) plays such an important part in determining the structural weight of a vehicle, as shown by the equation for isotensoid weight,

$$W_I = \frac{C_o V p n}{k_o}$$

the curves, shown in Figures 11, 12, and 13, were drawn in order to compare the volumes of various shapes and sizes. Volumes of other shapes are to be prepared as the study progresses.

An example of one of the uses for this type of curve can be found in Figure 4 which compares the volumes of a 200-foot diameter sphere, a 200-foot diameter torus and a 200-foot long cylinder for use as a 20-man space station.

Table 3. Range of Pressures for Various Types of Vehicles

STRUCTURAL CLASSIFICATION		TYPE OF VEHICLE	POSSIBLE RANGE OF PRESSURES
UNMANNED	Extremely Lightly Loaded	Passive Communication Satellite	0.0002 psi to 0.020 psi
	Lightly Loaded	Solar Concentrator	0.006 psi to 0.033 psi
		Antenna	0.006 psi to 0.033 psi
		Expandable Camera	0.125 psi to 1.00 psi
	Highly Loaded	Fuel Storage Tank	5.0 psi to 35.0 psi
MANNED	Lightly Loaded	Space Hangar	3.0 psi to 5.0 psi
	Highly Loaded	Space Station	5.0 psi to 15.0 psi
		Escape Vehicle	5.0 psi to 15.0 psi

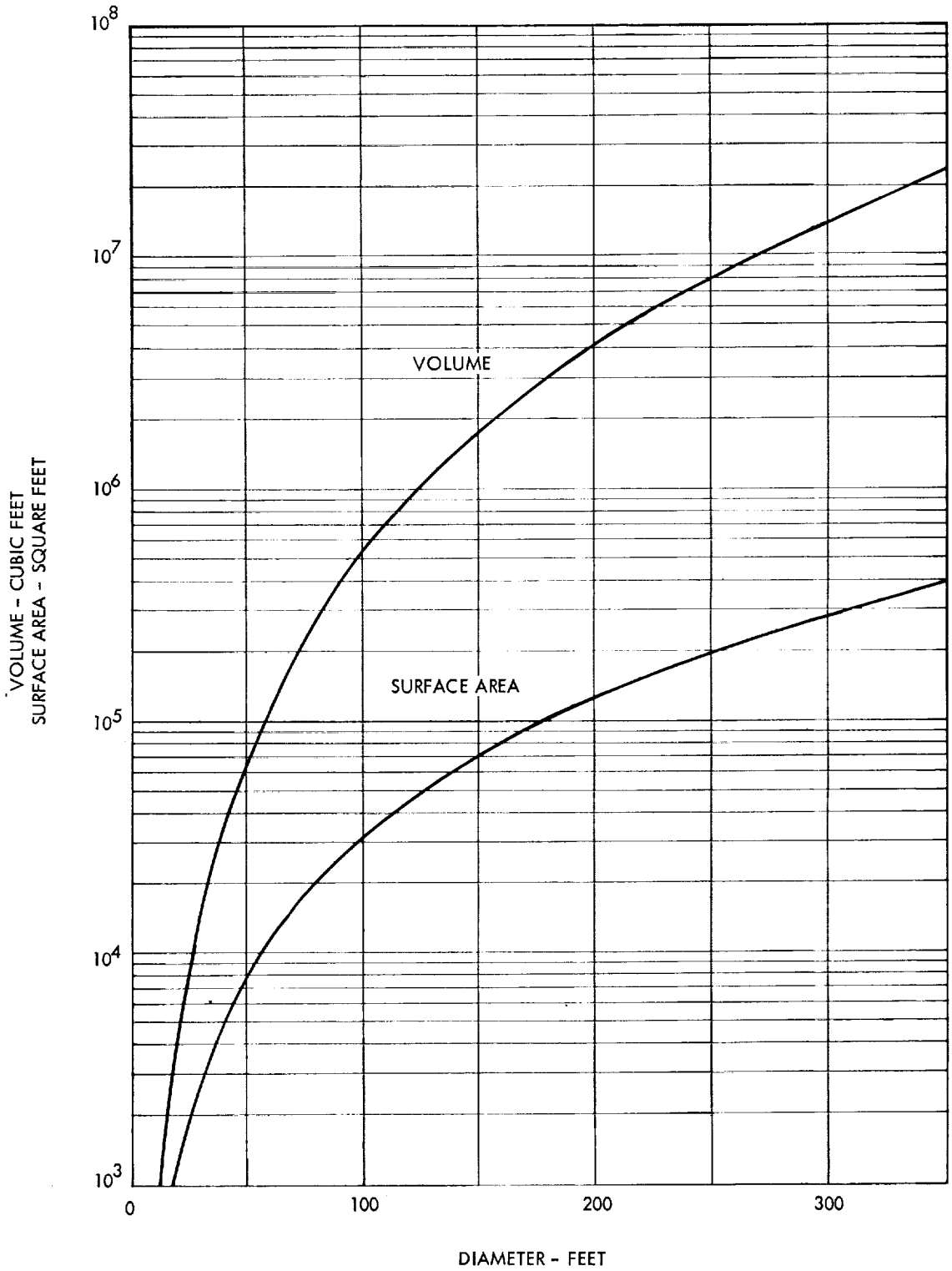

Figure 11. Volume and Surface Area of a Sphere

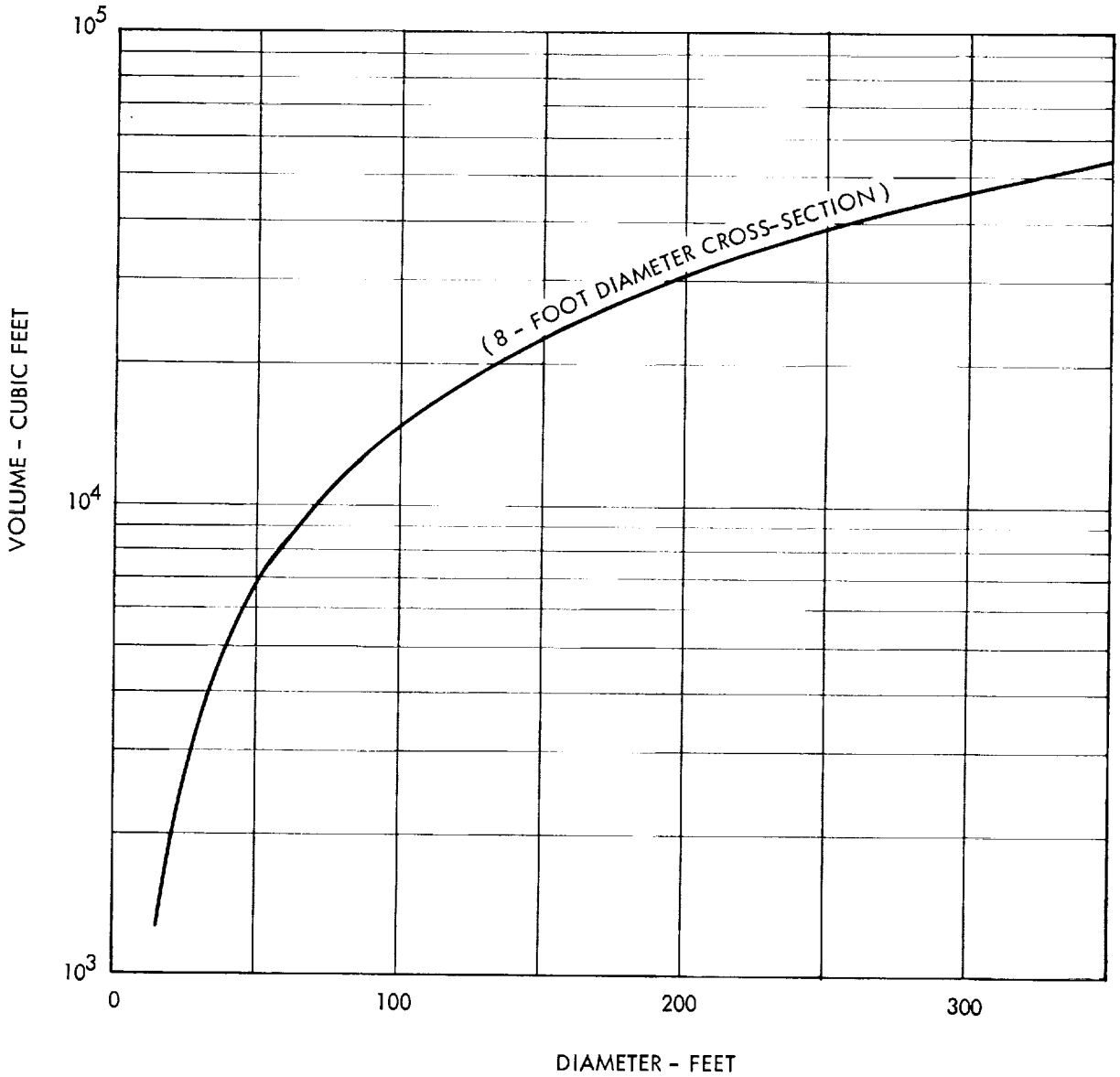

Figure 12. Volume of a Torus (8-Foot Diameter Cross-Section)

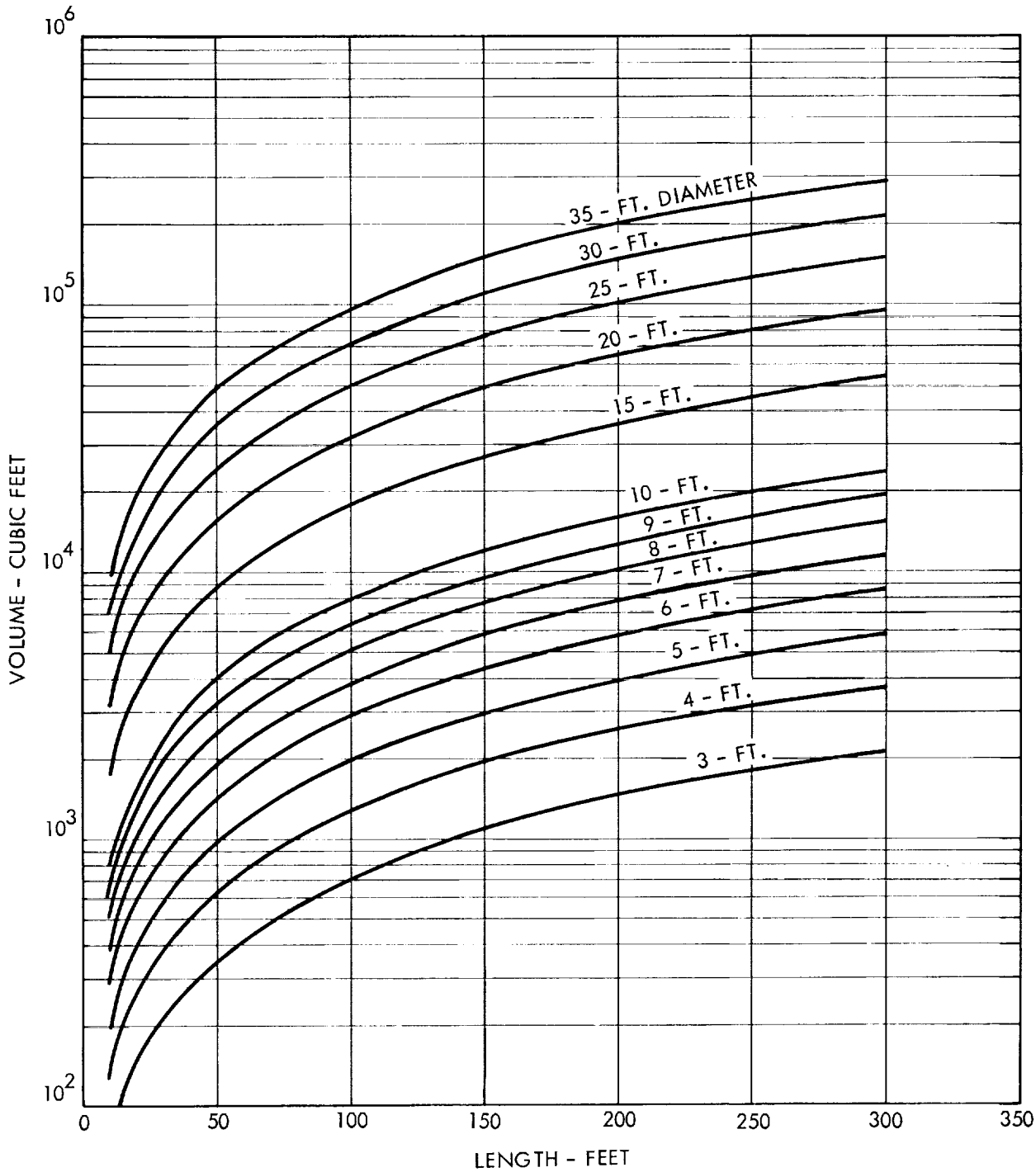

Figure 13. Volume of Cylinders of Various Lengths and Diameters

B. SECONDARY STRUCTURAL WEIGHT

Investigations of the pressurization system weight (W_{PS}) and the weight of partitions (W_P), which are two of the factors that make up the Secondary Structural Weight, were initiated, but not enough was accomplished at reporting time to warrant coverage in this report.

C. SUPPORTING STUDIES

In the area of supporting studies, a report on the "Structural Investigation of Torus-Cylinder Intersection" has been completed, and will be included in the next quarterly progress report. Other supporting studies will be included in subsequent quarterly progress reports as they are completed. Some of the studies being considered are:

1. Structural Instability Study
2. Dynamic Stability of Various Configurations
3. Dynamic Response of Space Stations to Docking Loads
4. Determination of Absolute Strength of Various Materials
5. Dynamics of Deployment
6. Development of Stress Analysis Methods for Joints, Cutouts, and Seams
7. Study the Propagation of Structural Failures Resulting from Small Holes or Tears
8. Reliability Factors in the Choice of Configuration and Method of Construction of Space Structures
9. Identification of Fruitful Areas for Additional or Accelerated Research and Development.
10. Thermal Coating Study
11. Meteoroid Protection (as it pertains to this study)
12. Internal Environment

SECTION IV - ANALYSIS OF RESULTS TO DATE

A. INTERPRETATION OF RESULTS

During the first quarter, considerable effort was expended in devising: (1) a plan of attack for the study, (2) a firm philosophy to follow, and (3) a detailed breakdown of the work. All these things have been accomplished, and all that now remains is to complete the work as planned.

One of the vital factors in this study is the degree of accuracy to which the strength-weight ratio of all materials being considered, can be determined for combined environmental conditions. Environmental test data is being compiled, but the quality and quantity has not yet been determined. As a back-up in case actual test data for combined environmental conditions prove inadequate, a theoretical method for determining the allowable stress of a material under combined environmental conditions is being studied. The method makes use of the cumulative damage theory which is also under consideration for determining material safety factors for time-dependent environmental conditions.

The coefficient C_1 in the basic weight equation,

$$W_B = \frac{C_1 Vnp}{k_1}$$

is determined from the shape of the structure and the manner in which the structural material is distributed (filament wound, constant thickness-variable stress, and variable thickness-constant stress). A study to determine how C_1 varies revealed that for all shapes, except the torus, C_1 varied from 1.5 to 3.0. The torus is a rather special case. For small major diameters its coefficient can vary from 2.0 to infinity, but for diameters of practical size the coefficient approaches 2.0 (refer to Table 2 and Section III-A-2).

B. RECOMMENDED ACTION

Several areas have been uncovered where it appears that test data is lacking, but recommended action will be withheld until the matter is studied in more detail.

C. SUCCESS IN MEETING OBJECTIVES

To conduct a general parametric study of space structures for orbital-type vehicles is a gigantic task if all types of orbital vehicles are to be considered to be in one class. The decision to consider each type of vehicle separately for this study is one that is bound to simplify the task considerably by breaking the task down into smaller, more manageable sections and is one that will result in more meaningful and useful results.

There is little doubt that a method can be established for evaluating orbital space structures, but the accuracy of the method will depend largely on the quality of the test data available. It is too early in the study to forecast the degree of success that can be expected in this area.

SECTION V - WORK TO BE ACCOMPLISHED NEXT QUARTER

During the second quarter of the study program, it is anticipated that the following work will be accomplished:

1. Continue to compile and analyze materials test data, in order to establish strength-weight ratios for the various classes of materials being considered for this program.
2. Continue to investigate the cumulative damage theory for possible use in determining safety factors, and strength-weight ratios of materials subjected to combined environmental conditions.
3. Determine the relative importance of the parameters affecting the weight and design of passive communication satellites, solar concentrators and antennas.
4. Establish the factors governing the structural instability of expandable shapes.
5. Investigate the factors governing the weight of partitions needed for expandable structures.
6. Determine the pressurization system weights for various types of vehicles of various shapes and sizes.
7. Establish weights of elastomeric and sealant materials required for various types of vehicles and different structural materials.
8. Determine the effect of seams on the weight of the structure.
9. Investigate the absolute strength of materials.

SECTION VI - REFERENCES

1. Schuerch, H., Space Structure Design with Composite Materials, American Rocket Society Paper No. 1096-60, presented at Structural Design of Space Vehicles Conference, Santa Barbara, California, April 6-8, 1960.

2. Marketos, J. D., Application of Expandable Structure to Space Station Configuration, Goodyear Aircraft Corporation, GER-9875, June, 1960.

3. Costakos, N. C. and Jorgenson, J. S., Stress Analysis of INFLATOPLANE Model GA-468, Goodyear Aircraft Corporation, GER-9861, 18 January 1961.

4. Jeppesen, N. L., and Topping, A. D., Proposal for Structural Evaluation of Expandable Structures for Space Applications, Goodyear Aircraft Corporation, GAP-1259, 12 February 1962.

5. Cross, W. B. and Fasnacht, D. P., Effects of High Vacuum and Temperature on Creep Strength of Coated and Uncoated Nylon Yarns, Goodyear Aircraft Corporation, GER-10153, 1 February 1961.

6. Topping, A. D., Structural Safety with Fabrics and Materials Exhibiting Creep-Rupture Characteristics, Goodyear Aircraft Corporation, GER 7974, 18 June 1957.

APPENDIX A

BASIC STRUCTURAL WEIGHT OF PRESSURE VESSELS IN THE FORM OF SURFACES OF REVOLUTION

A. GENERAL ANALYSIS.

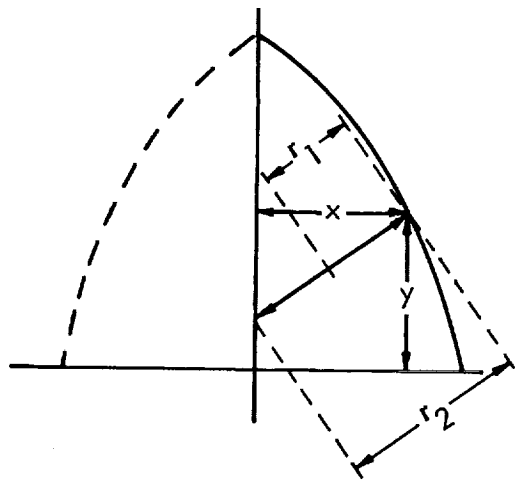

Figure A-1. Surface of Revolution

Figure A-1 shows the generating curve of a surface of revolution in rectangular coordinates, where r_1 and r_2 are the principal radii of curvature. It is assumed that the surface represents a membrane which is a part of a closed pressure vessel, the weight of which is to be determined in terms of the pressure, volume, and material properties. In the following analysis the weight is determined for the case in which the material thickness varies throughout the surface, depending on the larger of the two principal stresses at any point, and the case in which the material thickness is constant throughout the surface, depending on the maximum stress in the structure. In the cases in which the pressure vessel is formed by two or more different surfaces of revolution, as in the case of the cone and spherical segment, there is usually a discontinuity in the hoop stress at the juncture of two different surfaces. For these cases the weight equations are also developed assuming uniform

but different material thicknesses in each part of the structure in which there is a different equation for the meridian curve. In every case it is stipulated that the pressure stresses must be positive throughout the structure.

The equations for the principal pressure stresses in a surface of revolution are given below.

$$N_\phi = \frac{pr_2}{2} \tag{1}$$

$$N_\theta = pr_2 \left(\frac{2r_1 - r_2}{2r_1} \right) \tag{2}$$

In the case in which the thickness varies, (optimum sheet) the unit weight of the membrane is given by

$$w = \frac{nN}{k_1} \tag{3}$$

at any point, where N is the larger of N_ϕ or N_θ.

The area of an elemental ring is

$$dA = 2\pi x \sqrt{(dx)^2 + (dy)^2} \tag{4}$$

and the weight of an elemental ring is given by

$$dw = wdA = \frac{2nN\pi x}{k_1} \sqrt{(dx)^2 + (dy)^2} \quad . \tag{5}$$

For an optimum sheet structure,

$$W = \frac{2\pi n}{k_1} \int Nx \sqrt{(dx)^2 + (dy)^2} = \frac{2\pi n}{k_1} \int Nxds \tag{6}$$

where N at every point must be the larger of N_ϕ or N_θ.

For a uniform sheet structure,

$$w = \frac{nN_{max}}{k_1} \tag{7}$$

where N_{max} is the largest stress in the structure, and

$$W = wA = \frac{nN_{max}A}{k_1} \tag{8}$$

where A is the total surface area.

B. ELLIPSOIDS OF REVOLUTION

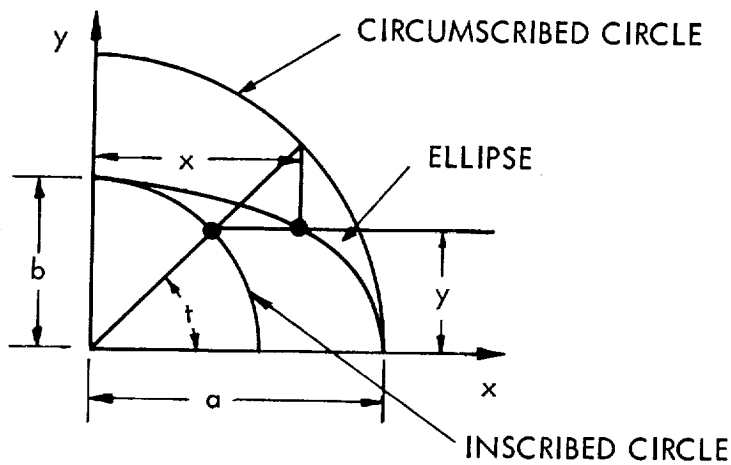

Figure A-2. Geometry of the Ellipse

The radii of curvature (see Figure A-2) are:

$$r_1 = \frac{(a^2\sin^2 t + b^2\cos^2 t)^{3/2}}{ab} \tag{9}$$

$$r_2 = \frac{a}{b}\sqrt{a^2\sin^2 t + b^2\cos^2 t}\ . \tag{10}$$

The coordinates are

$$x = a \cos t \tag{11}$$

$$y = b \sin t \tag{12}$$

and

$$dx = - a \sin t \, dt \tag{13}$$

$$dy = b \cos t \, dt \ . \tag{14}$$

The stresses are

$$N_\phi = \frac{pa}{2b} \sqrt{a^2 \sin^2 t + b^2 \cos^2 t} \tag{15}$$

$$N_\theta = \frac{pa}{2b} \sqrt{a^2 \sin^2 t + b^2 \cos^2 t} \left[2 - \frac{a^2}{(a^2 \sin^2 t + b^2 \cos^2 t)} \right] \ . \tag{16}$$

If $a > b$, the ellipsoid is an oblate spheroid, and N_ϕ is everywhere equal to or greater than N_θ. Substituting for N_ϕ, x, dx, and dy, Equation 6 becomes

$$W = \frac{2\pi n a^2 p}{k_1 b} \int_0^{\frac{\pi}{2}} \cos t \, (a^2 \sin^2 t + b^2 \cos^2 t) \, dt \ . \tag{17}$$

Integrating,

$$W = \frac{2\pi n p a^2}{k_1 b} \Bigg|_0^{\frac{\pi}{2}} \left[\frac{b^2 \sin t \, (\cos^2 t + 2)}{3} + \frac{a^2 \sin^3 t}{3} \right] \tag{18}$$

$$W = \frac{2\pi n p a^2 b}{k_1} \left(\frac{a^2 + 2b^2}{3b^2} \right) \ . \tag{19}$$

The volume is

$$V = (4/3)\pi a^2 b \ . \tag{20}$$

Substituting for $\pi a^2 b$, the weight of an optimum sheet structure is

$$W = \frac{pnV}{k_1} \left(\frac{a^2 + 2b^2}{2b^2} \right) \ . \tag{21}$$

The largest stress occurs when $t = 90^{o}$ and is equal to

$$N_{\phi max} = \frac{pa^2}{2b} . \tag{22}$$

The surface area of the oblate spheroid is

$$A = 2\pi a^2 + \frac{\pi b^2}{\sqrt{1 - b^2/a^2}} \ln \left[\frac{1 + \sqrt{1 - b^2/a^2}}{1 - \sqrt{1 - b^2/a^2}} \right] . \tag{23}$$

Substituting into Equation 8, the weight of a uniform sheet structure is

$$W = \frac{np\pi a^2 b}{2k_1} \left\{ \frac{2a^2}{b^2} + \frac{1}{\sqrt{1 - b^2/a^2}} \ln \left[\frac{1 + \sqrt{1 - b^2/a^2}}{1 - \sqrt{1 - b^2/a^2}} \right] \right\} \tag{24}$$

or

$$W = \frac{pnV}{k_1} \left\{ \frac{3}{8} \left[\frac{2a^2}{b^2} + \frac{1}{\sqrt{1 - b^2/a^2}} \ln \frac{1 + \sqrt{1 - b^2/a^2}}{1 - \sqrt{1 - b^2/a^2}} \right] \right\} . \tag{25}$$

If $b > a$, the ellipsoid is a prolate spheroid, and N_θ is everywhere equal to or greater than N_ϕ. Substituting for x, dx, dy, and N_θ, Equation 6 becomes

$$W = \frac{2\pi n a^2 p}{k_1 b} \int_0^{\pi/2} \cos t \, (a^2 \sin^2 t + b^2 \cos^2 t) \left[2 - \frac{a^2}{(a^2 \sin^2 t + b^2 \cos^2 t)} \right] dt . \tag{26}$$

The first integral of Equation 26 is the same as that of Equation 17, the solution of which is given by Equation 19. Substituting into Equation 26, the weight of an optimum sheet structure is

$$W = \frac{2\pi n p a^2 b}{k_1} \left[2 \frac{(a^2 + 2b^2)}{3b^2} - \frac{a^2}{b^2} \int_0^{\pi/2} \cos t \, dt \right]$$

or

$$W = \frac{2\pi n p a^2 b}{k_1} \left(\frac{4b^2 - a^2}{3b^2} \right) . \tag{27}$$

Substituting for $\pi a^2 b$,

$$W = \frac{pnV}{k_1} \left(\frac{4b^2 - a^2}{2b^2} \right) . \tag{28}$$

The largest stress occurs when t = 0 and is equal to

$$N_{\theta\,max} = \frac{pa}{2} \left(2 - \frac{a^2}{b^2} \right) . \tag{29}$$

The surface area of the prolate spheroid is

$$A = 2\pi a^2 + 2\pi ab \frac{\arcsin \sqrt{1 - a^2/b^2}}{\sqrt{1 - a^2/b^2}} . \tag{30}$$

Substituting into Equation 8, the weight of a uniform sheet structure is

$$W = \frac{np\pi a^2 b}{k_1} \left(2 - \frac{a^2}{b^2} \right) \left(\frac{a}{b} + \frac{\arcsin \sqrt{1 - a^2/b^2}}{\sqrt{1 - a^2/b^2}} \right) \tag{31}$$

or

$$W = \frac{pnV}{k_1} \left[\frac{3}{4} \left(2 - \frac{a^2}{b^2} \right) \left(\frac{a}{b} + \frac{\arcsin \sqrt{1 - a^2/b^2}}{\sqrt{1 - a^2/b^2}} \right) \right] . \tag{32}$$

Equations 21, 25, 28 and 32 can all be written in the form

$$W = \frac{C\,p\,n\,V}{k_1} . \tag{33}$$

In Figure A-3 Equations 21, 25, 28, and 32 are plotted for the range of the ratio a/b in which the pressure stresses are tensile.

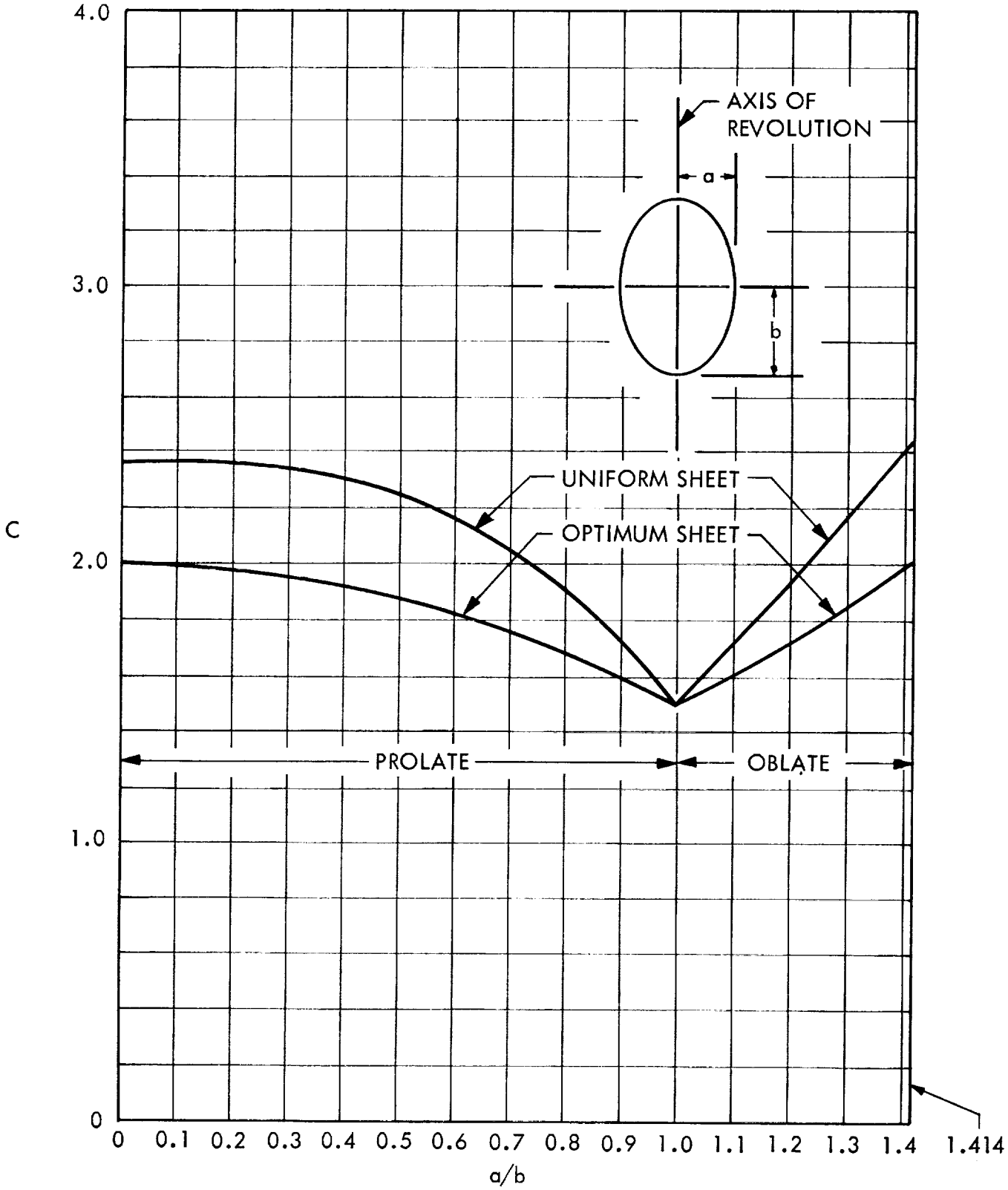

Figure A-3. Plot of Coefficient, C, for Ellipsoids of Revolution

C. PARABOLOID AND SPHERICAL SEGMENT

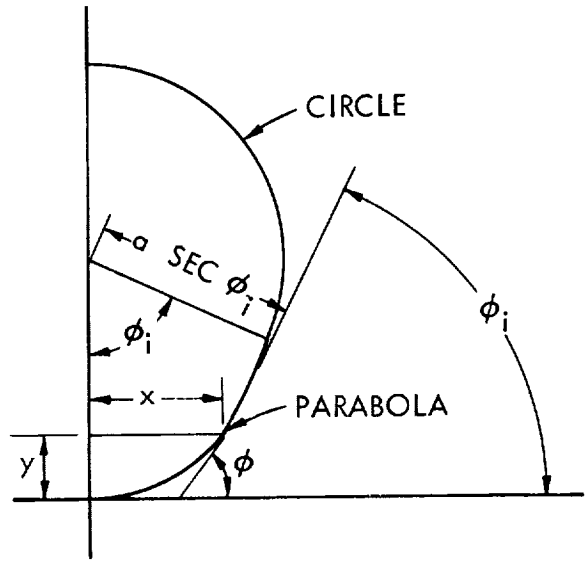

Figure A-4. Paraboloid and Spherical Segment Geometry

The parabola in Figure A-4 has the equation

$$y = \frac{x^2}{2a} \quad . \tag{34}$$

If the angle ϕ is defined such that

$$\tan \phi = \frac{dy}{dx} , \tag{35}$$

the radii of curvature are expressed as

$$r_1 = a \sec^3 \phi \tag{36}$$

$$r_2 = a \sec \phi \tag{37}$$

and the principal stresses are

$$N_\phi = \frac{pa}{2} \sec \phi \tag{38}$$

$$N_\theta = \frac{pa}{2} \sec \phi \, (2 - \cos^2 \phi) . \tag{39}$$

It is clear that N_θ is everywhere greater than N_ϕ. Substituting into Equation 6, the weight of the paraboloidal segment is found to be

$$W_p = p\pi a^3 n \, \frac{\sec^2 \phi_i}{2k_1} \, (\sec^2 \phi_i - 1) . \tag{40}$$

The volume of the paraboloid is equal to

$$V_p = \frac{\pi a^3 \tan^4\phi_i}{4} \tag{41}$$

and the surface area is given by

$$A_p = (2/3)\pi a^2(\sec^3 \phi_i - 1). \tag{42}$$

The largest value of N_θ occurs when $\phi = \phi_i$. In this case

$$N_{\theta\,max} = \frac{pa}{2} \sec \phi_i \,(2 - \cos^2 \phi_i). \tag{43}$$

If the paraboloid is made from a uniform sheet, the weight is obtained by substituting Equations 42 and 43 into Equation 8.

$$W_p = \frac{np\pi a^3}{3k_1} \sec \phi_i \,(2 - \cos^2 \phi_i)\,(\sec^3 \phi_i - 1) \tag{44}$$

The weight of the spherical segment is obtained from Equation 8 for either the optimum sheet case or the uniform sheet case. The surface area of the spherical segment is

$$A_S = 2\pi a^2 \sec \phi_i \,(1 + \sec \phi_i). \tag{45}$$

The stress everywhere in the spherical segment is equal to $\frac{p\,a \sec \phi_i}{2}$. Equation 8 gives

$$W_S = \frac{np\pi a^3 \sec^2 \phi_i}{k_1}(1 + \sec \phi_i) \tag{46}$$

for the optimum sheet case or for the case in which the spherical and paraboloidal segments have uniform but not equal thicknesses. If there is uniform thickness throughout the pressure vessel, the spherical segment weight is obtained by substituting Equations 43 and 45 into Equation 8.

$$W_S = \frac{np\pi a^3}{k_1} \sec^2 \phi_i \,(1 + \sec \phi_i)\,(2 - \cos^2 \phi_i). \tag{47}$$

The volume of the spherical segment is

$$V_S = \frac{\pi a^3}{3} \,(1 + \sec \phi)^2\,(2 \sec \phi - 1). \tag{48}$$

For the optimum sheet case the total weight is obtained by adding Equations 40 and 46

$$W = \frac{np\pi a^3 \sec^2 \phi_i (\sec \phi_i + 1)^2}{2k_1} . \tag{49}$$

The total volume of the structure is obtained by adding Equations 41 and 48

$$V = \pi a^3 \left[\frac{\tan^4 \phi_i}{4} + \frac{(1 + \sec \phi_i)^2 (2 \sec \phi_i - 1)}{3} \right] . \tag{50}$$

Equations 49 and 50 give

$$W = \frac{pnV}{k_1} \left[\frac{\sec^2 \phi_i (\sec \phi_i + 1)^2}{2 \left\{ \frac{\tan^4 \phi_i}{4} + \frac{(1 + \sec \phi_i)^2 (2 \sec \phi_i - 1)}{3} \right\}} \right] \tag{51}$$

For the case in which the paraboloid and spherical segments have uniform but not equal thicknesses, the weight is obtained by adding Equations 44 and 46.

$$W = \frac{np\pi a^3}{k_1} \left[\sec^2 \phi_i (1 + \sec \phi_i) + \sec \phi_i (2 - \cos^2 \phi_i) \frac{(\sec^3 \phi_i - 1)}{3} \right] \tag{52}$$

Equations 50 and 52 give

$$W = \frac{pnV}{k_1} \left[\frac{\sec^2 \phi_i (1 + \sec \phi_i) + \sec \phi_i (2 - \cos^2 \phi_i) \frac{(\sec^3 \phi_i - 1)}{3}}{\frac{\tan^4 \phi_i}{4} + \frac{(1 + \sec \phi_i)^2 (2 \sec \phi_i - 1)}{3}} \right] . \tag{53}$$

For the case in which the thickness is uniform throughout the structure, the weight is obtained by adding Equations 44 and 47:

$$W = \frac{np\pi a^3 \sec \phi_i (2 - \cos^2 \phi_i)}{k_1} \left[\frac{\sec^3 \phi_i - 1}{3} + \sec \phi_i (1 + \sec \phi_i) \right] . \tag{54}$$

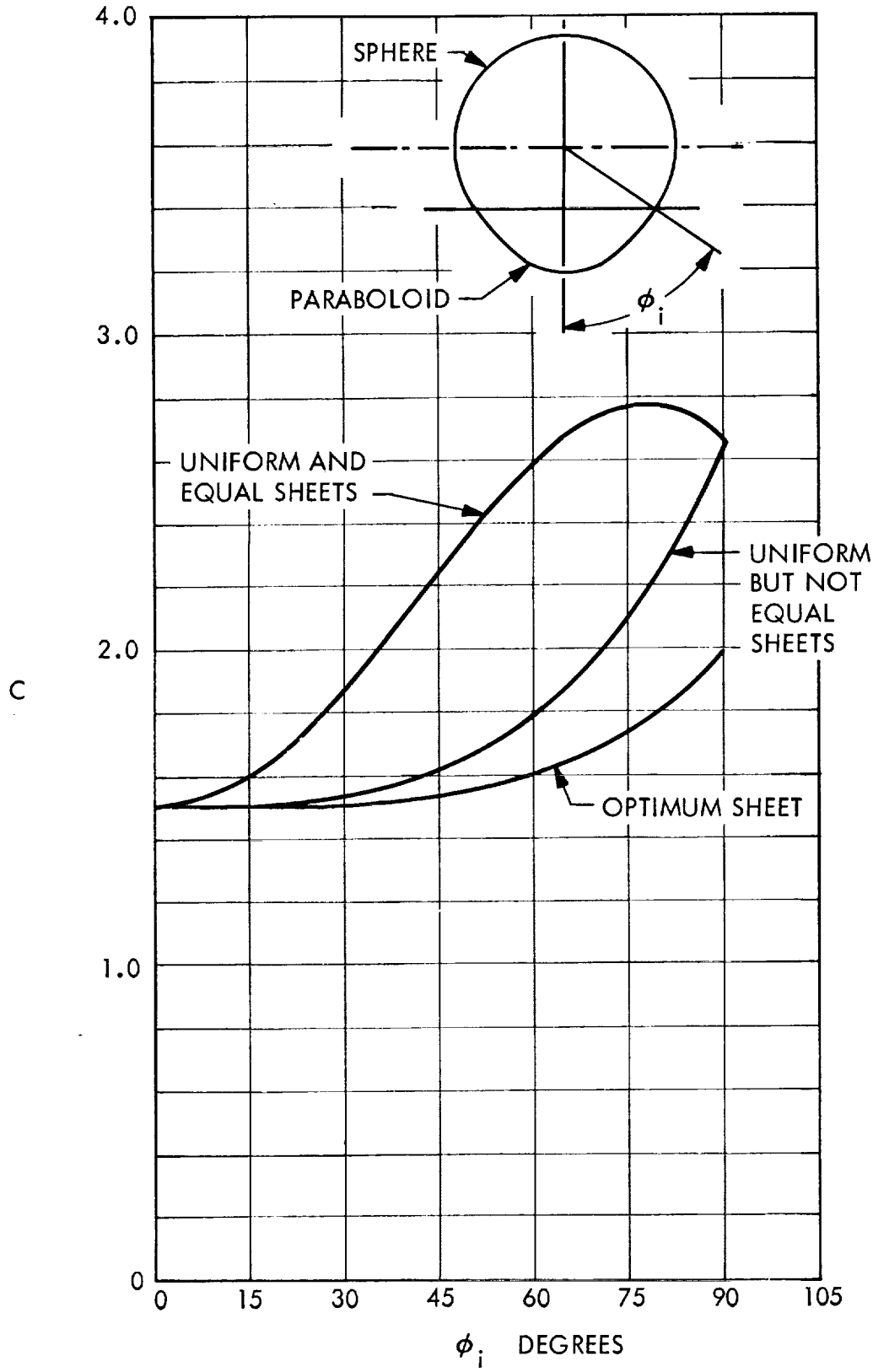

Figure A-5. Plot of Coefficient, C, for Paraboloid and Spherical Segment

Equations 50 and 54 give

$$W = \frac{pnV}{k_1} \left\{ \frac{\sec \phi_i \, (2 - \cos^2 \phi_i) \left[\frac{(\sec^3 \phi_i - 1)}{3} + \sec \phi_i \, (1 + \sec \phi_i) \right]}{\frac{\tan^4 \phi_i}{4} + \frac{(1 + \sec \phi_i)^2 \, (2 \sec \phi_i - 1)}{3}} \right\} \tag{55}$$

Equations 51, 53, and 55 are all of the form of Equation 33. In Figure A-5 the coefficient, C, is plotted as a function of ϕ_i.

D. CIRCULAR TORUS

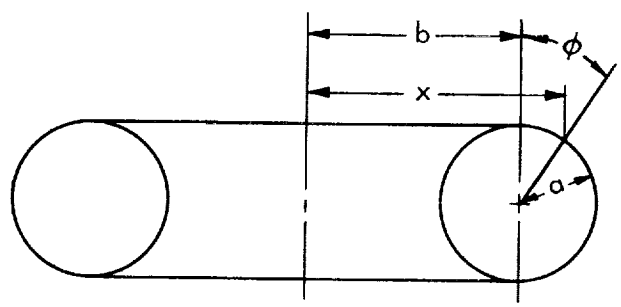

Figure A-6. Circular Torus Geometry

The principal pressure stresses in a circular torus (see Figure A-6) are:

$$N_\phi = \frac{pa}{2} \left(\frac{x + b}{x} \right) \tag{56}$$

$$N_\theta = \frac{pa}{2} \, . \tag{57}$$

The stress, N_ϕ, is always larger than N_θ. Substituting into Equation 6,

$$W = \frac{2\pi n}{k_1} \int \frac{pa}{2} \left(\frac{x + b}{x} \right) ds.$$

Substituting $ds = a \, d\phi$ and $x = b + a \sin \phi$,

$$W = \frac{4np\pi^2 a^2 b}{k_1} \, . \tag{58}$$

The volume of the torus is

$$V = 2\pi^2 a^2 b \tag{59}$$

Equations 58 and 59 give

$$W = \frac{pnV}{k_1} \quad [2] \tag{60}$$

for the optimum sheet case.

The maximum value of N_ϕ is $\frac{pa}{2}\left(\frac{2b-a}{b-a}\right)$. The area of the torus is

$$A = 4\pi^2 ab\,. \tag{61}$$

Substituting into Equation 8,

$$W = \frac{2np\pi^2 a^2 b}{k_1}\left(\frac{2b - a}{b - a}\right). \tag{62}$$

Equations 59 and 62 give

$$W = \frac{pnV}{k_1}\left(\frac{2b - a}{b - a}\right) \tag{63}$$

for the uniform sheet case.

In Figure A-7 the coefficient, C, is plotted for toroidal pressure vessels.

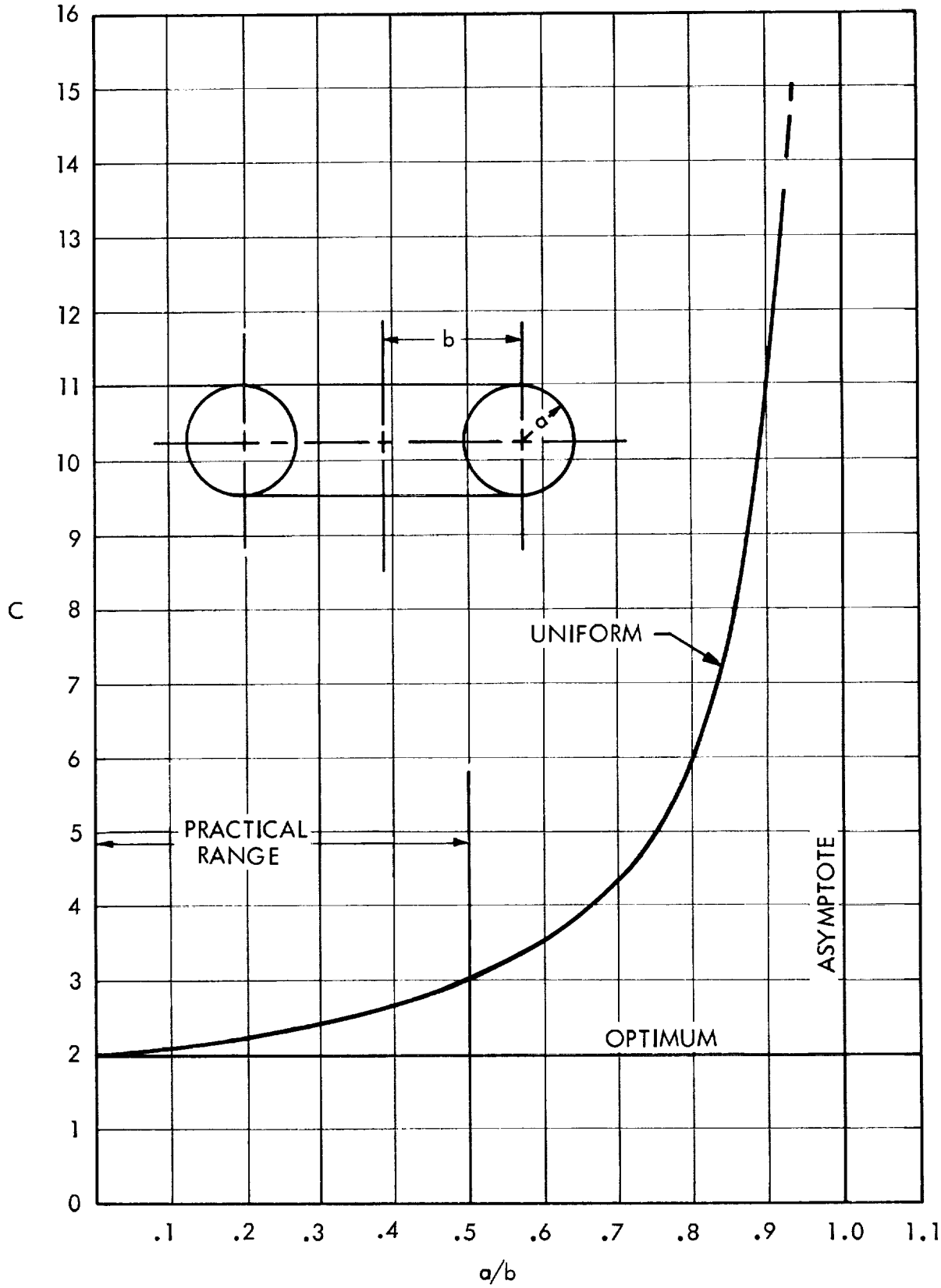

Figure A-7. Plot of Coefficient, C, for Toroidal Pressure Vessel

E. CONE AND SPHERICAL SEGMENT

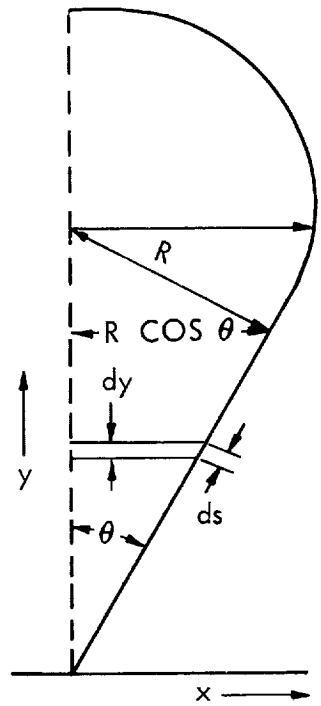

Figure A-8. Cone and Spherical Segment Geometry

The equation of the straight line (see Figure A-8) is:

$$y = \frac{x}{\tan\theta} \tag{64}$$

and

$$dy = \frac{dx}{\tan\theta} \tag{65}$$

The area of an elemental ring is:

$$dA = 2\pi x ds = 2\pi x \sqrt{1 + \left(\frac{dy}{dx}\right)^2}\, dx$$

or

$$dA = \frac{2\pi x dx}{\sin\theta} \tag{66}$$

The stresses in the cone are:

$$N_\phi = \frac{px}{2\cos\theta} \tag{67}$$

$$N_\theta = \frac{px}{\cos\theta} \tag{68}$$

N_θ is everywhere greater than N_ϕ. Substituting Equations 66 and 68 into 6 and integrating,

$$W_c = \int_0^{R\cos\theta} \frac{2\pi npx^2 dx}{k_1 \sin\theta \cos\theta} = \frac{2\pi npR^3 \cos^2\theta}{3k_1 \sin\theta} \tag{69}$$

for the optimum sheet case.

The surface area of the cone is equal to:

$$A_c = \frac{\pi R^2 \cos^2\theta}{\sin\theta} \tag{70}$$

The maximum value of N_θ is:

$$N_{\theta max} = pR \tag{71}$$

and the uniform sheet case weight is given by substituting Equations 70 and 71 into Equation 8:

$$W_c = \frac{np\pi R^3 \cos^2\theta}{k_1 \sin\theta} \quad . \tag{72}$$

The weight of the spherical segment can be obtained for the optimum sheet case or for the case in which the spherical and conical segments have uniform but not equal thicknesses by substituting $\theta = \pi/2 - \phi_i$ and $R = a \sec \phi_i$ into Equation 46. Thus

$$W_S = \frac{np\pi R^3 (1 + \sin\theta)}{k_1} \quad . \tag{73}$$

If there is uniform thickness throughout the structure, the spherical segment is designed for stress $N_{\theta\,max}$ given by Equation 71, instead of $N_\theta = N_\phi = \frac{pR}{2}$. In this case the value of W_S is twice that given by Equation 73. Thus:

$$W_S = \frac{2np\pi R^3 (1 + \sin\theta)}{k_1} \quad . \tag{74}$$

For the optimum sheet case the total weight is obtained by adding Equations 69 and 73:

$$W = \frac{np\pi R^3}{k_1} \left(\frac{2}{3} \frac{\cos^2\theta}{\sin\theta} + 1 + \sin\theta \right) \tag{75}$$

For the case in which the thicknesses in the two segments are uniform but not equal, the weight is obtained by adding Equations 72 and 73:

$$W = \frac{np\pi R^3}{k_1}\left(\frac{\cos^2\theta}{\sin\theta} + 1 + \sin\theta\right) . \tag{76}$$

For the uniform sheet case, the weight is obtained by adding Equations 72 and 74:

$$W = \frac{np\pi R^3}{k_1}\left(\frac{\cos^2\theta}{\sin\theta} + 2 + 2\sin\theta\right) \tag{77}$$

The total volume is equal to

$$V = \pi R^3\left[\frac{\cos^4\theta}{3\sin\theta} + (1+\sin\theta)^2\left(2/3 - \frac{\sin\theta}{3}\right)\right] \tag{78}$$

Writing Equations 75, 76, and 77, respectively, in terms of V,

$$W = \frac{pnV}{k_1}\left[\frac{\frac{2\cos^2\theta}{3\sin\theta} + 1 + \sin\theta}{\frac{\cos^4\theta}{3\sin\theta} + (1+\sin\theta)^2\left(2/3 - \frac{\sin\theta}{3}\right)}\right] \text{(optimum sheet)} \tag{79}$$

$$W = \frac{pnV}{k_1}\left[\frac{\frac{\cos^2\theta}{\sin\theta} + 1 + \sin\theta}{\frac{\cos^4\theta}{3\sin\theta} + \left(1+\sin\theta\right)^2\left(2/3 - \frac{\sin\theta}{3}\right)}\right] \text{(uniform but not equal sheets)} \tag{80}$$

$$W = \frac{pnV}{k_1}(3) \quad \text{(uniform and equal sheets).} \tag{81}$$

Equation 79, 80, and 81 are plotted as a function of θ in Figure A-9.

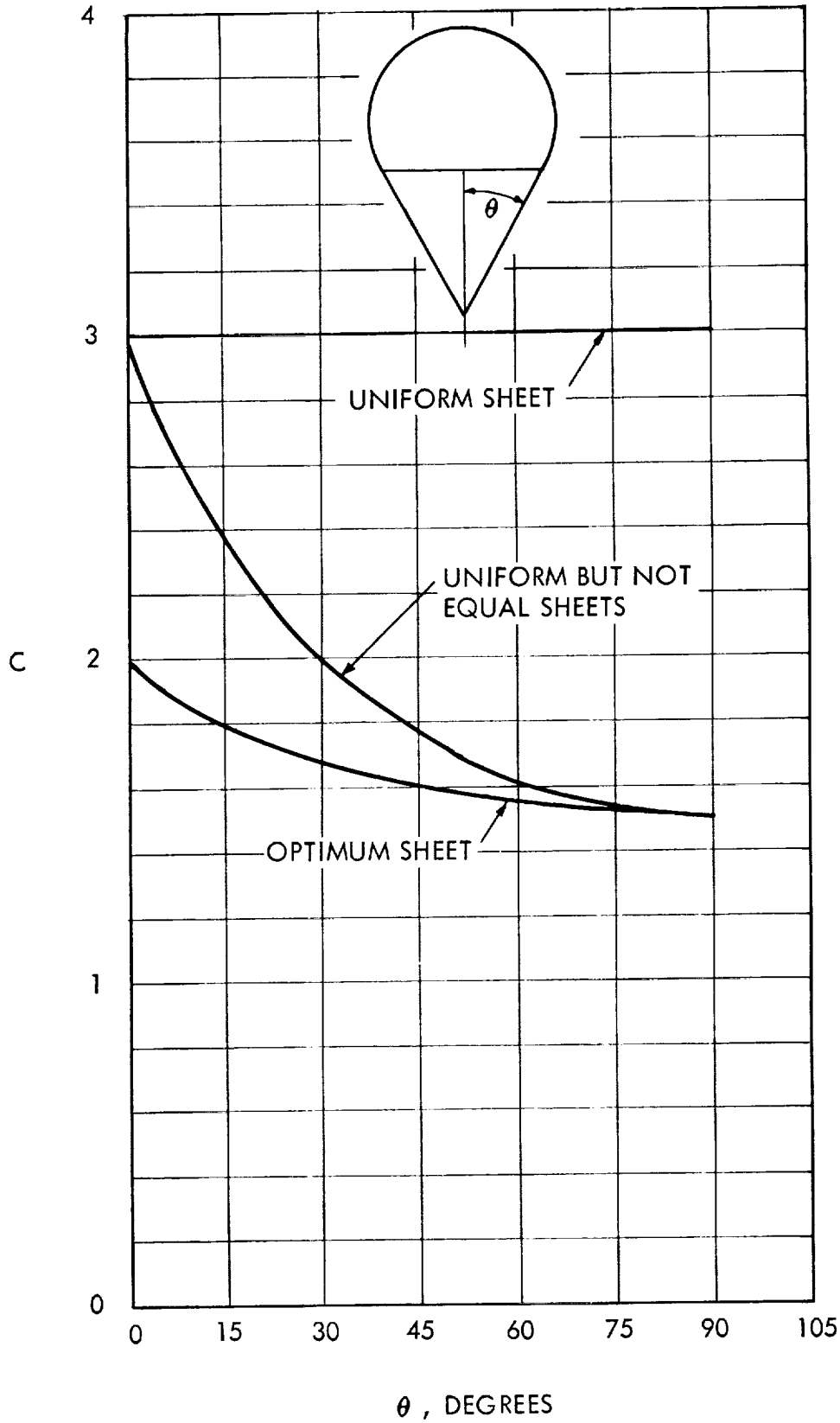

Figure A-9. Plot of Coefficient, C, for Cone and Spherical Segment Pressure Vessel

F. CYLINDER WITH HEMISPHERICAL ENDS

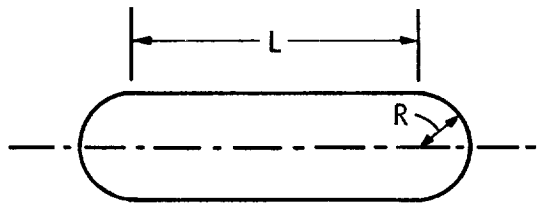

Figure A-10. Cylinder

The stresses in the cylinder (see Figure A-10) are:

$$N_\phi = \frac{pR}{2} \tag{82}$$

$$N_\theta = pR \tag{83}$$

The surface area of the cylinder is:

$$A_{CYL} = 2\pi RL \tag{84}$$

Equation 8 gives the cylinder weight for both the optimum and uniform sheet cases:

$$W_{CYL} = \frac{2np\pi R^2 L}{k_1} \tag{85}$$

The surface area of the spherical ends is

$$A_S = 4\pi R^2 \tag{86}$$

The stress in the sphere is everywhere equal to pR/2. If the sphere and cylinder sheets are not the same thickness, the weight of the spherical ends is:

$$W_S = \frac{2np\pi R^3}{k_1} \tag{87}$$

If the sphere is made from the same sheet as the cylinder, its weight is:

$$W_S = \frac{4np\pi R^3}{k_1} \tag{88}$$

For unequal thickness sheets the total weight is obtained by adding Equations 85 and 87:

$$W = \frac{2np\pi R^3}{k_1} (1 + L/R) \tag{89}$$

and if the cylinder and ends are all the same thickness sheet, the weight is obtained by adding equations 85 and 88:

$$W = \frac{2np\pi R^3}{k_1} (2 + L/R) \tag{90}$$

The total volume is:

$$V = 4/3\pi R^3 + \pi R^2 L = \pi R^3 (4/3 + L/R) \tag{91}$$

Writing Equations 89 and 90 in terms of V,

$$W = \frac{pnV}{k_1} \left[\frac{2(1 + L/R)}{4/3 + L/R} \right] \quad \text{(unequal thickness and optimum)} \tag{92}$$

and

$$W = \frac{pnV}{k_1} \left[\frac{2(2 + L/R)}{4/3 + L/R} \right] \quad \text{(equal thickness)} \tag{93}$$

G. SPHERE

The weight of the sphere is given by Equation 87 and the volume by the first term of equation 91. Thus

$$W = \frac{pnV}{k_1} \left[\frac{3}{2} \right] \tag{94}$$

H. SUMMARY OF BASIC STRUCTURAL WEIGHT ANALYSIS

In Figures A-3, A-5, A-7, and A-9, the coefficient C in the general expression for basic structural weight is plotted for some of the more involved cases. Each of these expressions, although complex, contains only one variable. The curves therefore eliminate the need for any computation to obtain the values of the coefficient. For ease of comparison, the expressions for C for all of the structures analyzed are also summarized in Table A-1.

Table A-1. Coefficient, C, in the Basic Weight Equation, $W = \frac{CnpV}{k_1}$

Configuration	Optimum Sheet	Uniform But Not Equal Sheets	Uniform and Equal Sheets
Sphere	3/2 (Derived from Equation 94.)	Does Not Apply	3/2 (Derived from Equation 94.)
Cylinder With Hemispherical Ends	$\frac{2\,(1 + L/R)}{4/3 + L/R}$ (Derived from Equation 92.)	$\frac{2\,(1 + L/R)}{4/3 + L/R}$ (Derived from Equation 92.)	$\frac{2\,(2 + L/R)}{4/3 + L/R}$ (Derived from Equation 93.)
Circular Torus	2 (Derived from Equation 60.)	Does Not Apply	$\frac{2b - a}{b - a}$ (Derived from Equation 63.)
Cone With Spherical Segment	$\frac{2/3\,\frac{\cos^2\theta}{\sin\theta} + 1 + \sin\theta}{\frac{\cos^4\theta}{3\sin\theta} + (1 + \sin\theta)^2\left(2/3 - \frac{\sin\theta}{3}\right)}$ (Derived from Equation 79.)	$\frac{\frac{\cos^2\theta}{\sin\theta} + 1 + \sin\theta}{\frac{\cos^4\theta}{3\sin\theta} + (1 + \sin\theta)^2\left(2/3 - \frac{\sin\theta}{3}\right)}$ (Derived from Equation 80.)	3 (Derived from Equation 81.)
Paraboloid With Spherical Segment	$\frac{\sec^2\phi_i\,(\sec\phi_i + 1)^2}{2\left[\frac{\tan^4\phi_i}{4} + \frac{(1 + \sec\phi_i)^2\,(2\sec\phi_i - 1)}{3}\right]}$ (Derived from Equation 51.)	$\frac{\sec^2\phi_i(1 + \sec\phi_i) + \sec\phi_i\,(2 - \cos^2\phi_i)\left(\frac{(\sec^3\phi_i - 1)}{3}\right)}{\frac{\tan^4\phi_i}{4} + \frac{(1 + \sec\phi_i)^2\,(\sec\phi_i - 1)}{3}}$ (Derived from Equation 53.)	$\frac{\sec\phi_i\,(2 - \cos^2\phi_i)\left[\frac{\sec^3\phi_i - 1}{3} + \sec\phi_i(1 + \sec\phi_i)\right]}{\frac{\tan^4\phi_i}{4} + \frac{(1 + \sec\phi_i)^2\,(2\sec\phi_i - 1)}{3}}$ (Derived from Equation 55.)
Prolate Spheroid	$\frac{4b^2 - a^2}{2b^2}$ (Derived from Equation 28.)	Does Not Apply	$3/4\left(2 - \frac{a^2}{b^2}\right)\left(\frac{a}{b} + \frac{\arcsin\sqrt{1 - a^2/b^2}}{\sqrt{1 - a^2/b^2}}\right)$ (Derived from Equation 32.)
Oblate Spheroid	$\frac{a^2 + 2b^2}{2b^2}$ (Derived from Equation 21.)	Does Not Apply	$\frac{3}{8}\left\{\frac{2a^2}{b^2} + \frac{1}{\sqrt{1 - b^2/a^2}}\ln\left[\frac{1 + \sqrt{1 - b^2/a^2}}{1 - \sqrt{1 - b^2/a^2}}\right]\right\}$ (Derived from Equation 25.)

APPENDIX B

ULTIMATE TENSILE STRENGTH-TO-WEIGHT RATIO AT STANDARD ATMOSPHERE AND ROOM TEMPERATURE

A. GENERAL

The strengths used in this appendix are quick-break strengths for those materials that exhibit creep-rupture. The strength-weight ratios given in Table B-1 are for the structural material only (yarn only, not yarn and coating) in the direction of fiber length or as indicated.

B. REFERENCES

1. Lynch, C. T., Wahldick, F. W., Robinson, L. B., Growth and Analysis of Alumina "Whiskers," ASD-TDR-62-272, May 1962.
2. Hodgman, C. D., Ed., Handbook of Chemistry and Physics, 31 Ed, Chemical Rubber Publishing Co., 2310 Superior Ave. N. E., Cleveland, Ohio.
3. Modern Plastics Encyclopedia Issue, 1960; pgs 626 to 680.
4. Textile Fiber Materials for Industry, Owens-Corning Fiberglas.
5. Textile World's Man-Made Fiber Table - 1959 Revision, Compiled by the editors of Textile World, McGraw Hill Publishing Co.
6. Clay, W. R., and Long, W. C., Physical and Chemical Properties of HT-1, E. I. duPont de Nemours & Co., Inc., Textile Fibers Department, Textile Research Laboratory, Wilmington, Delaware, May, 1961.
7. Pfannmuller, J. H., Final Technical Report Avco Drag Brake - Phase I Fabric Structure Design Study and Material Evaluation, Goodyear Aircraft Corporation, Akron, Ohio, GER-9863, 15 July 1960.
8. The Technical Editor Speaks, Revised Edition 1951, Copyright, 1951 - The International Nickel Company, Inc., New York, N. Y. p33.
9. Goodyear Specifications for Fabrics & Cloths, Drawing Number 59QS889.

Table B-1
Ultimate Tensile Strength-To-Weight Ratio at Standard Atmosphere and Room Temperature

Material Class	Material	Ultimate Tensile Strength (lb/sq in.)	Density (lb/cubic in.)	Ultimate Tensile Strength-to-Weight Ratio (in.)	Reference
Whisker	Iron	1,900,000	28.4×10^{-2}	6.69×10^{6}	1,2
	Copper	400,000	32.2×10^{-2}	1.243×10^{6}	1,2
	Gold	230,000	69.7×10^{-2}	3.30×10^{5}	1,2
	Silicone	550,000	8.66×10^{-2}	6.35×10^{6}	1,2
	Sodium Chloride	160,000	7.81×10^{-2}	2.05×10^{6}	1,2
	Aluminum Oxide	1,800,000	12.63×10^{-2} To 14.07×10^{-2}	1.425×10^{7} To 1.28×10^{7}	1,2
	Graphite	3,000,000	6.50×10^{-2} To 7.58×10^{-2}	4.62×10^{7} To 3.96×10^{7}	1,2
Film	Acrylonitrile Styrene Copolymer	10,000 to 15,000	3.93×10^{-2}	2.55×10^{5} To 3.82×10^{5}	3
	Cellulose Acetate	5,400 to 13,900	4.73×10^{-2}	1.143×10^{5} To 2.94×10^{5}	3
	Cellulose Triacetate	9,000 To 16,000	4.73×10^{-2}	1.903×10^{5} To 3.38×10^{5}	3
	Cellulose Acetate Butyrate	4,100 To 9,700	4.41×10^{-2}	9.30×10^{4} To 2.20×10^{5}	3
	Cellulose Nitrate	10,000 To 11,000	5.27×10^{-2}	1.897×10^{5} To 2.09×10^{5}	3
	Ethyl Cellulose	6,800 To 10,600	4.18×10^{-2}	1.627×10^{5} To 2.54×10^{5}	3
	Methyl Cellulose	4,200 To 9,700	4.44×10^{-2}	9.47×10^{4} To 2.18×10^{5}	3
	Polyamide (Nylon)	9,000	4.12×10^{-2}	2.18×10^{5}	3
	Polytrifluorochloroethylene	6,300 To 6,600	7.95×10^{-2}	7.93×10^{4} To 8.30×10^{4}	3
	Polymethyl Methacrylate	8,200 To 8,800	4.30×10^{-2}	1.907×10^{5} To 2.05×10^{5}	3
	Polyethylene (Low Density)	1,350 To 2,500	3.34×10^{-2}	4.04×10^{4} To 7.49×10^{4}	3

GOODYEAR AIRCRAFT

Table B-1

Ultimate Tensile Strength-To-Weight Ratio at Standard Atmosphere and Room Temperature (Cont)

Material Class	Material	Ultimate Tensile Strength (lb/sq in.)	Density (lb/cubic in.)	Ultimate Tensile Strength-to-Weight Ratio (in.)	Reference
Film (cont)	Polyethylene (Medium Density)	2,000 To 3,500	3.39×10^{-2}	5.90×10^{4} To 1.033×10^{5}	3
	Polyethylene (High Density)	2,400 To 6,100	3.49×10^{-2}	6.88×10^{4} To 1.749×10^{5}	3
	Polypropylene	4,500 To 10,000	3.25×10^{-2}	1.383×10^{5} To 3.08×10^{5}	3
	Polyester (Mylar)	17,000 To 23,700	5.02×10^{-2}	3.39×10^{5} To 4.72×10^{5}	3
	Linear Co-Polyester	8,500	4.84×10^{-2}	1.755×10^{5}	3
	Polytetrafluoroethylene	1,500 To 4,000	7.95×10^{-2}	1.888×10^{4} To 5.03×10^{4}	3
	Polystyrene (Extrusion)	7,100 To 12,100	3.83×10^{-2}	1.854×10^{5} To 3.16×10^{5}	3
	Polystyrene (Oriented)	8,000 To 12,000	3.83×10^{-2}	2.09×10^{5} To 3.13×10^{5}	3
	Polyvinyl Alcohol	4,000 To 10,000	4.73×10^{-2}	8.46×10^{4} To 2.11×10^{5}	3
	Polyvinyl Chloride (Nonrigid)	1,400 To 5,600	5.24×10^{-2}	2.67×10^{4} To 1.068×10^{5}	3
	Vinyl Chloride-Acetate Copolymers (Nonrigid)	2,000 To 4,500	4.87×10^{-2}	3.41×10^{4} To 9.23×10^{4}	3
	Vinylidene Chloride-Vinyl Chloride Copolymer	8,000 To 20,000	6.07×10^{-2}	1.318×10^{5} To 3.29×10^{5}	3
	Regenerated Cellulose (Cellophane)	7,000 To 15,000	5.42×10^{-2}	1.29×10^{5} To 2.77×10^{5}	3
	Rubber Hydrochloride	3,500 To 5,000	4.01×10^{-2}	8.73×10^{4} To 1.248×10^{5}	3
	Vinylnitrile Rubber	2,500 To 4,000	4.33×10^{-2}	5.77×10^{4} To 9.23×10^{4}	3

GOODYEAR AIRCRAFT

Table B-1
Ultimate Tensile Strength-To-Weight Ratio at Standard Atmosphere and Room Temperature (Cont)

Material Class	Material	Ultimate Tensile Strength (lb/sq in.)	Density (lb/cubic in.)	Ultimate Tensile Strength-to-Weight Ratio (in.)	Reference
Yarn	Fiberglas-ECD-1800-1/0-1.0Z		9.17×10^{-2}	1.905×10^{6}	4, 5
	Fiberglas-ECD-1800 1/0-5.0Z		9.17×10^{-2}	1.905×10^{6}	4, 5
	Fiberglas-ECD-450 1/0-10.0Z		9.17×10^{-2}	2.07×10^{6}	4, 5
	Fiberglas-ECD-900 1/3-8.5S		9.17×10^{-2}	1.905×10^{6}	4, 5
	Fiberglas-ECD-450 4/0-5.0Z		9.17×10^{-2}	2.06×10^{6}	4, 5
	Fiberglas-ECE-225 1/2-4.4S		9.17×10^{-2}	1.905×10^{6}	4, 5
	Fiberglas-ECE-55 1/0-1.0Z		9.17×10^{-2}	1.61×10^{6}	4, 5
	Fiberglas-ECD-450 3/3-4.4S		9.17×10^{-2}	2.06×10^{6}	4, 5
	Fiberglas-ECG-150 1/3-3.8S		9.17×10^{-2}	1.692×10^{6}	4, 5
	Fiberglas-ECG-450 4/3-4.4S		9.17×10^{-2}	2.06×10^{6}	4, 5
	Fiberglas-ECK-75 1/2-3.8S		9.17×10^{-2}	1.507×10^{6}	4, 5
	Fiberglas-ECK-75 3/0-4.0Z		9.17×10^{-2}	1.507×10^{6}	4, 5
	Fiberglas-ECG-150 4/8-3.5S		9.17×10^{-2}	1.692×10^{6}	4, 5
	Fiberglas-ECG-150 4/18		9.17×10^{-2}	1.692×10^{6}	4, 5
Yarn	Fortisan (Regular)	136,000	5.41×10^{-2}	2.51×10^{6}	5
	Fortisan -36	> 155,000	5.41×10^{-2}	2.86×10^{6}	5
	Nylon 6, 6 (Regular)	67,000 To 86,000	4.12×10^{-2}	1.625×10^{6} To 2.09×10^{6}	5
	Nylon 6, 6 (High Tenacity)	86,000 To 134,000	4.12×10^{-2}	2.09×10^{6} To 3.25×10^{6}	5
	Nylon 6 (Regular)	73,000 To 84,000	4.12×10^{-2}	1.772×10^{6} To 2.04×10^{6}	5
	Nylon 6 (High Tenacity)	109,000 To 125,000	4.12×10^{-2}	2.65×10^{6} To 3.03×10^{6}	5
	Dacron (Regular)	77,000 To 88,000	4.98×10^{-2}	1.546×10^{6} To 1.768×10^{6}	5
	Dacron (High Tenacity)	111,000 To 138,000	4.98×10^{-2}	2.23×10^{6} To 2.77×10^{6}	5

GOODYEAR AIRCRAFT

Table B-1
Ultimate Tensile Strength-To-Weight Ratio at Standard Atmosphere and Room Temperature (Cont)

Material Class	Material	Ultimate Tensile Strength (lb/sq in.)	Density (lb/cubic in.)	Ultimate Tensile Strength-to-Weight Ratio (in.)	Reference
	Cotton	44,000 To 109,000	5.56×10^{-2}	7.92×10^{5} To 1.961×10^{6}	5
	Glass	200,000 To 220,000	9.17×10^{-2}	2.18×10^{6} To 2.40×10^{6}	5
	Dacron Type 52 (High Tenacity)	141,300	4.98×10^{-2}	2.83×10^{6}	5
	Dacron Type 51 (High Tenacity)	109,500	4.98×10^{-2}	2.20×10^{6}	5
	Dacron Type 55 (Regular)	84,800	4.98×10^{-2}	1.703×10^{6}	5
	Dacron Type 56 (Regular)	77,700	4.98×10^{-2}	1.562×10^{6}	5
	Dacron Type 57 (Regular)	72,400	4.98×10^{-2}	1.454×10^{6}	5
	Dacron Type 59 (High Tenacity)	123,700	4.98×10^{-2}	2.49×10^{6}	5
	HT-1 Untwisted	102,300	4.98×10^{-2}	2.05×10^{6}	6
Wire and Cables	0.0016" dia. René 41	236,000	2.98×10^{-1}	7.93×10^{5}	7
	René 41-7-.0015" dia wires	196,000	2.98×10^{-1}	6.58×10^{5}	7
	René 41-.0015" dia wire	178,000	2.98×10^{-1}	5.98×10^{5}	7
	René 41-.0021" dia wire	169,000	2.98×10^{-1}	5.67×10^{5}	7
	Stainless 304-.0016" wire	106,000	2.90×10^{-1}	3.65×10^{5}	8
	1/32" René 41 Cable (3 x 7 x .0048)	103 lb			8
	3/32" René 41 Cable (7x7x.0104)	959 lb			8
	René 41 - .0021" dia	179,500	2.98×10^{-1}	6.02×10^{5}	8
Woven Cloth	611 Cotton warp		5.56×10^{-2}	1.112×10^{6}	9
	611 Cotton Fill		5.56×10^{-2}	1.281×10^{6}	9
	612 Cotton Warp		5.56×10^{-2}	1.095×10^{6}	9
	612 Cotton Fill		5.56×10^{-2}	1.143×10^{6}	9
	613 Cotton Warp		5.56×10^{-2}	1.112×10^{6}	9

GOODYEAR AIRCRAFT

Table B-1
Ultimate Tensile Strength-To-Weight Ratio at Standard Atmosphere and Room Temperature (Cont)

Material Class	Material	Ultimate Tensile Strength (lb/sq in.)	Density (lb/cubic in.)	Ultimate Tensile Strength-to-Weight Ratio (in.)	Reference
Woven Cloth	613 Cotton Fill		5.56×10^{-2}	1.192×10^{6}	9
	614 Cotton Warp		5.56×10^{-2}	1.103×10^{6}	9
	614 Cotton Fill		5.56×10^{-2}	1.175×10^{6}	9
	616 Cotton Warp		5.56×10^{-2}	1.043×10^{6}	9
	616 Cotton Fill		5.56×10^{-2}	1.125×10^{6}	9
	618 Cotton Warp		5.56×10^{-2}	1.035×10^{6}	9
	618 Cotton Fill		5.56×10^{-2}	1.160×10^{6}	9
	619 Cotton Warp		5.56×10^{-2}	1.109×10^{6}	9
	619 Cotton Fill		5.56×10^{-2}	1.171×10^{6}	9
	620 Cotton Warp		5.56×10^{-2}	1.133×10^{6}	9
	620 Cotton Fill		5.56×10^{-2}	1.171×10^{6}	9
	621 Cotton Warp		5.56×10^{-2}	1.007×10^{6}	9
	621 Cotton Fill		5.56×10^{-2}	1.145×10^{6}	9
	622 Cotton Warp		5.56×10^{-2}	1.124×10^{6}	9
	622 Cotton Fill		5.56×10^{-2}	1.195×10^{6}	9
	661 Cotton Warp		5.56×10^{-2}	8.15×10^{5}	9
	661 Cotton Fill		5.56×10^{-2}	9.02×10^{5}	9
	666 Cotton Warp		5.56×10^{-2}	1.013×10^{6}	9
	666 Cotton Fill		5.56×10^{-2}	1.098×10^{6}	9
	667 Cotton Warp		5.56×10^{-2}	8.28×10^{5}	9
	667 Cotton Fill		5.56×10^{-2}	8.28×10^{5}	9
	1417 Cotton Warp		5.56×10^{-2}	5.96×10^{4}	9
	1417 Cotton Fill		5.56×10^{-2}	5.96×10^{4}	9
	475 Dacron Warp		4.98×10^{-2}	1.400×10^{6}	9
	475 Dacron Fill		4.98×10^{-2}	1.417×10^{6}	9
	476 Dacron Warp		4.98×10^{-2}	2.07×10^{6}	9
	476 Dacron Fill		4.98×10^{-2}	2.07×10^{6}	9
	477 Dacron Warp		4.98×10^{-2}	1.985×10^{6}	9
	477 Dacron Fill		4.98×10^{-2}	1.949×10^{6}	

Table B-1
Ultimate Tensile Strength-To-Weight Ratio at Standard Atmosphere and Room Temperature (Cont)

Material Class	Material	Ultimate Tensile Strength (lb/sq in.)	Density (lb/cubic in.)	Ultimate Tensile Strength-to-Weight Ratio (in.)	Reference
Woven Cloth	478 Dacron Warp		4.98×10^{-2}	1.325×10^{6}	9
	478 Dacron Fill		4.98×10^{-2}	1.266×10^{6}	9
	479 Dacron Warp		4.98×10^{-2}	1.983×10^{6}	9
	479 Dacron Fill		4.98×10^{-2}	1.921×10^{6}	9
	481 Dacron Warp		4.98×10^{-2}	2.01×10^{6}	9
	481 Dacron Fill		4.98×10^{-2}	1.945×10^{6}	9
	482 Dacron Warp		4.98×10^{-2}	2.01×10^{6}	9
	482 Dacron Fill		4.98×10^{-2}	1.323×10^{6}	9
	483 Dacron Warp		4.98×10^{-2}	1.997×10^{6}	9
	483 Dacron Fill		4.98×10^{-2}	1.993×10^{6}	9
	484 Dacron Warp		4.98×10^{-2}	1.997×10^{6}	9
	484 Dacron Fill		4.98×10^{-2}	1.953×10^{6}	9
	Fiberglas-106 Plain Warp			2.24×10^{6}	4
	Fiberglas-106 Plain Fill			2.53×10^{6}	4
	Fiberglas-112 Plain Warp			1.603×10^{6}	4
	Fiberglas-112 Plain Fill			1.606×10^{6}	4
	Fiberglas-* Plain Warp			1.416×10^{6}	4
	Fiberglas-* Plain Fill			2.21×10^{6}	4
	Fiberglas-* Plain Warp			2.12×10^{6}	4
	Fiberglas-* Plain Fill			1.768×10^{6}	4
	Fiberglas-* Plain Warp			1.773×10^{6}	4
	Fiberglas-* Plain Fill			1.597×10^{6}	4
	Fiberglas-* Plain Warp			1.823×10^{6}	4
	Fiberglas-* Plain Fill			1.641×10^{6}	4
	Fiberglas-* Plain Warp			1.711×10^{6}	4
	Fiberglas-* Plain Fill			1.812×10^{6}	4
	Fiberglas-* Plain Warp			1.750×10^{6}	4
	Fiberglas-* Plain Fill			1.585×10^{6}	4
	Fiberglas-* Plain Warp			2.02×10^{6}	4
	Fiberglas-* Plain Fill			2.02×10^{6}	4

*Styles so indicated have been developed by the weavers of glass fabrics.

Table B-1
Ultimate Tensile Strength-To-Weight Ratio at Standard Atmosphere and Room Temperature (Cont)

Material Class	Material	Ultimate Tensile Strength (lb/sq in.)	Density (lb/cubic in.)	Ultimate Tensile Strength-to-Weight Ratio (in.)	Reference
Woven Cloth	Monel, .0021 x 200 x 190 Plain Warp	55,000	3.19×10^{-1}	1.723×10^{5}	8
	Monel, .0021 x 200 x 190 Plain Fill	83,000	3.19×10^{-1}	2.60×10^{5}	8
	293N-Nylon Warp		4.12×10^{-2}	1.992×10^{6}	9
	293N-Nylon Fill		4.12×10^{-2}	1.992×10^{6}	9
	296N-Nylon Warp		4.12×10^{-2}	1.992×10^{6}	9
	296N-Nylon Fill		4.12×10^{-2}	1.992×10^{6}	9
	3511N-Nylon Warp		4.12×10^{-2}	1.918×10^{6}	9
	3511N-Nylon Fill		4.12×10^{-2}	1.918×10^{6}	9
	3523N-Nylon Warp		4.12×10^{-2}	1.247×10^{6}	9
	3523N-Nylon Fill		4.12×10^{-2}	2.81×10^{6}	9
	3525N-Nylon Warp		4.12×10^{-2}	1.643×10^{6}	9
	3525N-Nylon Fill		4.12×10^{-2}	2.61×10^{6}	9
	3564N-Nylon Warp		4.12×10^{-2}	1.333×10^{6}	9
	3564N-Nylon Fill		4.12×10^{-2}	1.448×10^{6}	9
	3581N-Nylon Warp		4.12×10^{-2}	1.864×10^{6}	9
	3581N-Nylon Fill		4.12×10^{-2}	1.864×10^{6}	9
	René 41-.0016" - 200 x 200 Plain Warp	132,500	2.98×10^{-1}	4.45×10^{5}	7
	René 41-.0016" - 200 x 200 Plain Fill	202,000	2.98×10^{-1}	6.78×10^{5}	7
	René 41-7-.0015" x 100 x 100 Plain Fill	172,000	2.98×10^{-1}	5.77×10^{5}	7
	René 41-7-.0015" x 100 x 100 Plain Fill	147,000	2.98×10^{-1}	4.93×10^{5}	7
	René 41-.0021" x 200 x 200 Plain Fill	138,000	2.98×10^{-1}	4.63×10^{5}	7

Table B-1
Ultimate Tensile Strength-To-Weight Ratio at Standard Atmosphere and Room Temperature (Cont)

Material Class	Material	Ultimate Tensile Strength (lb/sq in.)	Density (lb/cubic in.)	Ultimate Tensile Strength-to-Weight Ratio (in.)	Reference
Woven Cloth	René 41-.0021" - 200 x 200 Plain Warp	99,000	2.98×10^{-1}	3.32×10^{5}	7
	René 41-.0016" - 200 x 200 2 x 2 Twill Fill	195,000	2.98×10^{-1}	6.55×10^{5}	7
	René 41-.0016" - 200 x 200 2 x 2 Twill Warp	172,000	2.98×10^{-1}	5.77×10^{5}	7
	René 41, .0016 x 200 x 200 Plain Warp	117,000	2.98×10^{-1}	3.93×10^{5}	8
	René 41, .0016 x 200 x 200 Plain Fill	151,000	2.98×10^{-1}	5.07×10^{5}	8
Woven Cloth Coated	René 41 - .0016" - 200 x 200 Plain Fill	206,000	2.98×10^{-1}	6.92×10^{5}	7
	René 41-.0016" - 200 x 200 Plain Warp	141,000	2.98×10^{-1}	4.73×10^{5}	7
	304 Stainless -.0016 x 200 x 200 Plain Fill	105,000	2.90×10^{-1}	3.62×10^{5}	8
	304 Stainless -.0016 x 200 x 200 Plain Warp	104,000	2.90×10^{-1}	3.59×10^{5}	8
	304 Stainless -.0021 x 200 x 200 Plain Warp	69,000	2.90×10^{-1}	2.38×10^{5}	8
	304 Stainless -.0021 x 200 x 200 Plain Fill	92,000	2.90×10^{-1}	3.17×10^{5}	8

GOODYEAR AIRCRAFT

APPENDIX C

CREEP-RUPTURE DATA

A. GENERAL

This appendix contains the creep-rupture data for various pliable structural materials. Table C-1 identifies the materials by code numbers and briefly describes the composition of each material. Table C-2 presents by code numbers the strength-weight ratios for the structural material only, i.e. the yarn but not the yarn with coating, in the direction of the fiber length unless otherwise indicated.

For Table C-2 it should be noted that ATMOSPHERE and RADIATION columns are established for future use even though all data currently reported are for sea level atmosphere and for conditions of no radiation exposure.

B. REFERENCES

1. Reynolds B.W., and Sutcliffe, A.B., Load-Time Tests of Dacron Airship Envelope Fabric at Elevated Temperatures, Goodyear Aircraft Corp., GER-9657, 14 April 1960.

2. Jouriles N., Wolcott, R., Fasnacht, D.P., and Johnson, W.C., Load-Time Test of Airship Envelope Fabrics, Goodyear Aircraft Corp., GER-6110 Rev. E, 19 May 1958.

3. Williams, E.W., Time versus Load Tests for Neoprene-Coated Fortisan-Rayon Fabric, Goodyear Aircraft Corp., GER-2010, 28 January 1949.

Table C-1. Fabric Construction

Fabric Code No.	Type of Fabric	No. of Plies	CLOTH DESCRIPTION							
			Ply (*)	Weight oz/yd^2	Denier W x F	Count W x F	Weave	Code No.	Material	Ref
XA21A535	Nylon-Neoprene	2	B & S	2.05	-	98 x 98	1 x 1 Plain	3511	Nylon Type 300	2
N113A70	Cotton-Neoprene	3	B	2.90	53 x 53	115 x 104	1 x 1 Plain	661	Cotton	2
			B	2.00	80 x 80	122 x 122	1 x 1 Plain	677	Cotton	
			S	5.50	80 x 80	104 x 96	5 x 5 Basket	666	Cotton	
XA21A627	Orlon-Neoprene	2	B	3.00	200 x 200	71 x 52	Plain	10027	Orlon	2
			S	5.25	200 x 200	99 x 41	Basket	10037	Orlon	
XA21A26	Fortisan-Neoprene	2	S	1.20	50 x 60	100 x 84	Plain	WE4094	Fortisan	3
			S	1.20	50 x 60	100 x 84	Plain	WE4094	Fortisan	
Y502A280	Fortisan-Neoprene	2	B	3.50	90 x 90	78 x 75	2 x 2 Basket	373R	Fortisan	2
			S	4.50	60 x 60	74 x 70	2 x 2 Basket	376R	Fortisan	
N113A310	Cotton-Neoprene	3	S	2.90	53 x 53	115 x 104	1 x 1 Plain	661	Cotton	2
			B	5.50	80 x 80	104 x 96	5 x 5 Basket	666	Cotton	
			S	5.50	80 x 80	104 x 96	5 x 5 Basket	666	Cotton	
XA21A443	Fortisan-Neoprene	2	B	3.50	60 x 60	73 x 73	2 x 2 Basket	WE5370	Fortisan	2
			S	4.50	60 x 60	74 x 70	2 x 2 Basket	WE5404	Fortisan	

(*) B = Bias, S = Straight, Listed in order of sequence.

Table C-1. Fabric Construction (Continued)

Fabric Code No.	Type of Fabric	No. of Plies	CLOTH DESCRIPTION							
			Ply (*)	Weight oz/yd^2	Denier W x F	Count W x F	Weave	Code No.	Material	Ref
Y502A25	Fortisan-Neoprene	3	B	2.20	90 x 90	90 x 90	2 x 1 Twill	368R	Fortisan	2
			B	2.20	90 x 90	90 x 90	2 x 1 Twill	368R	Fortisan	
			S	3.50	90 x 90	78 x 75	2 x 2 Basket	373R	Fortisan	

(*) B = Bias, S = Straight, Listed in order of sequence.

Table C-2. Creep-Rupture Data

Material	Strength-Weight Ratio (Inches)	Break Time (Days)	Temperature (^{o}F)	Atmosphere	Radiation	Reference
Dacron-Neoprene						
N313A100	2.23×10^{6}	3.97×10^{-3}	75	Sea Level	None	1
N313A100	2.23×10^{6}	1.262×10^{-3}	75	Sea Level	None	1
N313A100	2.23×10^{6}	7.41×10^{-4}	75	Sea Level	None	1
N313A100	2.23×10^{6}	1.388×10^{-4}	75	Sea Level	None	1
N313A100	2.23×10^{6}	1.910×10^{-3}	75	Sea Level	None	1
N313A100	2.23×10^{6}	3.73×10^{-3}	75	Sea Level	None	1
N313A100	2.12×10^{6}	3.42×10^{-2}	75	Sea Level	None	1
N313A100	2.12×10^{6}	6.15×10^{-2}	75	Sea Level	None	1
N313A100	2.12×10^{6}	1.042×10^{-2}	75	Sea Level	None	1
N313A100	2.12×10^{6}	1.273×10^{-2}	75	Sea Level	None	1
N313A100	2.12×10^{6}	3.47×10^{-2}	75	Sea Level	None	1
N313A100	2.12×10^{6}	9.72×10^{-3}	75	Sea Level	None	1
N313A100	1.998×10^{6}	5.04×10^{-1}	75	Sea Level	None	1
N313A100	1.998×10^{6}	6.96×10^{-1}	75	Sea Level	None	1
N313A100	1.998×10^{6}	6.08×10^{-1}	75	Sea Level	None	1
N313A100	1.998×10^{6}	1.785×10^{0}	75	Sea Level	None	1
N313A100	1.998×10^{6}	5.24×10^{-1}	75	Sea Level	None	1
N313A100	1.998×10^{6}	1.360×10^{0}	75	Sea Level	None	1
N313A100	2.10×10^{6}	1.424×10^{-2}	100	Sea Level	None	1
N313A100	2.10×10^{6}	2.07×10^{-2}	100	Sea Level	None	1
N313A100	2.10×10^{6}	2.24×10^{-3}	100	Sea Level	None	1
N313A100	2.10×10^{6}	4.86×10^{-3}	100	Sea Level	None	1
N313A100	2.10×10^{6}	7.85×10^{-4}	100	Sea Level	None	1
N313A100	2.10×10^{6}	7.85×10^{-4}	100	Sea Level	None	1
N313A100	2.10×10^{6}	2.36×10^{-2}	100	Sea Level	None	1

Table C-2. Creep-Rupture Data (Continued)

Material	Strength-Weight Ratio (Inches)	Break Time (Days)	Temperature (°F)	Atmosphere	Radiation	Reference
Dacron-Neoprene						
N313A100	2.10×10^{6}	3.40×10^{-2}	100	Sea Level	None	1
N313A100	2.10×10^{6}	2.99×10^{-2}	100	Sea Level	None	1
N313A100	1.984×10^{6}	1.750×10^{-1}	100	Sea Level	None	1
N313A100	1.984×10^{6}	1.528×10^{-2}	100	Sea Level	None	1
N313A100	1.984×10^{6}	1.368×10^{-1}	100	Sea Level	None	1
N313A100	1.984×10^{6}	1.000×10^{-1}	100	Sea Level	None	1
N313A100	1.984×10^{6}	4.07×10^{-1}	100	Sea Level	None	1
N313A100	1.984×10^{6}	9.17×10^{-2}	100	Sea Level	None	1
N313A100	1.984×10^{6}	6.64×10^{-1}	100	Sea Level	None	1
N313A100	1.984×10^{6}	1.125×10^{-1}	100	Sea Level	None	1
N313A100	1.984×10^{6}	9.03×10^{-3}	100	Sea Level	None	1
N313A100	1.870×10^{6}	8.32×10^{-1}	100	Sea Level	None	1
N313A100	1.870×10^{6}	2.60×10^{-1}	100	Sea Level	None	1
N313A100	1.870×10^{6}	4.32×10^{0}	100	Sea Level	None	1
N313A100	1.870×10^{6}	7.66×10^{-1}	100	Sea Level	None	1
N313A100	1.870×10^{6}	2.59×10^{0}	100	Sea Level	None	1
N313A100	1.870×10^{6}	5.08×10^{0}	100	Sea Level	None	1
N313A100	1.870×10^{6}	3.98×10^{0}	100	Sea Level	None	1
N313A100	1.870×10^{6}	5.99×10^{-1}	100	Sea Level	None	1
N313A100	1.870×10^{6}	3.81×10^{0}	100	Sea Level	None	1
N313A100	2.05×10^{6}	4.40×10^{-3}	120	Sea Level	None	1
N313A100	2.05×10^{6}	2.31×10^{-3}	120	Sea Level	None	1
N313A100	2.05×10^{6}	3.01×10^{-3}	120	Sea Level	None	1
N313A100	2.05×10^{6}	5.78×10^{-5}	120	Sea Level	None	1
N313A100	2.05×10^{6}	4.63×10^{-5}	120	Sea Level	None	1

GOODYEAR AIRCRAFT

Table C-2. Creep-Rupture Data (Continued)

Material	Strength-Weight Ratio (Inches)	Break Time (Days)	Temperature (°F)	Atmosphere	Radiation	Reference
Dacron-Neoprene						
N313A100	2.05×10^{6}	4.34×10^{-3}	120	Sea Level	None	1
N313A100	2.05×10^{6}	1.160×10^{-4}	120	Sea Level	None	1
N313A100	2.05×10^{6}	5.78×10^{-5}	120	Sea Level	None	1
N313A100	2.05×10^{6}	6.44×10^{-3}	120	Sea Level	None	1
N313A100	1.939×10^{6}	1.528×10^{-2}	120	Sea Level	None	1
N313A100	1.939×10^{6}	2.29×10^{-2}	120	Sea Level	None	1
N313A100	1.939×10^{6}	2.46×10^{-2}	120	Sea Level	None	1
N313A100	1.939×10^{6}	1.389×10^{-2}	120	Sea Level	None	1
N313A100	1.939×10^{6}	7.50×10^{-4}	120	Sea Level	None	1
N313A100	1.939×10^{6}	2.15×10^{-2}	120	Sea Level	None	1
N313A100	1.939×10^{6}	2.50×10^{-3}	120	Sea Level	None	1
N313A100	1.939×10^{6}	1.632×10^{-2}	120	Sea Level	None	1
N313A100	1.939×10^{6}	2.31×10^{-1}	120	Sea Level	None	1
N313A100	1.820×10^{6}	1.401×10^{0}	120	Sea Level	None	1
N313A100	1.820×10^{6}	1.365×10^{0}	120	Sea Level	None	1
N313A100	1.820×10^{6}	4.24×10^{0}	120	Sea Level	None	1
N313A100	1.820×10^{6}	1.597×10^{-2}	120	Sea Level	None	1
N313A100	1.820×10^{6}	1.764×10^{-1}	120	Sea Level	None	1
N313A100	1.820×10^{6}	8.24×10^{-1}	120	Sea Level	None	1
N313A100	1.820×10^{6}	1.451×10^{-1}	120	Sea Level	None	1
N313A100	1.820×10^{6}	2.97×10^{-1}	120	Sea Level	None	1
N313A100	1.820×10^{6}	1.183×10^{0}	120	Sea Level	None	1
N313A100	1.984×10^{6}	1.389×10^{-3}	140	Sea Level	None	1
N313A100	1.984×10^{6}	2.71×10^{-2}	140	Sea Level	None	1
N313A100	1.984×10^{6}	4.46×10^{-3}	140	Sea Level	None	1
N313A100	1.984×10^{6}	3.59×10^{-4}	140	Sea Level	None	1

Table C-2. Creep-Rupture Data (Continued)

Material	Strength-Weight Ratio (Inches)	Break Time (Days)	Temperature (^{o}F)	Atmosphere	Radiation	Reference
Dacron-Neoprene						
N313A100	1.984×10^{6}	3.70×10^{-4}	140	Sea Level	None	1
N313A100	1.984×10^{6}	6.48×10^{-3}	140	Sea Level	None	1
N313A100	1.984×10^{6}	2.08×10^{-4}	140	Sea Level	None	1
N313A100	1.984×10^{6}	6.02×10^{-4}	140	Sea Level	None	1
N313A100	1.984×10^{6}	4.03×10^{-3}	140	Sea Level	None	1
N313A100	1.870×10^{6}	5.35×10^{-2}	140	Sea Level	None	1
N313A100	1.870×10^{6}	1.302×10^{0}	140	Sea Level	None	1
N313A100	1.870×10^{6}	1.806×10^{-1}	140	Sea Level	None	1
N313A100	1.870×10^{6}	2.01×10^{-2}	140	Sea Level	None	1
N313A100	1.870×10^{6}	7.29×10^{-3}	140	Sea Level	None	1
N313A100	1.870×10^{6}	1.111×10^{-2}	140	Sea Level	None	1
N313A100	1.870×10^{6}	1.181×10^{-2}	140	Sea Level	None	1
N313A100	1.870×10^{6}	2.78×10^{-2}	140	Sea Level	None	1
N313A100	1.870×10^{6}	2.50×10^{-2}	140	Sea Level	None	1
N313A100	1.750×10^{6}	2.95×10^{-1}	140	Sea Level	None	1
N313A100	1.750×10^{6}	9.43×10^{0}	140	Sea Level	None	1
N313A100	1.750×10^{6}	1.307×10^{0}	140	Sea Level	None	1
N313A100	1.750×10^{6}	2.01×10^{0}	140	Sea Level	None	1
N313A100	1.750×10^{6}	1.750×10^{-1}	140	Sea Level	None	1
N313A100	1.750×10^{6}	1.649×10^{0}	140	Sea Level	None	1
N313A100	1.750×10^{6}	4.24×10^{-1}	140	Sea Level	None	1
N313A100	1.750×10^{6}	6.92×10^{0}	140	Sea Level	None	1
N313A100	1.750×10^{6}	5.16×10^{-1}	140	Sea Level	None	1
N313A100	1.939×10^{6}	4.43×10^{-3}	160	Sea Level	None	1
N313A100	1.939×10^{6}	9.17×10^{-4}	160	Sea Level	None	1

Table C-2. Creep-Rupture Data (Continued)

Material	Strength-Weight Ratio (Inches)	Break Time (Days)	Temperature (^{o}F)	Atmosphere	Radiation	Reference
Dacron-Neoprene						
N313A100	1.939×10^{6}	4.31×10^{-3}	160	Sea Level	None	1
N313A100	1.939×10^{6}	6.74×10^{-4}	160	Sea Level	None	1
N313A100	1.939×10^{6}	3.47×10^{-5}	160	Sea Level	None	1
N313A100	1.939×10^{6}	1.389×10^{-3}	160	Sea Level	None	1
N313A100	1.939×10^{6}	3.47×10^{-5}	160	Sea Level	None	1
N313A100	1.939×10^{6}	1.507×10^{-3}	160	Sea Level	None	1
N313A100	1.939×10^{6}	6.25×10^{-4}	160	Sea Level	None	1
N313A100	1.820×10^{6}	6.46×10^{-2}	160	Sea Level	None	1
N313A100	1.820×10^{6}	1.362×10^{-1}	160	Sea Level	None	1
N313A100	1.820×10^{6}	2.48×10^{-1}	160	Sea Level	None	1
N313A100	1.820×10^{6}	3.99×10^{-2}	160	Sea Level	None	1
N313A100	1.820×10^{6}	1.042×10^{-2}	160	Sea Level	None	1
N313A100	1.820×10^{6}	2.43×10^{-2}	160	Sea Level	None	1
N313A100	1.820×10^{6}	3.47×10^{-3}	160	Sea Level	None	1
N313A100	1.820×10^{6}	2.71×10^{-2}	160	Sea Level	None	1
N313A100	1.820×10^{6}	7.85×10^{-2}	160	Sea Level	None	1
N313A100	1.706×10^{6}	1.665×10^{0}	160	Sea Level	None	1
N313A100	1.706×10^{6}	5.475×10^{0}	160	Sea Level	None	1
N313A100	1.706×10^{6}	1.144×10^{0}	160	Sea Level	None	1
N313A100	1.706×10^{6}	1.868×10^{-1}	160	Sea Level	None	1
N313A100	1.706×10^{6}	3.44×10^{-1}	160	Sea Level	None	1
N313A100	1.706×10^{6}	2.23×10^{0}	160	Sea Level	None	1
N313A100	1.706×10^{6}	1.990×10^{0}	160	Sea Level	None	1
N313A100	1.706×10^{6}	3.58×10^{0}	160	Sea Level	None	1
N313A100	1.706×10^{6}	2.59×10^{0}	160	Sea Level	None	1
N313A100	2.130×10^{6}	4.43×10^{-3}	86	Sea Level	None	1

Table C-2. Creep-Rupture Data (Continued)

Material	Strength-Weight Ratio (Inches)	Break Time (Days)	Temperature (^{o}F)	Atmosphere	Radiation	Reference
Dacron-Neoprene						
N313A100	2.130×10^{6}	3.61×10^{-3}	86	Sea Level	None	1
N313A100	2.130×10^{6}	3.88×10^{-3}	86	Sea Level	None	1
N313A100	1.894×10^{6}	1.038×10^{0}	86	Sea Level	None	1
N313A100	1.894×10^{6}	2.26×10^{0}	86	Sea Level	None	1
N313A100	1.894×10^{6}	3.81×10^{0}	86	Sea Level	None	1
Nylon-Neoprene						
XA21A535	2.28×10^{6}	1.04×10^{-3}	R. T.	Sea Level	None	2
XA21A535	2.28×10^{6}	6.83×10^{-4}	R. T.	Sea Level	None	2
XA21A535	2.28×10^{6}	7.26×10^{-3}	R. T.	Sea Level	None	2
XA21A535	2.28×10^{6}	1.21×10^{-2}	R. T.	Sea Level	None	2
XA21A535	2.28×10^{6}	6.92×10^{-3}	R. T.	Sea Level	None	2
XA21A535	2.03×10^{6}	8.12×10^{-2}	R. T.	Sea Level	None	2
XA21A535	2.03×10^{6}	8.20×10^{-2}	R. T.	Sea Level	None	2
XA21A535	2.03×10^{6}	9.16×10^{-2}	R. T.	Sea Level	None	2
XA21A535	2.03×10^{6}	7.01×10^{-2}	R. T.	Sea Level	None	2
XA21A535	1.80×10^{6}	3.50×10^{0}	R. T.	Sea Level	None	2
XA21A535	1.80×10^{6}	3.50×10^{0}	R. T.	Sea Level	None	2
XA21A535	1.80×10^{6}	5.30×10^{0}	R. T.	Sea Level	None	2
XA21A535	1.80×10^{6}	2.00×10^{0}	R. T.	Sea Level	None	2
XA21A535	1.80×10^{6}	6.00×10^{0}	R. T.	Sea Level	None	2
XA21A535	1.80×10^{6}	1.10×10	R. T.	Sea Level	None	2
XA21A535	1.80×10^{6}	2.90×10	R. T.	Sea Level	None	2

Table C-2. Creep-Rupture Data (Continued)

Material	Strength-Weight Ratio (Inches)	Break Time (Days)	Temperature (^{o}F)	Atmosphere	Radiation	Reference
Nylon-Neoprene						
XA21A535	1.65×10^{6}	2.17×10	R. T.	Sea Level	None	2
XA21A535	1.65×10^{6}	5.10×10	R. T.	Sea Level	None	2
XA21A535	1.65×10^{6}	9.20×10	R. T.	Sea Level	None	2
XA21A535	1.52×10^{6}	2.10×10	R. T.	Sea Level	None	2
XA21A535	1.52×10^{6}	2.40×10	R. T.	Sea Level	None	2
XA21A535	1.52×10^{6}	2.70×10	R. T.	Sea Level	None	2
XA21A535	1.52×10^{6}	1.56×10^{2}	R. T.	Sea Level	None	2
XA21A535	1.52×10^{6}	5.00×10^{0}	R. T.	Sea Level	None	2
XA21A535	1.52×10^{6}	1.41×10^{2}	R. T.	Sea Level	None	2
XA21A535	1.52×10^{6}	1.98×10^{2}	R. T.	Sea Level	None	2
XA21A535	1.52×10^{6}	1.11×10^{2}	R. T.	Sea Level	None	2
XA21A535	1.52×10^{6}	1.61×10^{2}	R. T.	Sea Level	None	2
XA21A535	1.52×10^{6}	1.80×10^{2}	R. T.	Sea Level	None	2
Cotton-Neoprene						
N113A70	1.30×10^{6}	1.09×10^{-4}	R. T.	Sea Level	None	2
N113A70	1.30×10^{6}	1.05×10^{-4}	R. T.	Sea Level	None	2
N113A70	1.30×10^{6}	5.67×10^{-5}	R. T.	Sea Level	None	2
N113A70	1.30×10^{6}	2.08×10^{-5}	R. T.	Sea Level	None	2
N113A70	1.30×10^{6}	3.01×10^{-5}	R. T.	Sea Level	None	2
N113A70	1.30×10^{6}	6.25×10^{-5}	R. T.	Sea Level	None	2
N113A70	1.15×10^{6}	1.50×10^{-3}	R. T.	Sea Level	None	2
N113A70	1.15×10^{6}	1.16×10^{-3}	R. T.	Sea Level	None	2

GOODYEAR AIRCRAFT

Table C-2. Creep-Rupture Data (Continued)

Material	Strength-Weight Ratio (Inches)	Break Time (Days)	Temperature (^{o}F)	Atmosphere	Radiation	Reference
Cotton-Neoprene						
N113A70	1.15×10^{6}	1.44×10^{-3}	R. T.	Sea Level	None	2
N113A70	1.15×10^{6}	1.06×10^{-3}	R. T.	Sea Level	None	2
N113A70	1.15×10^{6}	2.05×10^{-3}	R. T.	Sea Level	None	2
N113A70	1.15×10^{6}	8.13×10^{-4}	R. T.	Sea Level	None	2
N113A70	1.01×10^{6}	7.14×10^{-3}	R. T.	Sea Level	None	2
N113A70	1.01×10^{6}	1.11×10^{-2}	R. T.	Sea Level	None	2
N113A70	1.01×10^{6}	7.75×10^{-3}	R. T.	Sea Level	None	2
N113A70	1.01×10^{6}	2.64×10^{-3}	R. T.	Sea Level	None	2
N113A70	1.01×10^{6}	1.03×10^{-2}	R. T.	Sea Level	None	2
N113A70	1.01×10^{6}	1.07×10^{-2}	R. T.	Sea Level	None	2
N113A70	8.63×10^{5}	3.47×10^{-1}	R. T.	Sea Level	None	2
N113A70	8.63×10^{5}	6.43×10^{-1}	R. T.	Sea Level	None	2
N113A70	8.63×10^{5}	2.84×10^{-1}	R. T.	Sea Level	None	2
N113A70	8.63×10^{5}	2.38×10^{-1}	R. T.	Sea Level	None	2
N113A70	8.63×10^{5}	9.52×10^{-1}	R. T.	Sea Level	None	2
N113A70	7.19×10^{5}	3.80×10^{0}	R. T.	Sea Level	None	2
N113A70	7.19×10^{5}	1.92×10	R. T.	Sea Level	None	2
N113A70	7.19×10^{5}	1.64×10	R. T.	Sea Level	None	2
N113A70	7.19×10^{5}	1.63×10	R. T.	Sea Level	None	2
N113A70	7.19×10^{5}	1.56×10	R. T.	Sea Level	None	2
N113A70	7.19×10^{5}	2.06×10	R. T.	Sea Level	None	2
N113A70	5.75×10^{5}	1.77×10^{2}	R. T.	Sea Level	None	2
N113A70	5.75×10^{5}	1.57×10^{2}	R. T.	Sea Level	None	2
N113A70	5.75×10^{5}	1.68×10^{2}	R. T.	Sea Level	None	2
N113A70	5.75×10^{5}	2.34×10	R. T.	Sea Level	None	2

Table C-2. Creep-Rupture Data (Continued)

Material	Strength-Weight Ratio (Inches)	Break Time (Days)	Temperature (^{o}F)	Atmosphere	Radiation	Reference
Cotton-Neoprene						
N113A70	4.32×10^{5}	1.34×10^{3}	R. T.	Sea Level	None	2
N113A70	4.32×10^{5}	8.36×10^{2}	R. T.	Sea Level	None	2
N113A70	4.32×10^{5}	1.59×10^{3}	R. T.	Sea Level	None	2
N113A70	4.32×10^{5}	1.78×10^{3}	R. T.	Sea Level	None	2
N113A70	4.32×10^{5}	1.88×10^{3}	R. T.	Sea Level	None	2
Orlon-Neoprene						
XA21A627	1.00×10^{6}	9.27×10^{-4}	R. T.	Sea Level	None	2
XA21A627	1.00×10^{6}	1.30×10^{-3}	R. T.	Sea Level	None	2
XA21A627	1.00×10^{6}	6.40×10^{-4}	R. T.	Sea Level	None	2
XA21A627	1.00×10^{6}	9.80×10^{-4}	R. T.	Sea Level	None	2
XA21A627	8.90×10^{5}	1.04×10^{-2}	R. T.	Sea Level	None	2
XA21A627	8.90×10^{5}	1.74×10^{-2}	R. T.	Sea Level	None	2
XA21A627	8.90×10^{5}	3.80×10^{-2}	R. T.	Sea Level	None	2
XA21A627	8.90×10^{5}	1.67×10^{-2}	R. T.	Sea Level	None	2
XA21A627	8.90×10^{5}	2.30×10^{-2}	R. T.	Sea Level	None	2
XA21A627	7.78×10^{5}	1.50×10^{0}	R. T.	Sea Level	None	2
XA21A627	7.78×10^{5}	1.23×10^{0}	R. T.	Sea Level	None	2
XA21A627	7.78×10^{5}	1.20×10	R. T.	Sea Level	None	2
XA21A627	7.78×10^{5}	5.00×10^{-1}	R. T.	Sea Level	None	2
XA21A627	7.78×10^{5}	4.00×10^{0}	R. T.	Sea Level	None	2
XA21A627	6.67×10^{5}	4.00×10	R. T.	Sea Level	None	2
XA21A627	6.67×10^{5}	4.01×10	R. T.	Sea Level	None	2

Table C-2. Creep-Rupture Data (Continued)

Material	Strength-Weight Ratio (Inches)	Break Time (Days)	Temperature (^{o}F)	Atmosphere	Radiation	Reference
Orlon-Neoprene						
XA21A627	6.67×10^{5}	5.20×10	R. T.	Sea Level	None	2
XA21A627	6.67×10^{5}	8.20×10	R. T.	Sea Level	None	2
XA21A627	6.67×10^{5}	8.40×10	R. T.	Sea Level	None	2
XA21A627	6.67×10^{5}	8.90×10	R. T.	Sea Level	None	2
Fortisan-Neoprene						
XA21A26	1.36×10^{6}	1.55×10^{-3}	R. T.	Sea Level	None	3
XA21A26	1.36×10^{6}	6.83×10^{-4}	R. T.	Sea Level	None	3
XA21A26	1.36×10^{6}	1.11×10^{-4}	R. T.	Sea Level	None	3
XA21A26	1.14×10^{6}	1.71×10^{-2}	R. T.	Sea Level	None	3
XA21A26	1.14×10^{6}	9.02×10^{-4}	R. T.	Sea Level	None	3
XA21A26	1.14×10^{6}	8.40×10^{-3}	R. T.	Sea Level	None	3
XA21A26	1.14×10^{6}	3.37×10^{-2}	R. T.	Sea Level	None	3
XA21A26	1.14×10^{6}	2.81×10^{-4}	R. T.	Sea Level	None	3
XA21A26	9.09×10^{5}	2.83×10^{0}	R. T.	Sea Level	None	3
XA21A26	9.09×10^{5}	2.83×10^{0}	R. T.	Sea Level	None	3
XA21A26	9.09×10^{5}	2.83×10^{0}	R. T.	Sea Level	None	3
XA21A26	9.09×10^{5}	6.42×10^{0}	R. T.	Sea Level	None	3
XA21A26	6.93×10^{5}	1.50×10	R. T.	Sea Level	None	3
XA21A26	6.93×10^{5}	7.58×10	R. T.	Sea Level	None	3
XA21A26	6.93×10^{5}	1.67×10^{2}	R. T.	Sea Level	None	3

GOODYEAR AIRCRAFT

Table C-2. Creep-Rupture Data (Continued)

Material	Strength-Weight Ratio (Inches)	Break Time (Days)	Temperature (^{o}F)	Atmosphere	Radiation	Reference
Fortisan-Neoprene						
Y502A280	2.09×10^{6}	1.74×10^{-4}	R. T.	Sea Level	None	2
Y502A280	2.09×10^{6}	1.22×10^{-4}	R. T.	Sea Level	None	2
Y502A280	2.09×10^{6}	4.05×10^{-4}	R. T.	Sea Level	None	2
Y502A280	2.09×10^{6}	1.98×10^{-4}	R. T.	Sea Level	None	2
Y502A280	2.09×10^{6}	1.32×10^{-4}	R. T.	Sea Level	None	2
Y502A280	2.09×10^{6}	2.09×10^{-4}	R. T.	Sea Level	None	2
Y502A280	1.85×10^{6}	2.99×10^{-3}	R. T.	Sea Level	None	2
Y502A280	1.85×10^{6}	3.79×10^{-3}	R. T.	Sea Level	None	2
Y502A280	1.85×10^{6}	1.79×10^{-3}	R. T.	Sea Level	None	2
Y502A280	1.85×10^{6}	2.86×10^{-3}	R. T.	Sea Level	None	2
Y502A280	1.85×10^{6}	4.70×10^{-3}	R. T.	Sea Level	None	2
Y502A280	1.85×10^{6}	2.50×10^{-3}	R. T.	Sea Level	None	2
Y502A280	1.62×10^{6}	2.40×10^{-2}	R. T.	Sea Level	None	2
Y502A280	1.62×10^{6}	8.60×10^{-3}	R. T.	Sea Level	None	2
Y502A280	1.62×10^{6}	2.38×10^{-2}	R. T.	Sea Level	None	2
Y502A280	1.62×10^{6}	1.60×10^{-2}	R. T.	Sea Level	None	2
Y502A280	1.62×10^{6}	2.38×10^{-3}	R. T.	Sea Level	None	2
Y502A280	1.62×10^{6}	1.62×10^{-2}	R. T.	Sea Level	None	2
Y502A280	1.39×10^{6}	3.29×10^{-1}	R. T.	Sea Level	None	2
Y502A280	1.39×10^{6}	1.34×10^{-1}	R. T.	Sea Level	None	2
Y502A280	1.39×10^{6}	5.50×10^{-1}	R. T.	Sea Level	None	2
Y502A280	1.39×10^{6}	2.54×10^{-1}	R. T.	Sea Level	None	2
Y502A280	1.39×10^{6}	1.62×10^{-1}	R. T.	Sea Level	None	2
Y502A280	1.39×10^{6}	3.79×10^{-1}	R. T.	Sea Level	None	2
Y502A280	1.16×10^{6}	7.22×10^{0}	R. T.	Sea Level	None	2

GOODYEAR AIRCRAFT

Table C-2. Creep-Rupture Data (Continued)

Material	Strength-Weight Ratio (Inches)	Break Time (Days)	Temperature (°F)	Atmosphere	Radiation	Reference
Fortisan-Neoprene						
Y502A280	1.16×10^6	2.23×10^1	R. T.	Sea Level	None	2
Y502A280	1.16×10^6	1.06×10^1	R. T.	Sea Level	None	2
Y502A280	1.16×10^6	5.77×10^0	R. T.	Sea Level	None	2
Y502A280	1.16×10^6	9.00×10^0	R. T.	Sea Level	None	2
Y502A280	1.16×10^6	1.39×10^1	R. T.	Sea Level	None	2
Y502A280	9.28×10^5	3.89×10	R. T.	Sea Level	None	2
Y502A280	9.28×10^5	3.93×10	R. T.	Sea Level	None	2
Y502A280	9.28×10^5	4.17×10	R. T.	Sea Level	None	2
Y502A280	9.28×10^5	2.15×10	R. T.	Sea Level	None	2
Y502A280	9.28×10^5	1.71×10^2	R. T.	Sea Level	None	2
Y502A280	9.28×10^5	1.44×10^2	R. T.	Sea Level	None	2
Y502A280	9.28×10^5	1.78×10^2	R. T.	Sea Level	None	2
Y502A280	6.96×10^5	6.92×10^2	R. T.	Sea Level	None	2
Y502A280	6.96×10^5	6.92×10^2	R. T.	Sea Level	None	2
Y502A280	6.96×10^5	6.01×10^2	R. T.	Sea Level	None	2
Y502A280	6.96×10^5	8.57×10^2	R. T.	Sea Level	None	2
Y502A280	6.96×10^5	8.08×10^2	R. T.	Sea Level	None	2
Y502A280	6.96×10^5	7.55×10^2	R. T.	Sea Level	None	2

APPENDIX D

CUMULATIVE DAMAGE AND FACTOR OF SAFETY

A. CREEP-RUPTURE

In the case of fabrics creep-rupture is given as percent of quick-break versus $\log_{10}$ time. The term quick-break needs some clarification. For example, a two-ply nylon-neoprene, straight-bias fabric was tested in strip tension for various periods of time. From 27 tests, between 50% and 90% of quick-break (only one test at 50%), the following equation was derived using the method of least squares:

$$Q = -6.85 \log_{10} t_B + 73.8 \text{ percent} \tag{1a}$$

where t_B is the time in days. The particular quick-break value of 126 lb/in. was determined with the use of a Scott Testing Machine and by more or less following Federal Specification CCC-T-191b (Reference 1), Method 5104.1, which specifies a length between jaws of 3 inches and a testing rate of 12 inches per minute.

Equation 1a may be converted to lb/in. by

$$Q = \frac{F_{tu}}{126} \; 100 \quad . \tag{2}$$

Therefore:

$$F_{tu} = -8.63 \log_{10} t_B + 93.0 \text{ lb/in.} \tag{1b}$$

Neither equations 1a nor 1b give the stress in the nylon filaments in the familiar term of lb/sq in. This term can be arrived at if the cloth specifications are known.

The code number XA21A535 was given to a two-ply fabric of bias-straight, neoprene-coated nylon cloth. Both cloths were woven with type 300 bright nylon yarns, 96 per inch in warp and fill directions. The 70 denier yarns were composed of 34 monofilaments.

With this information and conversion factors the strengths of the nylon in two other sets of units (the density of nylon being 1.14 gm/cm^3 or 1.14 x 0.0363 = 0.0413 lb/in^3) are given below in equations 1c and 1d.

Since:

$$1 \text{ lb} = 453.59 \text{ grams},$$

and

$$\rho_g = \frac{\text{grams}}{\text{cm}^3}$$

where ρ_g is the density in the cgs system;

and since:

$$1 \text{ psi} = 12,800 \left(\frac{\text{gm}}{\text{denier}}\right)\left(\frac{\text{gm}}{\text{cm}^3}\right)$$

or

$$1 \text{ psi} = 12,800\left(\frac{\text{gm}}{\text{denier}}\right)\rho_g \quad ;$$

then, if the bias ply is neglected and if only the warp yarns are considered, the gram per denier strength is:

$$S_{gm/den.} = \frac{F_{tu} \times 453.59}{70 \times 96}$$

$$= -0.583 \log_{10} t_B + 6.28 \text{ gm/den} \tag{1c}$$

and the psi strength is:

$$\begin{aligned} S_{psi} &= S_{gm/den.} \times 12,800 \times 1.14 \\ &= -8530 \log_{10} t_B + 91,800 \text{ psi} \quad . \end{aligned} \tag{1d}$$

The value of 126 lb/in. corresponds to 8.52 gm/den. or 124,300 psi. Such a value is rather high for nylon. The reason is due to neglecting the aid from the bias ply, the fill yarns of the straight ply, and neoprene. Equation 1c is already a strength-over-weight ratio; while equation 1d may be converted to the engineering units of strength-over-weight ratio by dividing it by the density of nylon in lb/in.^{3}

Thus:

$$k = \frac{S_{psi}}{1.14 \times .03613} \text{ inches}$$

$$= -207,000 \log_{10} t_B + 2,230,000 \text{ in.} \tag{1e}$$

the strength-over-weight ratio that can be used to compare nylon with the conventional metals.

In cumulative damage theories it is convenient to use creep-rupture curves in a normalized form. A plot of equation 1b is shown in Figure D-1. The quick-break strength of 126 lb/in corresponds to a quick-break time calculated from Equation 1b.

$$\log_{10} t_B = \frac{93 - 126}{8.63} = -3.83$$

or

$$t_B = 1.477 \times 10^{-4} \text{ days } (12.75 \text{ sec})$$

Equation 1b can be transformed to a non-dimensional form by letting

$$F_{tu} = 1.26\, Q \tag{2}$$

$$t_B = 1.477 \times 10^{-4} \tau \tag{3}$$

or

$$\log_{10} t_B = \log_{10} \tau + \frac{93 - 126}{8.63}$$

which gives

$$Q = -6.85 \log_{10} \tau + 100 \tag{1f}$$

In order to convert equation 1f to real times and real stresses it is necessary to know that Q = 100% corresponds to 126 lb/in and 1.477×10^{-4} days. The two equations, 1b and 1f, are both plotted in Figure D-2.

Equations 1a to 1e may be put in a literal form to apply to other materials. Let

$$F_{tu} = -m \log_{10} t_B + b, \text{ lb/in.} \tag{2b}$$

represent the original data. If

F_{qb} = Quick-break value lb/in.

C = Count, yarns/in. (Picks or ends/in.)

D = Denier

ρ_g = Density, gm/cc; ρ_l = density, lb/in^3

then,

$$Q = \frac{F_{tu}}{F_{qb}} 100 = - \frac{100m}{F_{qb}} \log_{10} t_B + \frac{100b}{Fqb}, \ \% \tag{2a}$$

$$S_{gm/den.} = - \frac{454m}{CD} \log_{10} t_B + \frac{454b}{CD}, \delta gm/den \tag{2c}$$

$$S_{psi} = \left[- \frac{5.806 \ \rho_g n}{CD} \log_{10} t_B + \frac{5.806 \ \rho_g b}{CD} \right] 10^6, \ psi \tag{2d}$$

$$k = \left[- \frac{16.072m}{CD} \log_{10} t_B + \frac{16.072 \ b}{CD} \right] \ 10^7 \ in. \tag{2e}$$

and the quick-break values needed to normalize equations 1c, 1d and 1e are:

$$\left[S_{gm/den.} \right]_{qb} = 454 \ \frac{F_{qb}}{CD}, \ gm/den. \tag{3c}$$

$$\left[S_{psi} \right]_{qb} = 5.806 \times 10^6 \ \frac{F_{qb} \ \rho_g}{CD}, \ psi \tag{3d}$$

$$\left[k_1 \right]_{qb} = 16.072 \times 10^7 \ \frac{F_{qb}}{CD}, \ in. \tag{3e}$$

and each of equations 1c, 1d, and 1e will be transformed into 1a, which can in turn be transformed into the type 1f. Plots of equations 1a through 1f are given in Figure D-3 to illustrate the relationships among them. The normalized equation 1f in literal form is

$$Q = - \frac{100m}{F_{qb}} \log_{10} \tau + 100 \tag{2f}$$

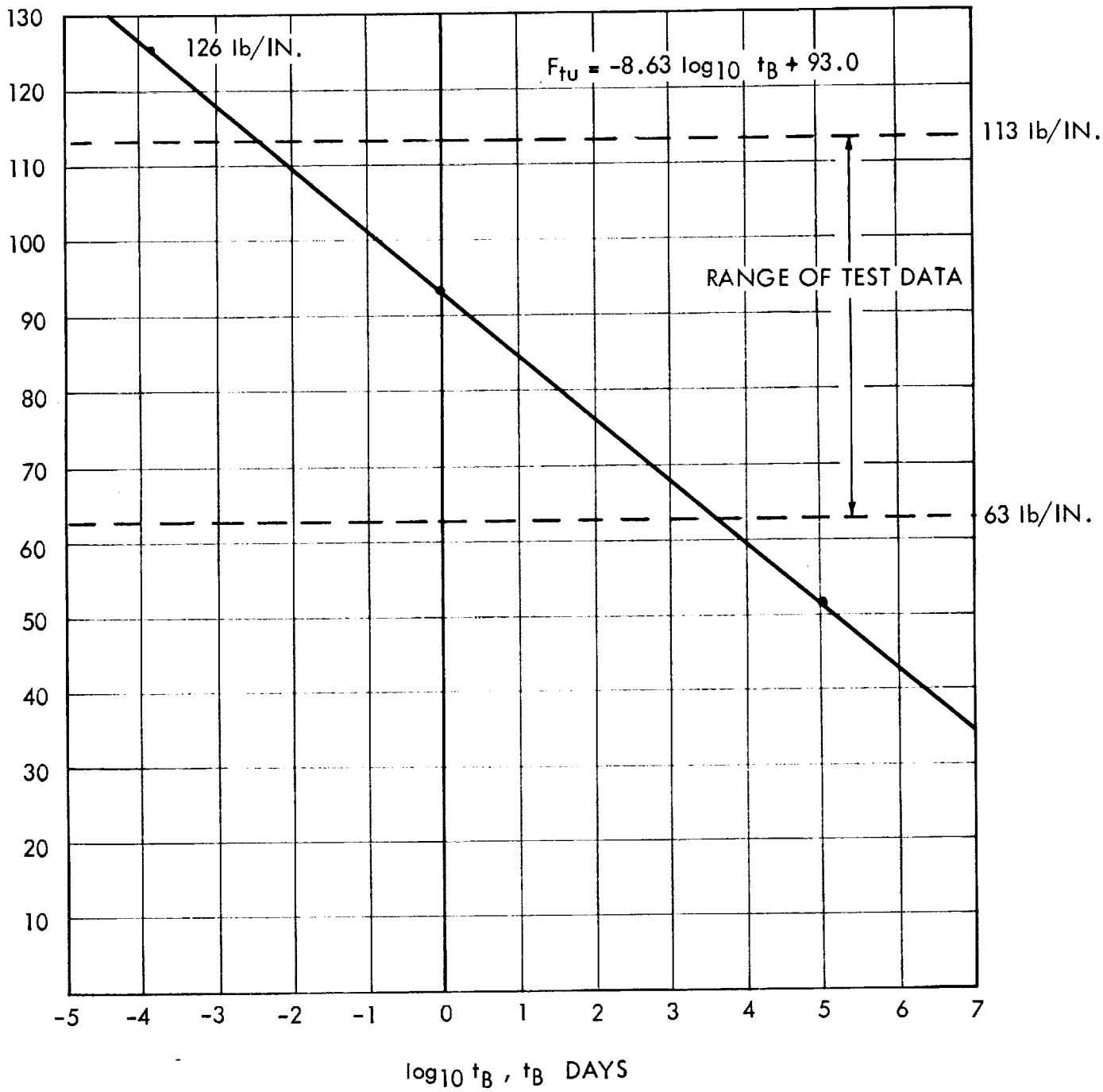

Figure D-1. Plot of Creep-Rupture Curve Representing Original Data

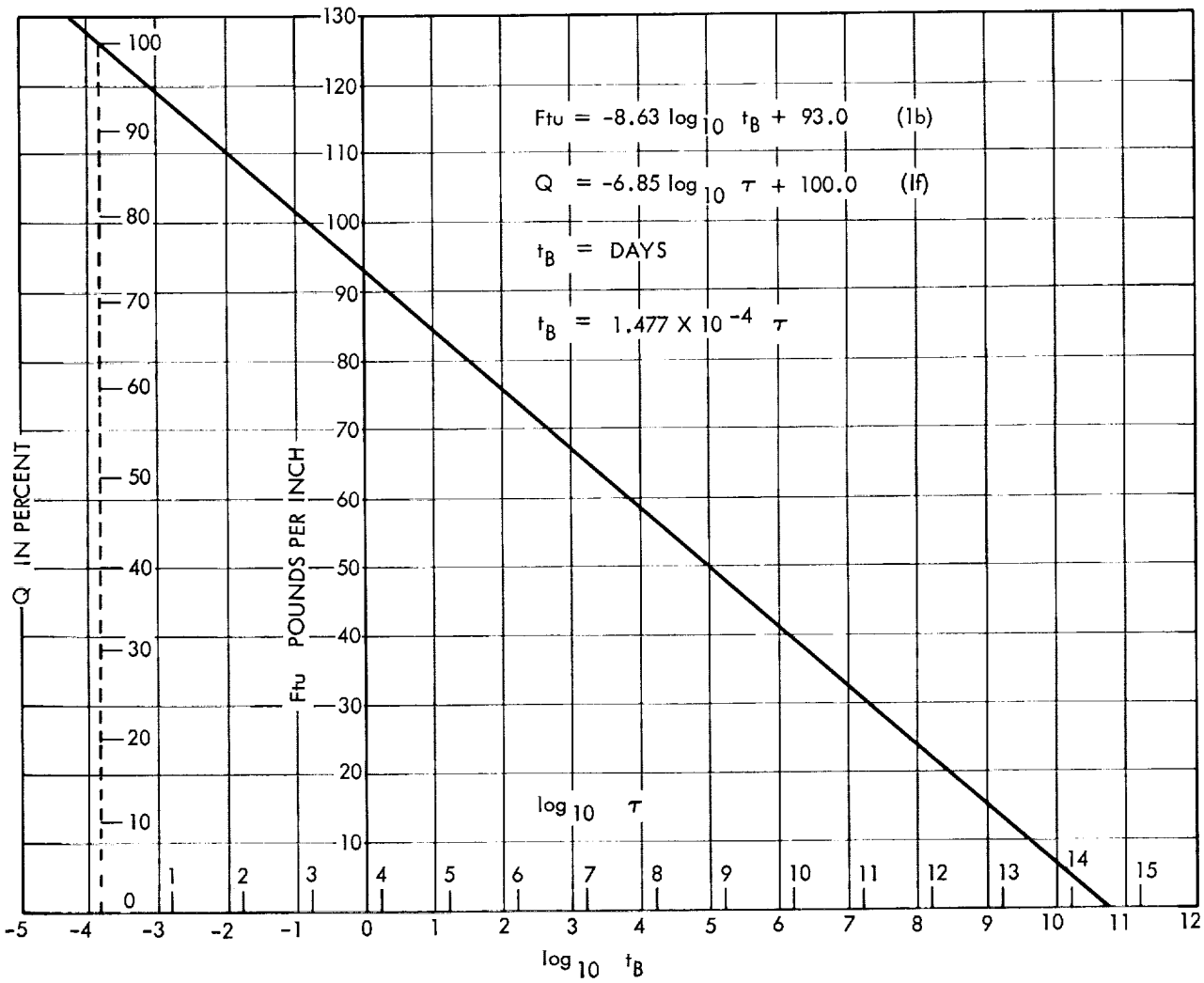

Figure D-2. Plots of Equations 1b and 1f

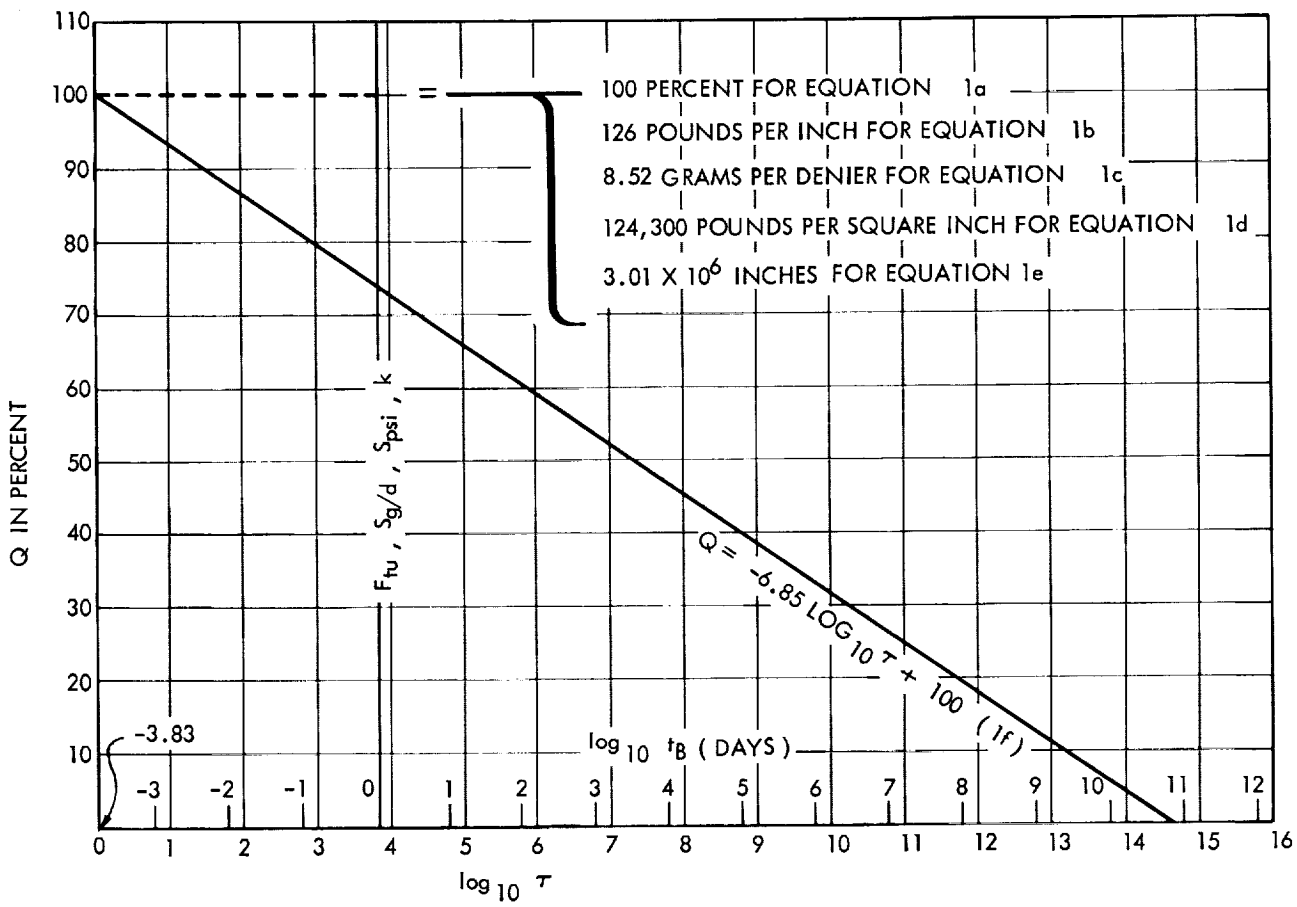

Figure D-3. Plots of Equations 1a through 1f

where

$$\log_{10} \tau = \frac{F_{qb} - b}{m} + \log_{10} t_B \,, \quad \tau = t_B \, 10^{\frac{F_{qb} - b}{m}}$$

$$\left(t_B\right)_{qb} = 10^{-\left(\frac{F_{qb} - b}{m}\right)}$$ is the quick break time.

B. OPERATING MARGIN AND FACTOR OF SAFETY

All polymeric materials to some extent exhibit creep. Structures made of these materials are always subjected to different stresses at different times; therefore, a load history must be known in order to design the structure. However, there is no proven theory available to evaluate the effect of the given load-time history on the strength of the structure. Furthermore, a load-time history implies fatigue as well as creep, but fatigue damage theory is almost always presented as range of stress versus cycles of variation, i.e. time is left out completely. The effect of creep and fatigue when both occur is generally considered by the designer in an empirical way. In order to better evaluate creep and fatigue damage, the concept of operating margin (OM) is introduced.

All of equations 1a through 1f are of the type $y = -m\,x + b$, where y is related to stress, x is related to time, and m and b are the slope and y-intercept respectively. If a stress Y_1 acts for a time T_1 ($X_1 = \log_{10} T_1$), the Operating Margin is defined as the vertical distance between the curve $y = -m\,x + b$ and one parallel to $y = -m\,x + b$ but passing through the point X_1, Y_1. This is illustrated in Figure D-4.

The distance OM is independent of the position along the curve $Y = -m\,X + B$; in particular, if the X-intercept is used, a stress Y_1 acting for a time T_1 · ($X_1 = \log_{10} T_1$) may be replaced by a zero stress acting for a time T_0 · ($X_0 = \log_{10} T_0$) and the operating margin is given by:

$$OM = -m\,X_0 + b \tag{4}$$

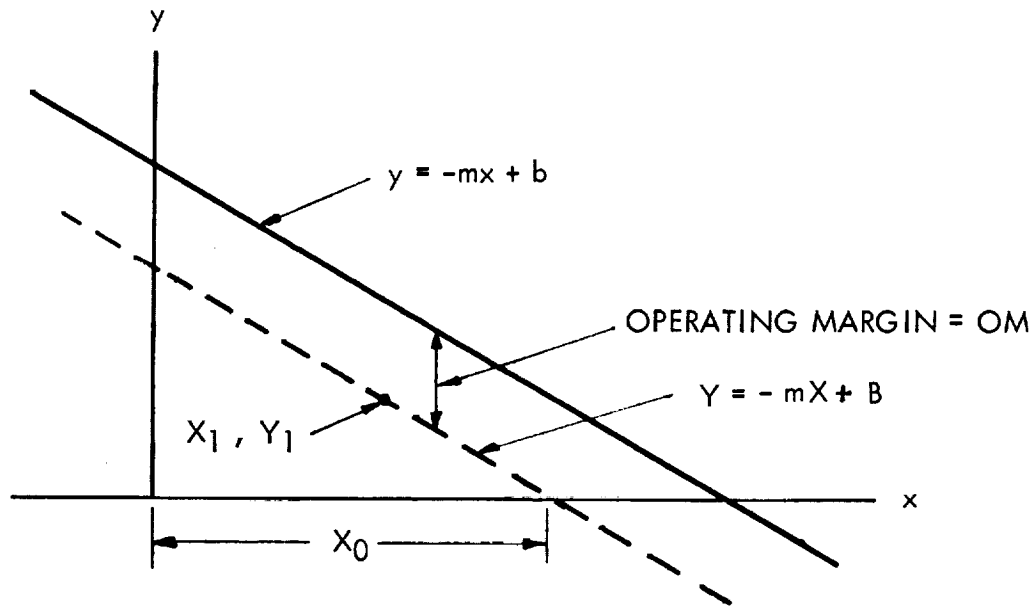

Figure D-4. Operating Margin

The stress Y_1 is reduced to zero for convenience. Any other stress could have been used. The reduction to zero has no physical meaning, and is done merely for mathematical convenience. The curves $y = -mx + b$ cannot be extrapolated indefinitely in either direction because impossible values result. Thus extrapolation to the left means that the strength of the material increases without limit as the time of application approaches zero. Extrapolation to the right yields a finite life under no stress whatsoever. In any event the final Operating Margin should not go too far beyond the available data.

A load-time history can be given as a set of X_i, Y_i. Each Y_i can be reduced to zero while each X_i is increased to an X_{0i}. From Figure D-4 the coordinates X_i, Y_i satisfy the equation

$$Y = -m X + B \tag{5}$$

hence,

$$B = Y_i + mX_i \tag{6}$$

If $Y = Y_{0i} = 0$ is substituted into equations 5 and 6, then

$$X_{0i} = \frac{Y_i}{m} + X_i \, . \tag{7}$$

For each X_{0i} there is a T_{0i} since $X_{0i} = \log_{10} T_{0i}$. Let the set of T_{0i} be summed, i.e.

$$T_\Sigma = \sum_{i=1}^{n} T_{0i} \tag{8}$$

and let

$$X_\Sigma = \log_{10} T_\Sigma \tag{9}$$

The net operating margin is

$$OM = -mX_\Sigma + b \tag{10}$$

The above concept of operating margin was developed in Reference 2 with some experimental verification in Reference 3. The significance of the operating margin is that any given stress-time coordinate can be made equivalent to another stress-time coordinate by merely "moving" parallel to the original creep-rupture curve. Such "motion" is at constant operating margin as is evident in Figure D-4.

The concept of factor of safety needs some clarification when the strength of a material is time dependent and when variability in material properties is present. Figure D-5 shows three normalized creep-rupture curves and three safety factor curves. The creep-rupture curves are:

$$Q = -6.85 \log_{10} \tau + 100 \text{ (least squares line)} \tag{11a}$$

$$Q = -6.58 \log_{10} \tau + 89.9 \text{ (97.5\% confidence limit)} \tag{11b}$$

$$Q = -6.59 \log_{10} \tau + 79.9 \text{ (99.95\% confidence limit)} \tag{11c}$$

An illustration of the meaning of these curves is given by the intersection of the line $Q = 25\%$ and each of the six curves. Table D-1 lists the quantities with some remarks. At present Reference 4 does not give the least squares (50%)

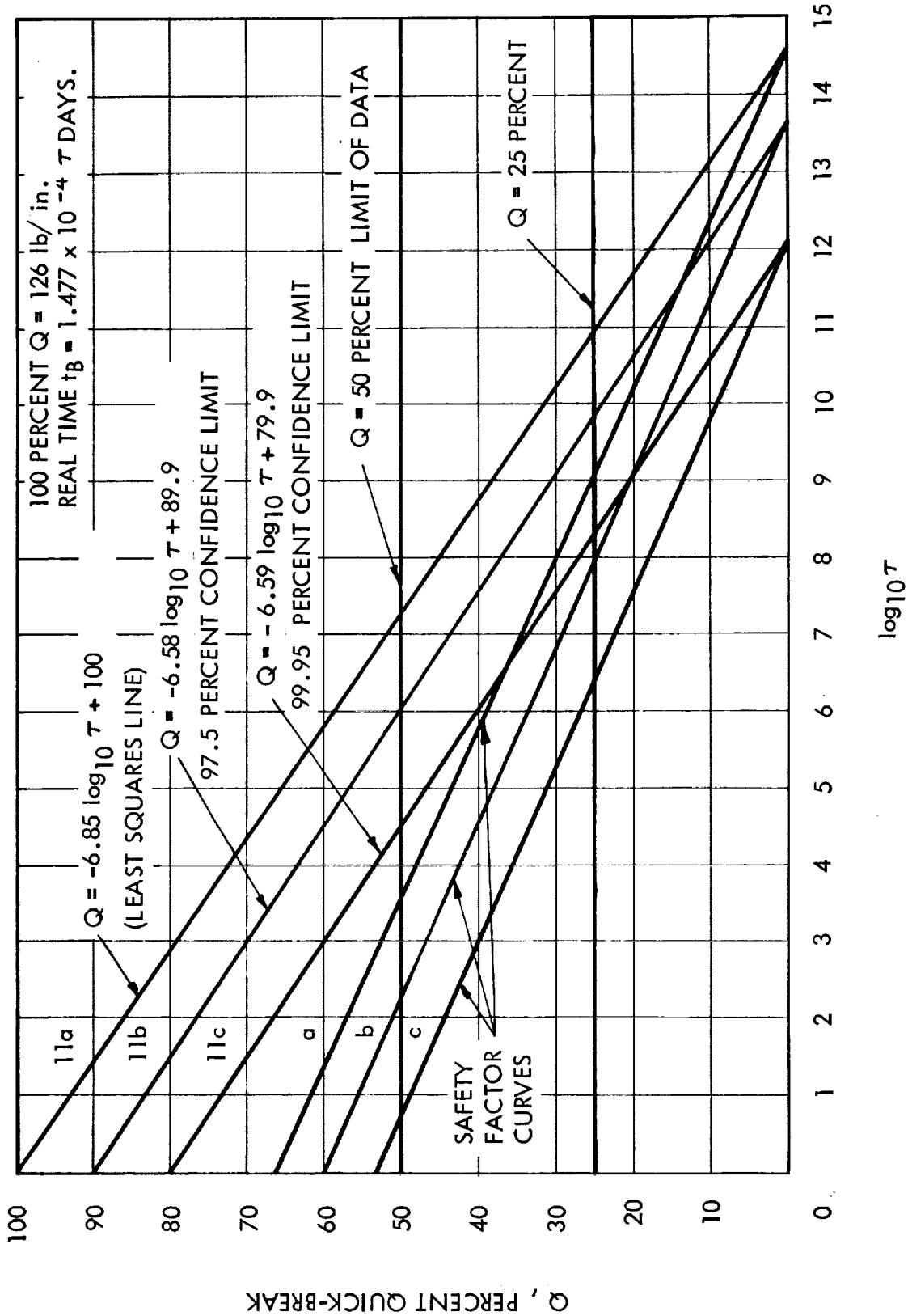

Figure D-5. Confidence Limit and Safety Factor Curves

Table D-1. Survival Times, Reliability, and Factor of Safety

CURVE	$\log_{10}\tau$	t_B, SURVIVAL TIME (DAYS)	CONFIDENCE (PERCENT)	FACTOR OF SAFETY
C	6.43	392	99.95	1.5
b	7.97	13,800	97.5	1.5
9	9.05	1.66×10^5	Least Squares	1.5
11c	8.30	2.95×10^4	99.95	1.0
11b	9.85	10.43×10^5	97.5	1.0
11a	10.93	12.6×10^6	Least Squares	1.0

value for aluminum alloys, but rather it gives conformance and confidence limits. In article 3.1.1.1.1, "Strength Properties," MIL-HDBK-5 (Reference 4) defines an "A" and a "B" value for both F_{tu} and F_{ty}. The "A" value is met by suppliers as 99% conformance and a 95% confidence. The "B" value means that 90% of the material supplied will meet or exceed the F_{tu} and F_{ty} values with a 95% confidence level. Thus the "A" and "B" values are really one-sided tolerance values and enable a supplier to describe his product. The values in Table D-1 are confidence limits because one is confident that a sample when loaded to a given Q will have a 97.5% or 99.95% chance of surviving the time given by the particular curve. The factor of safety is illustrative, and the actual value chosen will depend upon the mission and the confidence curve chosen.

A question will still arise concerning the relation between operating margin and safety factor. This can be resolved by transferring the net operating

margin at $Q = 0$, $T = T_\Sigma$ to a point (Q_E, T_E) where Q_E is the maximum stress expected during the life of the structure. Figure D-6 illustrates the calculation. The factor of safety is defined to be

$$n = \frac{\overline{Q}_E}{Q_E} \tag{12}$$

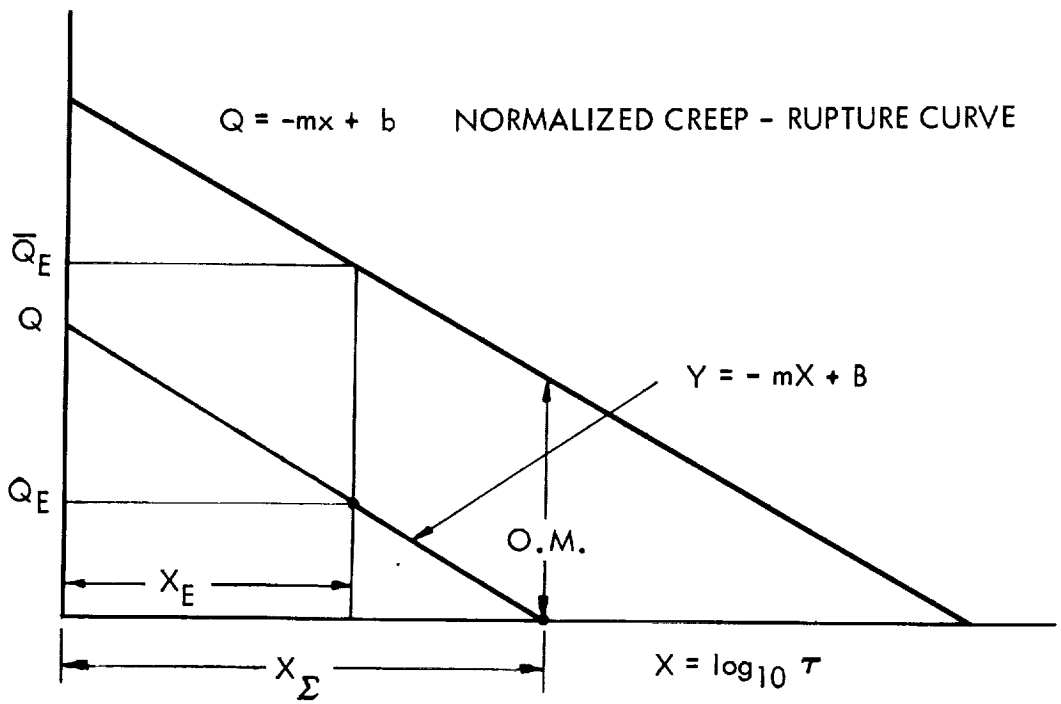

Figure D-6. Relation Between Operating Margin and Factor of Safety $n = \frac{\overline{Q}_E}{Q_E}$

Equation 12 means that if Q_E is the equivalent load for time T_Σ, then $n\,Q_E = \overline{Q}_E$ is the load that causes failure in the same time. The factor of safety, n, here is similar to the conventional one in which creep is not a factor. Since $X_\Sigma = \log_{10} T_\Sigma$ and $Q = 0$ $(Y = 0)$ at $X = X_\Sigma$, then

$$B = m\,X_\Sigma \tag{13}$$

and

$$X_E = \frac{Q_E - mX_\Sigma}{-m} = -\frac{Q_E}{m} + X_\Sigma \tag{14}$$

X_E gives $\overline{Q}_E$ when substituted into the original normalized creep curve. Therefore:

$$\overline{Q}_E = -mX_E + b$$

$$= Q_E - mX_\Sigma + b \tag{15}$$

and

$$n = 1 - \frac{mX_\Sigma}{Q_E} + \frac{b}{Q_E} \tag{16}$$

The procedures just discussed regarding creep-rupture at room temperature can be extended to other temperatures and to other means of damage such as fatigue, radiation, etc. In the case of fatigue the time variable is replaced by cycles to failure. In any case the stress and time or cycles should of course be normalized. At present such extension of operating margin to other damage means is not based on test results but rather is a theoretical extension that yields a simple means of evaluating damage.

The concept of safety factor just discussed and shown in Figure D-5 is not the only possible concept, even though it is similar to the conventional safety factor. In Reference 2 a factor of safety,

$$n = \frac{100}{100 - OM} \tag{17}$$

is given. This factor of safety is dependent upon the stress history but not on any particular stress. A comparison of the two concepts of safety factor are shown in Figure D-7. Two different values of safety factor are used. It is apparent from Figure D-7 that the two concepts are the same at $\tau = 0$ when the normalized creep-rupture curve is used. As the time under load increases the two concepts diverge. The safety factor from Reference 2 is the more conservative.

From Figure D-5 it can be seen that the 97.5% and 99.95% confidence limit curves are almost parallel to the least squares curve. Since the operating margin curves of Figure D-7 are parallel to the least squares curve, the

safety factor concept of Reference 2 gives allowable stress histories that occur at constant probability of failure. On this basis the safety factor concept of Reference 2 is better than the other safety factor. The fact that the safety factor is dependent only upon the stress-history is a further advantage.

The choice of actual numerical value of factor of safety will have to be made on allowable deformations as well as on strength. Excessive deformations render a structure useless even though sufficient strength remains.

C. COMPARISON OF SAFETY FACTORS OF POLYMERIC FABRICS AND METALS.

Fabrics whose load carrying elements are polymeric materials should usually be designed with larger safety factors when these are based on short-time ultimate strength than is the case with conventional metal structures. The main reason for a larger factor of safety (lower allowable stresses) is to reduce the deformation under operating conditions. If relatively large deformations are not detrimental, lower safety factors can be used.

Comparison in Table D-2 of the ratio of typical modulus of elasticities to typical ultimate strengths of several polymeric materials to the same ratio for several metals reveals a great difference in the deformation characteristics of the two kinds of materials. Table D-3 shows percent strain for various ratios of F_{tu} to F_t ($n = F_{tu}/F_t$) for a typical nylon 300 and a high strength alloy steel. It is evident in both tables that the deformations of polymeric structures can be one or two orders of magnitude greater than metallic structures. It is not necessary that inflated fabric structures and conventional metal structures have deformations of the same order of magnitude; nevertheless, deformations greater than 10% are excessive for many structures. Criteria of allowable deformation for a given structure will have to be determined. Such criteria must then ultimately be accounted for in the safety factor.

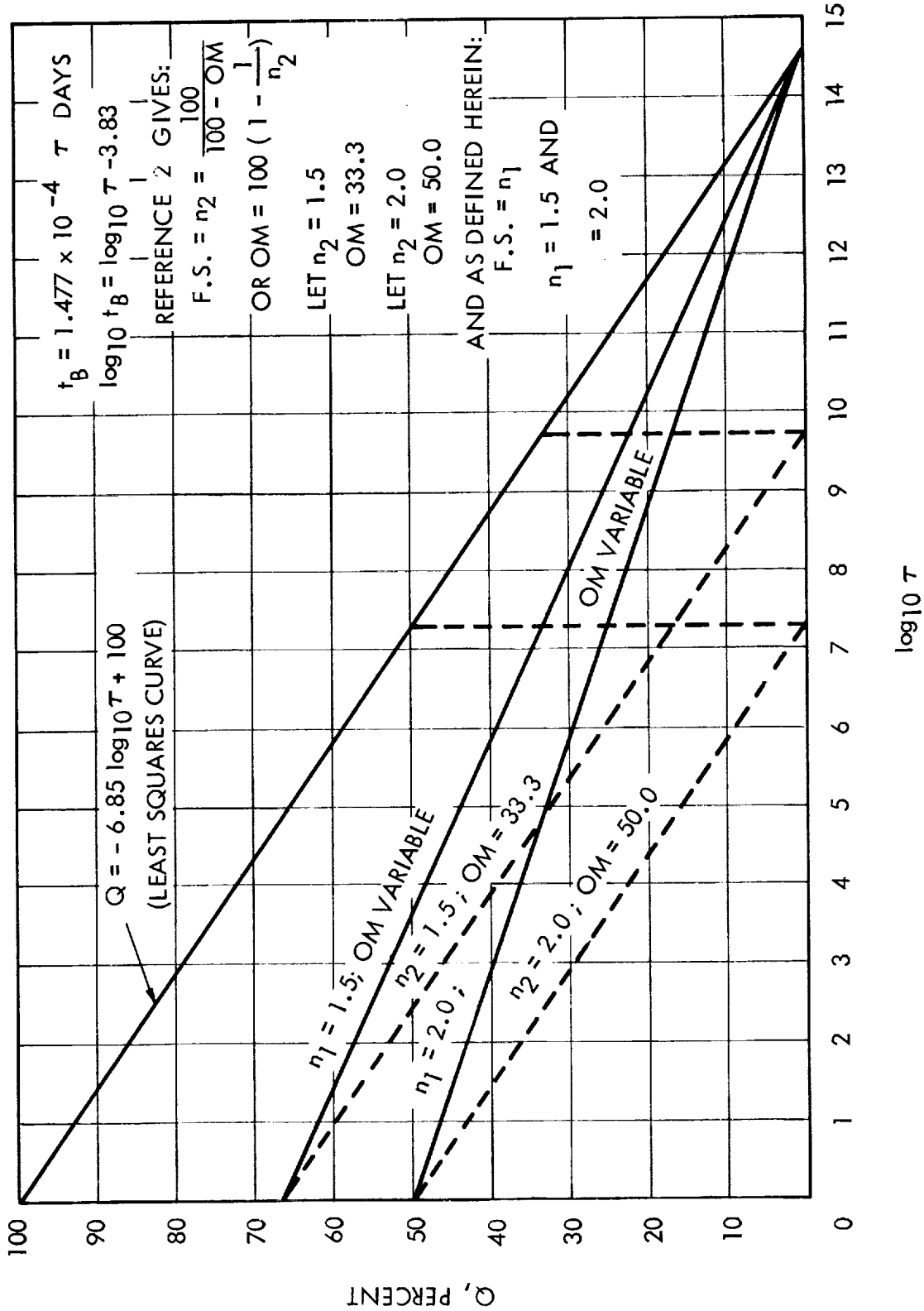

Figure D-7. Comparison of Two Safety Factor Concepts and Related Operating Margins

Table D-2. Ratio of Moduli of Elasticity to Ultimate Strength for Polymers and Metals

MATERIAL	E	F_{tu}	$\frac{E}{F_{tu}}$	REFERENCE
Type 300 Nylon	21 gm/den	6.5 gm/den	3.2	5
Type 200 Nylon	20 gm/den	5.7 gm/den	3.5	5
Type 51 Dacron	30 gm/den	6.2 gm/den	4.8	5
Rayon	20 gm/den	3.5 gm/den	5.7	5
Cotton	28 gm/den	3.5 gm/den	8.0	5
SAE 1025 Steel	29×10^6 psi	55,000 psi	530	4
Alloy Steel	29×10^6	260,000 psi	110	4
2024-T4	10×10^6	63,000 psi	160	4
AZ31B-H24(M_g)	6.5×10^6	40,000 psi	160	4
8Mn Ti Alloy	15.5×10^6	120,000 psi	130	4

Table D-3. Factor of Safety and Percent Elongation

Nylon (Reference 5)		Alloy Steel (Reference 4)	
$\frac{F_{ty}}{F_t} = n$	% Elong.	$\frac{F_{tu}}{F_t} = n$	% Elong.
17.5	1.0	4.9	0.25
10.0	3.0	1.86	0.50
7.3	5.0	1.37	0.75
3.5	10.0	1.18	1.00

The rather large deformations with large values of n (Table D-3) are due, in part, to the fact that the safety factor is based on the quick-break value. In practice the safety factor should be based on the conditions that prevail at the design life of the structure. This is illustrated in Figure D-5. At $\log_{10} \tau = 0$, $t_B = 1.477 \times 10^{-4}$ days and Q = 25%, n = 4; while at $\log_{10} \tau = 10^8$, $t_B = 13,800$ days and Q = 25%, n = 1.5, based on the strength at Q = 1.5 (25) = 37.5 for $t_B = 13,800$ days. Thus, a structure designed for a life of 13,800 days with Q = 25% would have an initial safety factor of 4, and this factor would decrease with time to a value of 1.5.

D. REFERENCES

1. Federal Specification CCC-T-191b, Textile Test Methods, Washington 25, D. C., 15 May 1951.
2. Topping, A. D., Structural Safety with Fabrics and Materials Exhibiting Creep-Rupture Characteristics, Goodyear Aircraft Corporation, GER 7974, 18 June 1957.
3. Jouriles, N., Load-Time Tests of Airship Envelope Fabric, Goodyear Aircraft Corporation, GER6110, May 26, 1954, Revised May 19, 1958.
4. MIL-HDBK-5, Strength of Metal Aircraft Elements, Armed Forces Supply Support Center, Washington 25, D. C.
5. deBordenave, J. F., Bringardner, D. J., and Pratt, H. T., "How Eight Fibers Compare in Stress-Strain Properties," Textile World, March 1958, p. 97.